

UNCLASSIFIED

AD NUMBER
ADB258619
NEW LIMITATION CHANGE
TO Approved for public release, distribution unlimited
FROM Distribution authorized to U.S. Gov't. agencies only; Proprietary Info.; Jul 99. Other requests shall be referred to U.S. Army Medical Research and Materiel Command, 504 Scott St., Fort Detrick, Maryland 21702-5012.
AUTHORITY
USAMRMC ltr, 26 Aug 2002

THIS PAGE IS UNCLASSIFIED

AD \_\_\_\_\_

GRANT NUMBER DAMD17-96-1-6038

TITLE: Growth Suppression and Therapy Sensitization of Breast Cancer

PRINCIPAL INVESTIGATOR: Ruth A. Gjerset, Ph.D.

CONTRACTING ORGANIZATION: Sidney Kimmel Cancer Center  
San Diego, California 92121

REPORT DATE: July 1999

TYPE OF REPORT: Annual

PREPARED FOR:  
U.S. Army Medical Research and Materiel Command  
Fort Detrick, Frederick, Maryland 21702-5012

DISTRIBUTION STATEMENT: Distribution authorized to U.S. Government agencies only (proprietary information, Jul 99). Other requests for this document shall be referred to U.S. Army Medical Research and Materiel Command, 504 Scott Street, Fort Detrick, Maryland 21702-5012.

The views, opinions and/or findings contained in this report are those of the author(s) and should not be construed as an official Department of the Army position, policy or decision unless so designated by other documentation.

**DTIC QUALITY INSPECTED 4**

**20001013 094**

## NOTICE

USING GOVERNMENT DRAWINGS, SPECIFICATIONS, OR OTHER DATA INCLUDED IN THIS DOCUMENT FOR ANY PURPOSE OTHER THAN GOVERNMENT PROCUREMENT DOES NOT IN ANY WAY OBLIGATE THE U.S. GOVERNMENT. THE FACT THAT THE GOVERNMENT FORMULATED OR SUPPLIED THE DRAWINGS, SPECIFICATIONS, OR OTHER DATA DOES NOT LICENSE THE HOLDER OR ANY OTHER PERSON OR CORPORATION; OR CONVEY ANY RIGHTS OR PERMISSION TO MANUFACTURE, USE, OR SELL ANY PATENTED INVENTION THAT MAY RELATE TO THEM.

### LIMITED RIGHTS LEGEND

Award Number: DAMD17-96-1-6038

Organization: Sidney Kimmel Cancer Center

Those portions of the technical data contained in this report marked as limited rights data shall not, without the written permission of the above contractor, be (a) released or disclosed outside the government, (b) used by the Government for manufacture or, in the case of computer software documentation, for preparing the same or similar computer software, or (c) used by a party other than the Government, except that the Government may release or disclose technical data to persons outside the Government, or permit the use of technical data by such persons, if (i) such release, disclosure, or use is necessary for emergency repair or overhaul or (ii) is a release or disclosure of technical data (other than detailed manufacturing or process data) to, or use of such data by, a foreign government that is in the interest of the Government and is required for evaluational or informational purposes, provided in either case that such release, disclosure or use is made subject to a prohibition that the person to whom the data is released or disclosed may not further use, release or disclose such data, and the contractor or subcontractor or subcontractor asserting the restriction is notified of such release, disclosure or use. This legend, together with the indications of the portions of this data which are subject to such limitations, shall be included on any reproduction hereof which includes any part of the portions subject to such limitations.

THIS TECHNICAL REPORT HAS BEEN REVIEWED AND IS APPROVED FOR PUBLICATION.

Atkinson Mintra  
08/28/00

# REPORT DOCUMENTATION PAGE

*Form Approved*  
**OMB No. 0704-0188**

Public reporting burden for this collection of information is estimated to average 1 hour per response, including the time for reviewing instructions, searching existing data sources, gathering and maintaining the data needed, and completing and reviewing the collection of information. Send comments regarding this burden estimate or any other aspect of this collection of information, including suggestions for reducing this burden, to Washington Headquarters Services, Directorate for Information Operations and Reports, 1215 Jefferson Davis Highway, Suite 1204, Arlington, VA 22202-4302, and to the Office of Management and Budget, Paperwork Reduction Project (0704-0188), Washington, DC 20503.

<b>1. AGENCY USE ONLY (Leave blank)</b>	<b>2. REPORT D</b> July 1999	<b>3. REPORT TYPE AND DATES COVERED</b> Annual (1 Jul 98 - 30 Jun 99)	
<b>4. TITLE AND SUBTITLE</b> Growth Suppression and Therapy Sensitization of Breast Cancer		<b>5. FUNDING NUMBERS</b> DAMD17-96-1-6038	
<b>6. AUTHOR(S)</b> Ruth A. Gjerset, Ph.D.			
<b>7. PERFORMING ORGANIZATION NAME(S) AND ADDRESS(ES)</b> Sidney Kimmel Cancer Center San Diego, California 92121		<b>8. PERFORMING ORGANIZATION REPORT NUMBER</b>	
<b>9. SPONSORING/MONITORING AGENCY NAME(S) AND ADDRESS(ES)</b> U.S. Army Medical Research and Materiel Command Fort Detrick, Frederick, Maryland 21702-5012		<b>10. SPONSORING/MONITORING AGENCY REPORT NUMBER</b>	
<b>11. SUPPLEMENTARY NOTES</b>			
<b>12a. DISTRIBUTION / AVAILABILITY STATEMENT</b> Distribution authorized to U.S. Government agencies only (proprietary information, Jul 99). Other requests for this document shall be referred to U.S. Army Medical Research and Materiel Command, 504 Scott Street, Fort Detrick, Maryland 21702-5012.		<b>12b. DISTRIBUTION CODE</b>	
<b>13. ABSTRACT (Maximum 200)</b>  The goal of this project is to provide a rationale and pre-clinical evaluation of p53-based approaches to growth suppression and therapy sensitization of breast cancer, including combination approaches using p53 gene therapy in combination with chemotherapy or DNA repair inhibitors. The scope of the third year's work was (1) to continue to evaluate how the c-Jun and p53 pathways interact to affect DNA repair, apoptosis, and the cellular response to chemotherapy, (2) to study how retinoids affect cisplatin adduct formation in specific regulatory regions of the genome, and (3) to set up an <i>in vivo</i> model for breast cancer metastasis to evaluate p53 combination approaches. We observed that inhibition of c-Jun N-terminal phosphorylation inhibits cisplatin-induced expression of GADD45, and enhances p53 mediated induction of bax and apoptosis, suggesting that GADD45 may provide a target for new therapeutics that collaborate with p53. With regard to retinoid induced cisplatin adduct formation on the RAR $\beta$ promoter, we have shown that a region encompassing the TATA box and RARE become preferentially targeted by cisplatin following retinoid treatment. We have set up an <i>in vivo</i> model for breast cancer metastasis and are presently testing the efficacy of p53 plus doxorubicin therapy in inhibiting metastasis.			
<b>14. SUBJECT TERMS</b> Breast Cancer		<b>15. NUMBER OF PAGES</b> 125	
		<b>16. PRICE CODE</b>	
<b>17. SECURITY CLASSIFICATION OF REPORT</b> Unclassified	<b>18. SECURITY CLASSIFICATION OF THIS PAGE</b> Unclassified	<b>19. SECURITY CLASSIFICATION OF ABSTRACT</b> Unclassified	<b>20. LIMITATION OF ABSTRACT</b> Limited



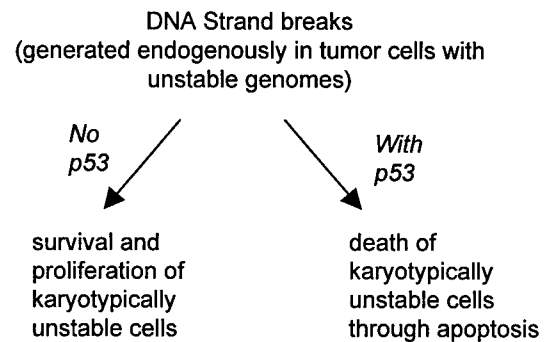
## TABLE OF CONTENTS

	<u>Page #</u>
FRONT COVER	
REPORT DOCUMENTATION PAGE	2
FOREWARD	3
TABLE OF CONTENTS	4
INTRODUCTION	5
BODY OF REPORT	6
KEY RESEARCH ACCOMPLISHMENTS	13
REPORTABLE OUTCOME	14
CONCLUSIONS	15
REFERENCES	17
APPENDICES	19

**Growth Suppression and Therapy Sensitization of Breast Cancer**  
**DAMD17-96-1-6038**  
**Progress Report #3**

## INTRODUCTION

The goal of this project is to provide a rationale and pre-clinical evaluation of p53-based approaches to growth suppression and therapy sensitization of breast cancer, including combination approaches in which p53 gene therapy is combined with traditional chemotherapy or inhibitors of DNA repair. p53 abnormalities occur in about 40% of breast cancers (1-4), and are a feature of more aggressive tumors with increased aneuploidy and genetic instability (5,6). Gene therapy approaches aimed at restoring wild-type p53 function would therefore be applicable to a large fraction of breast cancers and be particularly relevant to advanced disease. Because p53 gene transfer appears to have minimal consequences for normal cells, and because p53 adenovirus has been used successfully in animal models and Phase I clinical trials for various cancers without toxicity, p53 based approaches for breast cancer therapy hold promise as effective biological therapies with minimal to no adverse side effects. Loss of p53 plays a key role in tumor progression as well as therapy resistance, and this is most likely due to the function of p53 as a modulator of apoptosis following DNA damage (7-11). Karyotypic instability, which occurs in breast cancer and increases with disease progression, generates strand breaks and other forms of DNA damage that can stabilize p53 and activate it for transcriptional transactivation and induction of apoptosis. Loss of p53 function would then favor the growth of karyotypically unstable cancer cells by removing the trigger for apoptosis that would eliminate them, as proposed in (12) and as diagrammed above. This scheme is consistent with studies of mammary tumorigenesis in wnt-1 transgenic mice that showed a correlation between loss of p53 function and increased genomic instability and aneuploidy, suggesting that p53 deficiency relaxes constraints on chromosome number and organization during tumorigenesis. We have added further support for this scheme (Progress Report #2, tasks 2,3) by showing directly that cell lines with decreased DNA repair and increased genomic instability are more sensitive to p53-mediated apoptosis (13, copy attached). We have extended these studies this year to provide further evidence for inhibition of DNA repair in these cell lines and increased p53-mediated apoptosis through expression of bax (see below). Thus the trigger for p53-mediated apoptosis may lie in an abnormal DNA structure generated by the mechanisms that destabilize the genome of these cells. As a result of losing the p53-mediated DNA damage-induced apoptotic pathway, tumor cells become more resistant to radiation and DNA damaging chemotherapeutic drugs, most of which kill cells through the induction of apoptosis. We and others have shown that restoration of p53 function in tumor cells that have lost p53, restores apoptosis in response to DNA damaging therapies such as cisplatin and 5-fluorouracil (14,15). We have also shown that restoration of p53 function in T47D breast cancer cells and MDA-MB-435 breast cancer cells, both of which express endogenous mutant



p53, enhances sensitivity to the DNA damaging drug doxorubicin (adriamycin), The standard therapy for breast cancer. Because resistance to doxorubicin and other chemotherapies occurs in metastatic breast cancer, and constitutes one of the biggest obstacles to successful therapy of this disease, we have set up an orthotopic (mammary fat pad) model for metastatic breast cancer in nude mice (described below) and have initiated studies (tasks 6,7) to test the efficacy of a combined p53 adenovirus + doxorubicin approach in inhibiting metastases. Because the orthotopic model resulting in metastasis more closely resembles the clinical disease than does the model originally proposed for task 6 (subcutaneous implantation of ex vivo-modified cells), we have shifted our efforts to this one. The central hypothesis of this project, supported by our results discussed above (13), is that the level of DNA damage constitutes a key determinant of a tumor cell's susceptibility to p53-mediated apoptosis. Overall our results provide a strong rationale for the combined use of p53 along with DNA damaging chemotherapies or inhibitors of DNA repair for the treatment of breast cancer. We plan to continue *in vivo* studies to test this approach in year 4.

## BODY OF REPORT

Our objectives for the third year, as outlined in the Statement of Work included (task 3, Specific Aim 2 continued) correlating expression of DNA repair genes with mutant Jun expression, and sensitivity to p53-mediated apoptosis, and (Task 6,7) establishing a tumor model for *in vivo* studies. We have also extended the PCR-stop assay for DNA repair to analyze how retinoids may enhance the benefits of cisplatin therapy (28, copy attached).

## Results

*Correlation of DNA damage levels and DNA repair inhibition with sensitivity to p53.* We have provided direct evidence to support our central hypothesis, namely that the level of DNA damage constitutes a key determinant of a tumor cell's susceptibility to p53-mediated apoptosis (13). In these studies we used tumor cell clones modified to express a mutant form of the transcription factor c-Jun (a component of AP-1), altered by amino acid substitutions in its N-terminal domain so as to prevent its phosphorylation by Jun kinase. It is known that Jun kinase activation leading to increased c-Jun N-terminal phosphorylation (JNP) represents an early response to stress and DNA damage and that this activation is often constitutive in tumor cells. We found that cells modified to express mutant Jun and therefore inhibited in the JNP have a DNA repair defect that accounts for their increased sensitivity to DNA damaging chemotherapeutic agents (16). Consistent with such a mechanism, we did not observe increased sensitivity to agents that do not damage DNA such as taxotere (13). Furthermore, these cells showed elevated methotrexate-induced colony formation due to amplification of the dihydrofolate reductase gene, and increased sensitivity to p53-mediated apoptosis. Because gene amplification events and other forms of genome instability involve strand breaks as an initiating event, these results suggest that expression of mutant Jun leading to inhibition of DNA repair promotes the accumulation of strand breaks, which on the one hand favors gene amplification and on the other hand promotes DNA damaged induced stabilization of p53 and apoptosis. We have, in addition shown that the elevated p53-mediated apoptosis in mutant Jun cells correlates with elevated expression of the pro-apoptotic p53 target, bax, relative to the anti-apoptotic bcl2, as determined by Western

analysis (Figure 1). These results are summarized in the model diagrammed in Figure 2. In this model, activation of JNK and loss of p53 are shown as independent mechanisms by which tumor cells undergoing progression accommodate the accompanying increased levels of genome instability and insure survival while sustaining potentially lethal genome destabilizing events. By promoting DNA repair, the JNK pathway may limit endogenous DNA damage to levels compatible with survival. Loss of p53 would further enhance survival by eliminating DNA damage-induced apoptosis.

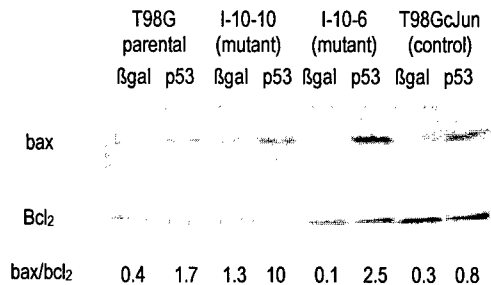


Figure 1. Western blot analysis of bax and bcl2 protein in lysates of parental cells (T98G parental), and two mutant Jun-expressing clones (I-10-10 and I-10-6), as well as a normal c-Jun modified clone (control), 48 hours after treatment with Adp53 or Adβgal (control vector), 100 pfu per cell for 3 hours. Results show that the bax to bcl2 ratio is elevated in mutant Jun expressing clones, consistent with enhanced apoptosis as shown in the model proposed in Figure 2.

### Responses to DNA damage in tumor cells

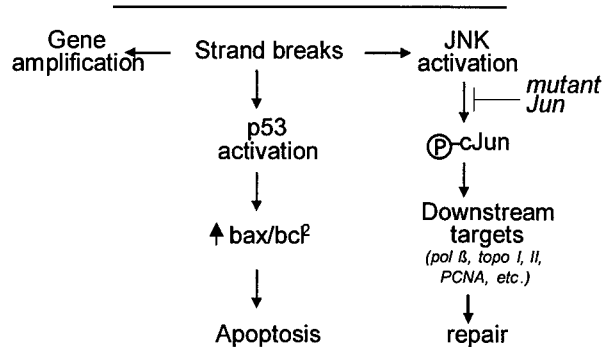


Figure 2. Model showing how, through inhibition of potential c-Jun downstream targets (DNA polymerase β, topoisomerase I,II, PCNA) mutant Jun promotes the accumulation of endogenous DNA strand breaks in genomically unstable tumor cells, which in turn leads to p53 activation, induction of bax and apoptosis.

This system may enable us to identify downstream targets of the c-Jun transcription factor, whose inhibition enhances p53-mediated apoptosis in a way similar to expression of mutant Jun. Such genes may themselves constitute new therapeutic targets for p53 combination therapies. We have therefore examined by quantitative RT-PCR the expression of several potential downstream targets of c-Jun (genes whose promoter regions contain one or more AP-1 or ATF2/CREB regulatory sequences) known also to be involved in DNA synthesis and repair, including PCNA, topoisomerase I, polymerase β, GADD45 as shown in Table 1. Of the genes examined, only GADD45 expression appears to be altered in c-Jun modified cells (Figure 3).

Table 1  
Genes whose expression patterns are similar in T98G parental cells and in mutant Jun expressing cells

Gene	DNA damage (cisplatin) induced change in expression	
	Parental T98G	CJun modified I-10-10
PCNA	No change	No change
Polymerase β	decrease	decrease
Topoisomerase I	decrease	decrease

Gene expression was analyzed by RT-PCR 24 hours following treatment with 100 μM cisplatin

## RT-PCR of GADD45

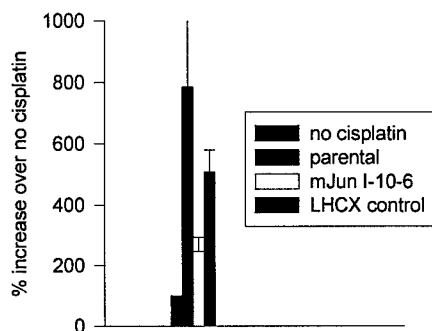


Figure 3. Bar graph showing changes in expression of GADD45 24 hours after a 1 hour exposure to 100  $\mu$ M cisplatin in T98G parental cells, in mutant Jun-expressing T98G cells clone I-10-6, and in control vector modified cells (LHCX). RNA was prepared and analyzed by quantitative RT-PCR.

We are presently extending this analysis to other DNA damage response genes, including GADD153.

These results could have clinical implication for late stage tumors where DNA repair mechanisms may be upregulated in response to exposure to DNA damaging therapies (17-21). Such tumors may require concurrent down regulation of DNA repair in order to respond optimally to p53 therapy. Down regulation of specific AP-1 regulated DNA synthesis and repair genes may provide a means to inhibit DNA repair and enhance sensitivity to p53. We have observed, for example, that T47D breast cancer cells have a highly efficient nucleotide excision repair (NER) pathway (Progress Report #2), suggesting that DNA repair may be a component of drug resistance in T47D cells. The selection of T47D clones expressing mutant Jun is in progress, and will enable us to extend these observation to a second tumor line.

Demonstration of a novel mechanism by which retinoids may synergize with cisplatin. As previously described in Progress report 2, we have obtained evidence for a novel mechanism by which retinoids such as 9-cis retinoic acid might synergize with cisplatin, an agent that forms primarily intrastrand bifunctional adducts on adjacent guanine-guanine or guanine-adenine dinucleotides, inducing a 45° bend in the helix toward the major groove (22). The formation of this structural motif may be critical to the anti-tumor activity of cisplatin and explain the differential biological activity of cisplatin compared to its clinically inert trans isomer (transplatin). In particular, cisplatin-DNA adducts are known to suppress transcription to a significantly greater degree than do transplatin-DNA adducts (23), and this could be the basis of their differential cytotoxicity. In fact, the structural features of the transcription complex, where transcription factor-binding induces distortions in the DNA structure, might create preferential targets for cisplatin but not transplatin adduct formation.

Consistent with this model, we have found that treatment of T47D breast cancer cells with 9-cis retinoic acid prior to treatment with cisplatin, alters the distribution of cisplatin adducts along the retinoic acid receptor beta gene, one of the target genes for 9-cis retinoic acid. The fact that this treatment did not alter the distribution of cisplatin adducts on the dihydrofolate reductase

(DHFR) gene, which is transcriptionally unresponsive to 9-cis retinoic acid, suggests that the altered distribution of adducts is directly related to 9-cis retinoic acid-induced activation of the RAR $\beta$  gene. In particular, 9-cis retinoic acid pretreatment resulted in more than a two fold enhancement of cisplatin adduct formation on the RAR $\beta$  promoter region, while having little effect on the downstream regions of the same gene. Thus 9-cis retinoic acid and other retinoids may, through their pleiotropic effects on gene expression, generate new targets for cisplatin adduct formation and enhance its cytotoxicity through inhibition of the transcription initiation complex.

In the past year we extended this analysis to subregions of the RAR $\beta$  gene promoter, as shown in Figure 4. In the absence of promoter activation with 9-cis retinoic acid, adduct formation was virtually undetectable in the central region, B, encompassing the TATA box and RARE (retinoic acid response element), and approximately equivalent in the regions A and C to what we had previously observed on the larger 1043 base region of the promoter. Some portion of the central region of the promoter included in fragment B may therefore be protected from platination in the uninduced state, and become accessible upon promoter activation.

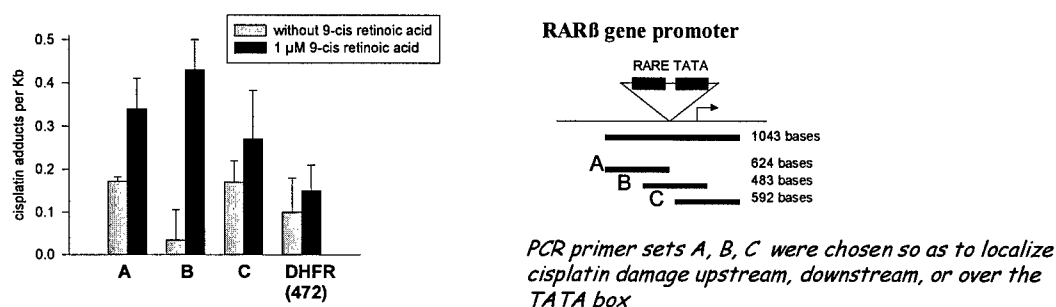


Figure 4. Analysis by PCR stop assay of cisplatin damage on three overlapping regions A, B, and C, or the RAR $\beta$  promoter region of T47D genomic DNA following exposure of cells to cisplatin, either in the presence or absence of 1  $\mu$ M 9-cis retinoic acid. Assays were performed in triplicate.

Upon promoter activation, cisplatin adduct densities increase on all fragments so as to account for the overall increase in adduct density observed on the larger 1043 base fragment. These results suggest that chromatin-remodeling following promoter activation may create sites that are preferentially vulnerable to cisplatin adduct formation. This preference may contribute to the highly effective anti-tumor activity of cisplatin and suggest that drugs that target promoters may have considerable anti-tumor efficacy. Retinoids may synergize with drugs such as cisplatin by creating new targets for cisplatin binding in genomic regions where the cell is particularly vulnerable. These results are described in a manuscript presently under revision (28, copy attached).

*In vivo animal model with MDA-MB-435 cells – pilot experiment 1.* We have tested the metastatic breast tumor line MDA-MB-435. This model provides the most realistic and rigorous test of the therapeutic approaches we are proposing, as drug resistance becomes a greater obstacle to treatment of metastatic disease. The MDA-MB-435 cell line is relatively resistant to adenovirus mediated gene transfer, but high efficiencies of infection (*in vitro*) can be achieved by

increasing the dosage of virus. In other animal tumor models we have used, high levels of adenovirus given in repeated doses are well tolerated and have been effective in combination approaches even with tumor models relatively resistant to Adenovirus, as in the case of the MDA-MB-435 line. P53-Adenovirus is being supplied by Introgen Therapeutics.

The pilot experiment was set up to gain experience in the mammary fat pad implantation technique. We used 4 animals (nude, female, 4-5 weeks, Harlan Sprague Dawley). Animals 1 and 2 were implanted with MDA-MB-435 cells received from ATCC. Animals 3 and 4 were implanted with MDA-MB-435 cells provided by Janet Price (M.D. Anderson, Houston, TX)). While both clones have metastatic potential (primarily to the lung), the cells from Janet Price have been selected through multiple passages through animals for greater metastatic potential, primarily to lungs. Animals were anesthetized with isoflourane. A small incision was made in the middle of the chest and  $2 \times 10^6$  cells in 50  $\mu$ l PBS were implanted under the skin in the mammary fat pad. The incision was closed with a surgical staple, and removed about 1 week later. Animals were monitored for tumor growth by measuring the length and width of tumors calculating volumes based on the formula  $\text{Volume} = (\frac{1}{2}) \text{length} \times (\text{width})^2$ . At 6 weeks and 4 months post implantation, animals 1 and 2, respectively, were sacrificed. At the time of sacrifice the tumor of animal 1 measured 570  $\text{mm}^3$  and the tumor of animal 2 measured 45  $\text{mm}^3$ . At 2.5 months post implantation, animals 3, 4 were sacrificed. At the time of sacrifice, the tumor of animal 3 measured 310  $\text{mm}^3$  and the tumor of animal 4 measured 120  $\text{mm}^3$ . Lungs were excised from sacrificed animals and fixed in 10% formaldehyde for histological analysis of metastasis. We did not observe metastases in any of these animals.

*In vivo model with MDA-MB-435 cells – pilot experiment 2.* This experiment was set up to further test the metastatic potential of the cell line received from Janet Price and to conduct an initial efficacy test of intratumoral or intravenous Adenovirus administration. 15 animals were implanted in the mammary fat pad with  $2 \times 10^6$  MDA-MB-435 cells. 16 days post-implantation, an attempt was made to approximately randomize animals with respect to tumor volume into 5 groups. Tumor volumes, however, showed considerable variation from animal to animal. Animals were then injected twice per week for 6 weeks with vector ( $2.5 \times 10^{10}$  vp/animal in 50  $\mu$ l PBS; equal to  $2.5 \times 10^8$  pfu Adp53 and  $10^9$  pfu AdLuc). Vector was either injected intravenously through the tail vein or intratumorally. Tumors were measured and volumes calculated two times per week. At 15 weeks, animals were sacrificed and lungs were removed and fixed in 10% formaldehyde. Histological slides were prepared for examination of lung metastases (see Table 2; Figure 6, with metastatic masses indicated by an "M").

Figure 5 shows that tumors increased in size and lung metastases developed in all treatment groups, possibly due to the large initial tumor cell inoculum. The small group size and wide range of tumor sizes per group did not enable us to draw any conclusions as to treatment efficacy.

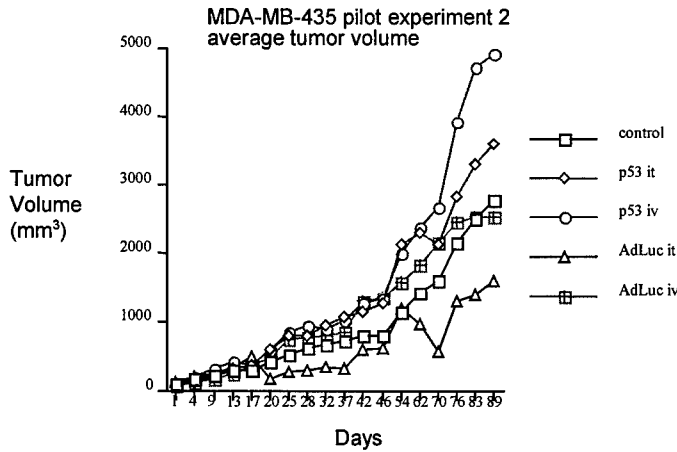


Figure 5. Tumor growth at the site of mammary fat pad inoculation of MDA-MB-435 cells (from Janet Price).  $2 \times 10^6$  cells were implanted and animals in vector treated groups received vector twice per week for six weeks beginning day 1 (which was 16 days post implantation).

Table 2  
MDA-MB-435 pilot experiment 2  
Histological analysis of lung metastases at 15 weeks post-implantation

Animal #	treatment	Lung metastases (relative amt)
1	None	+
2	None	+++
4	Adp53 (i.t.)	+
5	Adp53 (i.v.)	+
6	Adp53 (i.t.)	-
7	AdLuc (i.v.)	-
8	Adp53 (i.t.)	+
10	AdLuc (i.t.)	+
12	AdLuc (i.v.)	-
13	None	+
14	None	+
15	AdLuc (i.v.)	+

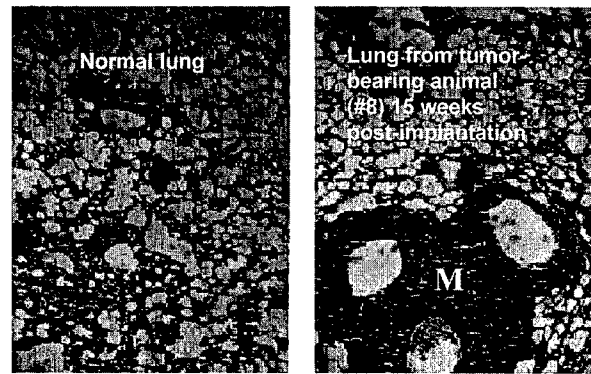


Figure 6. Hematoxylin/eosin-stained paraffin-embedded sections of lung tissue. Left: normal lung. Right: lung from tumor-bearing animal #8 (Table 3) sacrificed 15 weeks post-implantation of tumor cells. "M" indicates metastasis.

**Administration of doxorubicin.** In order to establish toxicity limits for doxorubicin to be used in subsequent combination studies, animals were injected at various doses with doxorubicin (2 mg/ml solution Doxorubicin HCl for injection, clinical grade, Bedford Laboratories, obtained through local pharmacies). Doses were chosen based on published doses in the range of 5 mg/kg to 50 mg/kg. Tail vein and intraperitoneal routes of injection were tried. By intraperitoneal injection, the maximum tolerated dose (3 weekly injections) without visible signs of illness was 5 mg/kg.

Two weekly intravenous-doses of 5mg/kg, 10 mg/kg, or 15/mg/kg, were equally well tolerated, although tissue necrosis at the site of injection was observed.

**Intravenous administration of adenovirus vector.** Intravenous administration of viral vector via the tail vein would enable us to extend the application of adenovirus to the treatment of

metastatic disease. In order to verify that intravenous delivery of viral vector could in fact achieve significant delivery efficiencies to the lung, we conducted a test in which animals received  $10^9$  plaque forming units of  $\beta$ -galactosidase adenovirus. 48 hours later, animals were sacrificed and lungs were excised and frozen for the preparation of thin sections. Sections were fixed in ethanol/acetone (1:1) followed by overnight staining in 0.1% X-gal solution (containing 5 mM potassium ferricyanate, 5 mM potassium ferrocyanate, 2 mM  $MgCl_2$  in PBS) to reveal the presence of blue,  $\beta$ -galactosidase-expressing cells. Slides were counterstained with nuclear fast red. Figure 7 shows that significant staining of lung tissue was achieved.



Figure 7. X-gal stain of frozen lung section taken from a mouse 48 hours following tail vein injection of  $10^9$  pfu of Adenovirus- $\beta$ galactosidase. Intense staining indicating gene transfer and expression of  $\beta$ galactosidase is shown by arrow.

*In vivo efficacy study of Ad p53 (intravenous) plus doxorubicin for treatment of breast cancer metastases (MDA-MB-435 model).* Based on the results of our pilot studies we have set up an efficacy study which is in progress, to test the efficacy of intravenous vector delivery along with doxorubicin (also intravenous) for the treatment of lung metastases of MDA-MB-435 tumors, initiated by mammary fat pad (m.p.f.) implantation. The protocol follows a protocol described by Janet Price and colleagues (27), in which tumors are initiated by implanting  $5 \times 10^5$  cells (m.f.p.), a lower inoculum than we used in our pilot experiments. At 8 weeks post implantation, when most tumors have metastasized to the lungs, the primary tumor is excised and animals are given treatment. The animals are sacrificed at 15-16 weeks post-implantation and analyzed for lung metastases. The following treatment groups have therefore been set up (week 1 refers to the first week of treatment, which is about 8 weeks post-implantation):

Treatment schedule for MD MB 435 metastases  
(3 cycles of treatment in weeks 1, 3, 5)  
9 animals per group

- 1) no treatment
- 2) doxorubicin only
- 3) Ad-p53
- 4) Ad-Luc (control vector)
- 5) Ad-p53 + doxorubicin
- 6) Ad-Luc + doxorubicin

} Doxorubicin 10 mg/kg day 1, 15, 29 (100  $\mu$ l)  
Vector 3x per week during weeks 1-6.  
Vector dose:  $5 \times 10^{10}$  vp per injection  
=  $5 \times 10^8$  pfu for Adp53 and  $2 \times 10^9$  pfu for AdLuc

## Key Research Accomplishments

We have observed the following:

- Restoration of wild-type p53 expression enhances sensitivity of breast cancer cells to doxorubicin, a DNA damaging drug, and the standard therapy for breast cancer.
- Inhibition of DNA repair in tumor cells enhances sensitivity to DNA damaging drugs, as well as p53-mediated induction of bax and apoptosis.
- Inhibition of c-Jun downstream targets (through inhibition of c-Jun N terminal phosphorylation) leads to DNA repair defects, increased gene amplification, and increased p53-mediated apoptosis.
- Inhibition of c-Jun N terminal phosphorylation inhibits cisplatin-induced expression of GADD45, suggesting that this may be one downstream target of phosphorylated c-Jun.
- Pretreatment of T47D breast cancer cells with 9-cis retinoic acid leads to increased cisplatin adduct formation in the promoter region of the 9-cis retinoic acid-responsive gene, retinoic acid receptor  $\beta$  (RAR $\beta$ ), suggesting that retinoids such as 9-cis retinoic acid, through their pleiotropic effects on gene expression, generate new targets for cisplatin, and enhance its cytotoxicity through inhibition of the transcription initiation complex.
- MDA-MB-435 cells, expressing endogenous mutant p53, are growth inhibited and sensitized to doxorubicin following restoration of wild-type p53 function. They also provide a useful *in vivo* model for breast cancer metastasis.

## Reportable Outcomes

### Manuscripts:

- (1) Gjerset, R.A., Lebedeva, S., Haghghi, A., Turla, S.T., and Mercola, D. (1999) Inhibition of the Jun kinase pathway blocks DNA repair, enhances p53-mediated apoptosis and promotes gene amplification. *Cell Growth and Differentiation*, *in press*.
- (2) Haghghi, A., Lebedeva, S., and Gjerset, R.A. Preferential platination of an activated cellular promoter by cis-diamminedichloroplatinum. (1999, manuscript submitted, under revision)
- (3) Gjerset, R.A., and Mercola, D. (1999) Sensitization of tumors to chemotherapy through gene therapy. In "Cancer Gene Therapy: Past Achievements and Future Challenges", N. Habib, ed., Plenum Publishing Corporation, New York, London, Moscow. *In press*.

### Abstracts, posters, oral presentations

- (1) Preferential DNA binding of Cis-diamminedichloroplatinum to an Activated Promoter, Haghghi, A., Lebedeva, S., and Gjerset, R.A. Poster presented at the Conference on Chromatin Structure and Function, June 16, 1998, Paris, France.
- (2) The Cellular Stress Response Modulates Sensitivity to p53 (poster and oral presentation) Gordon Research Conference on Cancer August 2-7, 1998, Newport, RI.

## Conclusions

We have shown that restoration of wild-type p53 activity sensitizes breast cancer cells to doxorubicin, a common DNA damaging chemotherapeutic drug used in the treatment of breast cancer. These observations extend our earlier observation on p53-mediated sensitization to cisplatin (15), and suggest a broad applicability of p53 as a general sensitizer to DNA damaging therapies.

Using clonal derivatives of the T98G cell line, modified so as to be suppressed in N-terminal c-Jun phosphorylation, and defective in DNA repair, we have demonstrated a correlation between decreased DNA repair, increased genome instability, and increased sensitivity to p53-mediated apoptosis through the bax pathway. This result supports our central hypothesis that DNA damage constitutes a key determinant of a tumor cell's susceptibility to p53-mediated apoptosis, and provides additional rationale for the combined use of p53 with DNA repair inhibitors, as well as DNA damaging drugs. We are presently selecting clones of T47D cells inhibited in the jun kinase pathway in order to extend and confirm the generality of our results with T98G cells. T47D cells display a particularly efficient nucleotide excision repair pathway, and thus represent an ideal model system in which to test the efficacy of a combined therapeutic approach in which drug resistance is reversed by inhibiting DNA repair and restoring p53.

We have addressed the mechanism of synergy between retinoids and cisplatin, as therapeutic synergy between these two agents has been observed in tumor models for breast cancer, and because we have observed the restoration of p53 further improves the therapeutic efficacy of retinoids with cisplatin. Earlier published studies show that retinoid pretreatment enhances the total platinum binding to DNA of target cells. Using the RAR $\beta$  gene as a model, we have observed that the enhanced cisplatin binding occurs preferentially at the promoter region, suggesting that retinoids synergize with cisplatin by generating hypersensitive sites in promoter regions to which cisplatin preferentially binds, and possibly leading in this way, to the inhibition of transcription observed with cisplatin, followed by apoptosis.

We are presently testing our hypotheses *in vivo* (tasks 6,7), using a nude mouse model for breast cancer metastasis. Animals will receive systemic treatment with p53 adenovirus in combination with doxorubicin. Based on the outcome of this study we plan to conduct an additional study in which the vector is delivered locally (intratumorally) or in which doxorubicin is replaced with a second chemotherapeutic agent (cisplatin).

## Materials and Methods.

Cell culture. MDA-MB-435 breast cancer cells used in this work were purchased either from ATCC or received from Dr. Janet Price (MD Anderson Cancer Center) and grown under 10% CO<sub>2</sub> in DMEM medium supplemented with 10% fetal calf serum, non-essential amino acids, glutamine, pyruvate and gentamycin.

DNA damage assays based on PCR (PCR-stop assay). We have used a DNA damage assay known as the "PCR stop assay" (30-32) to examine cisplatin adduct formation on different

genomic regions. The assay is based on the principle that every DNA lesion, including platinum adducts produced by cisplatin, can potentially block the progression of the Taq polymerase and decrease the yield of a given PCR product. It has been well demonstrated that the degree of inhibition of PCR correlates with the level of platination, indicating that the polymerase is inhibited by every lesion (32). In addition, when whole cells are incubated with varying levels of cisplatin, the degree of inhibition of amplification of a specific PCR fragment from DNA purified from these cells, correlates with platination levels determined by atomic absorption (32), with P (relative PCR efficiency) being related to the average number of adducts, n, per fragment by the Poisson formula:  $P = e^{-n}$ .

Genomic DNA was prepared from about  $10^6$  cells treated with 0.5 mM or 1 mM cisplatin either with or without 9-cis retinoic acid, using the Qiagen Qiaamp Blood Kit™ following the manufacturer's instructions, and resuspended in sterile H<sub>2</sub>O at a concentration of 0.5 mg/ml. PCR reactions are performed in 25  $\mu$ l containing 50 mM KCL, 10 mM Tris pH 8.3, 1.5 mM MgCl<sub>2</sub>, 250  $\mu$ M each of dNTP, 1  $\mu$ M of the forward and reverse primers and 0.1  $\mu$ M of the nested primer, 0.25  $\mu$ l Taq enzyme (Qiagen), and 0.5  $\mu$ l of Q™ solution (Qiagen). Quantitative amplification is as follows: one cycle (1'30" 94°C), 25 cycles (94°C for 1 minute, 57°C for 1 minute, 70°C for 2'30"), 1 cycle (94°C for 1 minute, 57°C for 1 minute, 70°C for 7 minutes, 4°C to hold). To confirm that the extent of reaction remains directly proportional to amount of template, we have performed control reactions with known amounts of DNA in 2 fold dilutions.

*Western blots.* Cell lysates were adjusted to a protein concentration of 5 mg/ml and about 50  $\mu$ g were electrophoresed on a 15% acrylamide gel, transferred to an 0.45  $\mu$ m PVDF-plus transfer membrane (Micron Separations, Inc.) and probed with rabbit polyclonal anti-bax or mouse monoclonal anti-c-myc (Santa Cruz Biotechnology, Inc.) at 1  $\mu$ g/ml followed by HRP-secondary antibody (1:1000) using the protocol supplied by the manufacturer. The blot was then treated with ECL Detection Reagents (Amersham) and exposed to Kodak Biomax MR film for 2 minutes.

*RT-PCR.* were treated as indicated and Total cellular RNA was prepared from about  $5 \times 10^5$  cells (at about 70% confluency) using the Rneasy™ kit from Qiagen and following the manufacturer's procedure. 5  $\mu$ g of RNA was reverse transcribed into cDNA in a 20  $\mu$ l reaction containing 0.5 mM dNTPs (Pharmacia), 100  $\mu$ g/ml oligo dT (Promega), 2 units RNAsin (Promega), 10 units Moloney Murine leukemia virus reverse transcriptase (Promega), reverse transcriptase buffer (Promega). This cDNA was then used as a template for quantitative PCR. Primers were chosen using MacVector™ software so as to amplify a 200-300 base region of the gene of interest. Amplification of a 246 base region of the coding sequence of the dihydrofolate reductase from exons 1 to 4 served as an internal control. Amplification conditions were as described above for the PCR-stop assay. Quantitative conditions were verified by amplifying serial two fold dilutions of the cDNA from 2  $\mu$ l to 0.25  $\mu$ l template and product formation was found to be proportional to input template under our conditions. Following amplification, products were analyzed by agarose gel electrophoresis followed by band quantitation using a Kodak digital camera.

## References

1. Bartek, J., Iggo, R., Gannon, J., and Lane J.P. (1990) Genetic and immunochemical analysis of mutant p53 in human breast cancer lines. *Oncogene*, 5:893-899.
2. Coles, C., Condie, A., Chetty, U., Steel, C.M., Evans, A.J. and Prosser, J. (1992) *Cancer Research* 52:5291-5298.
3. Singh, S., Simon, M., Meybohm, I., Jantke, I., Jonat, W., Maass, H., and Goedde, H.W. (1993) Human breast cancer: frequent p53 allele loss and protein overexpression. *Human Genet.*, 90:635-640.
4. Moll, U.M., Riou, G., and Levine, A.J. (1992) Two distinct mechanisms alter p53 in breast cancer: mutation and nuclear exclusion. *Proc. Natl. Acad. Sci., USA* 89:7262-7266.
5. Hendersin, I.C., Harris, J.R., Kinne, D.W., and Hellman, S. *Cancer of the breast. In Cancer, Principles and Practice of Oncology.* DeVita, V.T., Hellman, S., and Rosenberg, S.A., eds., J.P. Lippincott Comp., Philadelphia, 3rd ed., pp. 1197-1268.
6. Donehower, L.A., Godley, L.A., Aldaz, C.M., Pyle, R., Shi, Y-P., Pinkel, D., Gray, J., Bradley, A., Medina, D., Varmus, H.E. (1995) Deficiency of p53 accelerates mammary tumorigenesis in *wnt-t* transgenic mice and promotes chromosomal instability. *Genes and Development*, 9: 882-895.
7. Lowe S.W., Ruley H.E., Jacks T., Housman, D.E. (1993) p53-mediated apoptosis modulates the cytotoxicity of anti-cancer agents. *Cell* 74: 957-967.
8. Lotem, J. and Sachs, L. (1993) Hematopoietic cells from mice deficient in wild-type p53 are more resistant to induction of apoptosis by some agents. *Blood* 82:1092-1096.
9. Clarke, A.R., Purdie, C.A., Harrison, D.J., Morris, R.G., Bird, C.C., Hooper, M.L., Wyllie, A.H. (1993) Thymocyte apoptosis induced by p53-dependent and independent pathways. *Nature* 362: 849-852.
10. Yonish-Rouach E, Resnitzky D, Lotem J, Sachs, L., Kimchi, A., Oren, M. (1991) Wild-type p53 induces apoptosis of myeloid leukemic cells that is inhibited by interleukin-6. *Nature* 352: 345-347.
11. Shaw, P., Bovey, R., Tardy, S., Sahli, R., Sordat, B., Costa, J. (1992) Induction of apoptosis by wild-type p53 in a human colon tumor-derived cell line. *Proc Natl Acad Sci USA* 89:4495-4499.
12. Lane, D. P.(1992) p53:guardian of the genome. *Nature* 358: 15-16.
13. Gjerset, R.A., Lebedeva, S., Haghighi, A., and Mercola, D.M.(1999) Inhibition of the Jun Kinase pathway blocks DNA repair, enhances p53-mediated apoptosis and promotes gene amplification. *Cell Growth and Differentiation*, *in press.* (copy attached)
14. Lowe, S.W., Bodis, S., McClatchey, A., Remington, L., Ruley, H.E., Fisher, D.E., Housman, D.E., Jacks, T. (1994) p53 status and the efficacy of cancer therapy *in vivo*. *Science* 266: 807-810.
15. Gjerset, R.A., Turla, S.T., Sobol, R.E., Scalise, J.J., Mercola, D., Collins, H., Hopkins, P.J. (1995) Use of wild-type p53 to achieve complete treatment sensitization of tumor cells expressing endogenous mutant p53. *Molecular Carcinogenesis* 14: 275-285.
16. Potapova, O., Haghighi, A., Bost, F., Liu, C., Birrer, M., Gjerset, R., Mercola, D. (1997) The jun kinase/stress-activated protein kinase pathway functions to regulate DNA repair and inhibition of the pathway sensitizes tumor cells to cisplatin. *J. Biol. Chem.* 272: 14041-14044.

17. Scanlon, K.J., Kashini-Sabet, M., and Sowers, L.C. (1989) Overexpression of DNA replication and repair enzymes in cisplatin-resistant human colon carcinoma HCY8 cells and circumvention by azidothymidine. *Cancer Comm.* 1: 269-275.
18. Fravel, H.N.A., Rawlings, C.J., Roberts, J.J. (1978) Increased sensitivity of UV-repair-deficient human cells to DNA bound platinum adducts which, unlike thymidine dimers, are not recognized by an exonuclease from *Micrococcus luteus*. *Mutat. Res.* 51: 121-132.
19. Scanlon, K.J., Kashini-Sabet, M., Miyachi, H., Sowers, L., and Rossi, J. (1989) Molecular basis of cisplatin resistance in human carcinomas, model systems, and patients. *Anti-cancer Res.* 9:1301-1312.
20. Kashini-Sabet, M., Lu, Y., Leong, I., Haedicke, K., and Scanlon, K.J. (1990) Differential oncogene amplification in tumor cells from a patient treated with cisplatin and 5-fluorouracil. *Eur. J. Cancer* 26:383-390.
21. Scanlon, K.J., Jiao, L., Funato, T., Wang, W., Tone, T., Rossi, J.J., Kashini-Sabet, M. (1991) Ribozyme-mediated cleavage of c-fos mRNA reduces gene expression of DNA synthesis enzymes and metallothionein. *Proc. Natl. Acad. Sci. USA* 88: 10591-10595.
22. Takahara PM, Rosenzweig AC, Frederick CA, Lippard SJ (1995) Crystal structure of double-stranded DNA containing the major adduct of the anticancer drug cisplatin. *Nature* 377:649-652.
23. Mello JA, Lippard SJ, Essigmann JM (1995) DNA adducts of cis-diamminedichloroplatinum (II) and its trans isomer inhibit RNA polymerase II differentially in vivo. *Biochemistry* 34: 14783-14791.
24. Oshita, F., Saijo, N. (1994) Rapid polymerase chain reaction assay to detect variation in the extent of gene-specific damage between cisplatin- or VP-16-resistant and sensitive lung cancer cell lines. *Jpn. J. Cancer Res.* 85: 669-673.
25. Oshita, F. and Eastman, A. (1993) Gene-specific damage produced by cisplatin, ormaplatin and UV light in human cells as assayed by the polymerase chain reaction. *Oncology Research* 5: 111-118.
26. Jennerwein, M.M. and Eastman, A. (1991) A polymerase chain reaction-based method to detect cisplatin adducts in specific genes. *Nucleic Acids Research* 19: 6209-6214.
27. Price, J.E., Polyzos, A., Zhang, R.D., and Daniels, L.M. (1990) Tumorigenicity and metastasis of human breast carcinoma cell lines in nude mice. *Cancer Res.* 50: 717-721.
28. Haghghi, A., Lebedeva, S., and Gjerset, R.A. (1999) Preferential platination of an activated cellular promoter by cis-diamminedichloroplatinum. (manuscript submitted and presently under revision). (copy attached)

## APPENDIX

1. **Habib N., ed. (1999) Cancer Gene Therapy: Past Achievements and Future Challenges. Plenum Publishing Corp. N.Y. London, Moscow. *in press*.**
2. **Haghighi, A., Lebedeva, S., and Gjerset, R.A. (1999) Preferential platination of an activated cellular promoter by cis-diamminedichloroplatinum. (manuscript submitted and presently under revision).**
3. **Gjerset, R.A., Lebedeva, S., Haghighi, A., and Mercola, D.M.(1999) Inhibition of the Jun Kinase pathway blocks DNA repair, enhances p53-mediated apoptosis and promotes gene amplification. Cell Growth and Differentiation, *in press*. (copy attached)**

## SENSITIZATION OF TUMORS TO CHEMOTHERAPY THROUGH GENE THERAPY

Ruth A. Gjerset and Dan Mercola

Sidney Kimmel Cancer Center  
10835 Altman Row  
San Diego, California 92121

### 1. Introduction

The cellular response to DNA damage plays a critical role not only in tumor progression but also in the process of acquired drug resistance, a problem that affects about half of all cancer cases overall and remains one of the major obstacles to successful therapy of cancer. Modulation of these DNA damage response pathways may therefore provide us with a means to reverse acquired drug resistance and improve the outcome of therapy for a large fraction of cancer patients. In this article we will focus on two major pathways involved in the cellular response to DNA damage: The Jun kinase stress activated pathway, and the p53-mediated DNA damage response pathway leading to apoptosis. Through independent mechanisms, each of these pathways modulates the cellular response to DNA damaging chemotherapies and radiation. Therapeutic approaches based on inhibiting the Jun kinase pathway and/or restoring the p53 pathway may, therefore, provide us with new biological strategies for reversing acquired drug resistance, thus improving the outcome of therapy for most cancers.

### 2. The p53 tumor suppressor and the DNA damage response.

Over half of all cancers suffer loss of function of the p53 tumor suppressor (Levine, 1993), a key player in the induction of apoptosis in response to DNA damage (Clarke *et al.*, 1993; Gjerset *et al.*, 1995; Lotem *et al.*, 1993; Lowe *et al.*, 1993), in addition to its roles in cell cycle regulation and DNA repair (Levine, 1997). Its involvement in DNA damage-induced apoptosis may derive from its ability to bind, alone or possibly in combination with other DNA damage recognition proteins, to sites of damaged DNA, including single stranded ends and insertion-deletion loops (Bakalkin *et al.*, 1995; Lee *et al.*, 1995, Levine 1997 (review)). p53 might also bind to DNA adducts and strand breaks induced by various therapies. The frequent loss of p53 function in cancer, often associated with disease progression and increased genomic instability, may reflect at least in part the role of p53 in DNA damage recognition and apoptosis. Most genome destabilizing events, including gene amplification, gene deletion and gene translocation, involve DNA strand breaks (Stark, 1993). These breaks could serve as triggers for p53-mediated apoptosis and provide the driving force for loss of p53.

The same process that underlies the progression of cancer, that is, genomic instability accompanied by loss of p53-mediated apoptosis, can also lead to therapy resistance. Support for the idea that loss of p53 could desensitize a cell to the damaging effects of drugs and radiation comes from studies of p53-null transgenic mice. In these studies it was observed that normal transgenic hematopoietic cells (Lotem and Sachs, 1993), E1A-expressing transgenic fibroblasts (Lowe *et al.*, 1993), and transformed transgenic fibroblasts (Lowe *et al.*, 1994) were all more resistant to apoptosis following treatment with any of a wide variety of anti-cancer agents including radiation, than were

the comparable cells from the parental strain of mice that express wild-type p53. Cell killing was therefore enhanced in cells that expressed wild-type p53 and were able to trigger their own cell death program.

The possibility that p53 status is a factor in therapy responsiveness finds further support from a recent anti-cancer drug screening of human tumor cell lines expressing mutant or wild-type p53 (O'Connor *et al.*, 1997). In that study the growth inhibitory properties of some 123 anti-cancer agents were tested in 60 human tumor lines of known p53 status. It was found that cells expressing mutant p53 showed less growth inhibition than did wild-type p53-expressing cells lines following treatment with the majority of clinically used anti-cancer agents, including DNA cross-linking agents such as cisplatin, antimetabolites such as 5-fluorouracil, and topoisomerase I and II inhibitors. Since these agents are known to cause DNA damage, either directly or indirectly, these results are consistent with a role of p53 in mediating the cellular apoptotic response to DNA damage. One class of agents, the antimitotic agents, appeared to suppress growth in a p53-independent manner, consistent with the primary target for these agents being the mitotic apparatus rather than DNA.

Taken together, these studies suggest that p53 gene transfer could have clinical application in suppressing cancer and enhancing the responsiveness of tumors to a wide variety of DNA damaging therapies, a possibility that greatly expands the clinical application of p53-based approaches. Numerous *in vitro* studies in a variety of tumor cell systems support the use of p53 gene transfer to sensitize tumors to such therapy, including, 5-fluorouracil, cisplatin, topoisomerase I inhibitors and gamma radiation (see below).

#### 2.1 *In vitro* sensitization of tumor cells to chemotherapeutic drugs by p53.

In Figures 1 and 2 we have summarized the results of screening tumor cells for sensitivity to various chemotherapeutic agents following exposure of cells to a replication-defective adenovirus encoding wild-type p53 (Ad-p53, Ad-βgal, and Ad-Luc (luciferase) vectors provided by Dr. Deborah R. Wilson, Introgen Therapeutics, Inc.). The cells were treated with virus under conditions which achieve about 70-80% infection efficiency, as judged by infection of parallel cultures with a β-galactosidase adenovirus. Following infection, cells were replated at low density in 96-well plates and treated with varying levels of chemotherapeutic agent, followed by an additional 5-7 days of incubation and measurement of cell viability.

In numerous examples from a variety of cancer types, we have observed suppression of mutant-p53-expressing tumor cells *in vitro* following treatment with Ad-p53. As shown in Figure 1, restoration of wild-type p53 in mutant p53-expressing cells (DLD-1, T47D, PC-3, T98G) results in marked enhancement of sensitivity to a variety of DNA damaging treatments (5-fluorouracil, doxorubicin, cisplatin), consistent with possibility that we have restored the p53-mediated pathway of DNA damage recognition and apoptosis. Apoptosis was confirmed by (a) propidium iodide staining of fixed cells followed by FACS analysis to reveal a sub G1 peak of apoptotic cells, and (b) an ELISA assay (Boehringer Mannheim Corp, Indianapolis, IN) to detect oligonucleosomal

fragments released from the nuclei of cells in the early phases of apoptosis (see Gjerset *et al.*, 1995).

In contrast, this enhancement of sensitivity is not observed in two wild-type p53-expressing cell lines, MCF7 and LS174T (Figure 2). This suggests that wild-type p53 gene transfer may be effective in therapy sensitization only in the case of tumors that have lost wild-type p53 function.

## 2.2 *In vivo* sensitization of tumors to chemotherapeutic drugs by p53.

We have extended our *in vitro* observations on tumor suppression and therapy sensitization to *in vivo* models for human head and neck cancer and colon cancer (Gjerset *et al.*, 1997) and prostate cancer (Figure 3) in nude mice, where established tumors were treated *in vivo* with replication-defective p53-adenovirus, and chemotherapy. We have also studied chemosensitization by p53 using *ex vivo* modified cells in an orthotopic model of glioblastoma in Fisher rats (Dorigo *et al.*, 1998). The results are consistent with other *in vivo* studies in animal models showing a combined benefit of p53 and chemotherapy (Badie *et al.*, 1998; Fujiwara *et al.*, 1994; Miyake *et al.*, 1998; Nielsen *et al.*, 1998; Nguyen *et al.*, 1996). Together with the *in vitro* data, these results support the clinical application of adenovirus p53 combination approaches to tumors expressing mutant p53. In the experiment shown in Figure 3, PC-3 prostate cancer cells which express mutant p53, were implanted in 20 nude mice ( $5 \times 10^6$  cells/ animal) where they form rapidly growing subcutaneous tumors. At 5 days post-implantation, when tumor sizes had obtained a volume of about 50 mm<sup>3</sup>, animals were randomized by tumor size and treatment was initiated. The first day of treatment was then designated day 1 and consisted of intraperitoneal injection of cisplatin (Platinol™, Bristol Laboratories, obtained through local pharmacies), at 4mg/kg (LD10) on days 1 and 8. Vector (Ad-p53 or Ad-luc control) was administered intratumorally ( $10^8$  pfu per tumor) of days 1,3,5, 8, and 10. In both cases, some suppression was observed with Ad-p53 alone, with a significant enhancement of suppression when Ad-p53 was combined with chemotherapy. The vector doses used here were relatively low (10-30 pfu per tumor cell) and completely without side effects (as judged by periodic weight measurements on the animals and histological examination. We observe little or no toxicity in nude mice of vector doses as high as  $10^9$  pfu per animal (Gjerset *et al.*, 1997). Phase I clinical trials employing p53 adenovirus also demonstrate that this vector is well tolerated in patients (Roth *et al.*, 1998). Thus restoration of wild-type p53 function through gene therapy may provide a significant benefit for patients with advanced cancers, when used in combination with conventional therapies.

## 3. The Jun Kinase/Stress-Activated Protein Kinase Pathway and the DNA damage response.

Another important cellular pathway is also triggered in response to DNA damage: the Jun Kinase/Stress-activated protein kinase pathway (JNK/SAPK), one of several distinct Mitogen-Activated Protein Kinase (MAPK) Pathways involved in signal transduction. Besides its role in the DNA damage response (discussed below), the JNK/SAPK pathway is also induced by growth factors such as EGF-1 (Bost *et al.*, 1999), by oncogene expression (Binétruy *et al.*, 1991), and is essential for transformation of rat embryo fibroblasts (Smeal *et al.*, 1991). As we show below, inhibition of this pathway enhances

sensitivity to DNA damaging therapies in both p53 mutant and p53 wild-type tumors, as T98G glioblastoma cells, PC-3 prostate cancer cells, and U87 glioblastoma cells which express mutant p53, and MCF7 breast cancer cells which express wild-type p53, are all sensitized to various DNA damaging treatments by expression of a dominant-negative inhibitor of the pathway. Thus it may be possible to modulate this pathway by itself or in combination with p53 gene replacement to enhance tumor cell responsiveness to DNA damaging chemotherapies.

The Mitogen Activated Protein Kinase (MAPK) pathways play roles in several cellular processes, including cellular transformation, proliferation, differentiation, and the DNA damage response. Through these pathways extracellular growth and stress stimuli transmit signals through a cascade of kinases and phosphorylation events that result in the phosphorylation and activation of transcription factors such as c-Jun (a heterodimeric component of the AP-1 complex and related transcription complexes), ATF-2 and Elk-1 (Bost *et al.* 1997; Cavigelli *et al.* 1995; Dérijard *et al.* 1994; Gupta *et al.* 1995; Hibi *et al.* 1993; Livingstone *et al.* 1995; Potapova *et al.* 1997; Smeal *et al.* 1991,1992). This phosphorylation activates the transcriptional transactivation properties of AP-1 and related factors and leads to the subsequent induction of specific response genes. The cascade of events begins with the activation of the Mitogen Activated Protein Kinase Kinase Kinases (MAPKKK), followed by activation of the Mitogen Activated Protein Kinase Kinases (MAPKK), and finally activation of the Mitogen Activated Protein Kinases (MAPK), of which the Jun Kinase family of enzymes (including JNK 1,2,3) is one example.

### 3.1 *In vitro* sensitization to chemotherapeutic drugs through inhibition of the JNK/SAPK pathway.

T98G glioblastoma cells activate the JNK/SAPK pathway in response to treatment with the chemotherapeutic agent, cisplatin (Potapova *et al.*, 1997), which forms bifunctional DNA cross links between adjacent guanines or adenine-guanine dinucleotides. This is consistent with numerous other reports in which activation of the JNK/SAPK pathway has been observed in response to genotoxic DNA treatments, including UV irradiation (Dérijard *et al.*, 1994, Adler *et al.*, 1995a, 1995b, 1996), ionizing radiation (Kharbanda *et al.*, 1995), the mutagens methylmethane sulfate (MMS), N-nitro-N'-nitroso-guanidine (MNNG) and numerous genotoxic chemotherapeutic agents such as Ara-C (1-β-D-Arabinofuranosylcytosine) (van Dam *et al.*, 1995; Kharbanda *et al.*, 1995). For several of these agents such as UV-irradiation, the activation of the JNK/SAPK pathway is directly proportional to the number of DNA damaging events (Adler *et al.*, 1995a). Activation is often rapid, detectable within a few minutes. These characteristics have given rise to the hypothesis that the role of the JNK/SAPK pathway may be to mediate DNA repair (Potapova *et al.*, 1997).

To evaluate the role of JNK/SAPK activation in the cellular DNA damage response we selected clones of T98G cells modified to express a non-phosphorylatable mutant of c-Jun (T98G mJun), in which serines 63 and 73, the targets of Jun Kinase-mediated phosphorylation, have been replaced by alanines (Smeal *et al.*, 1991, 1992). These cells are therefore suppressed in JNK-mediated functions. We found that unlike control vector-modified cells (T98GLHCX) or wild-type c-Jun-modified cells (T98GcJun), both

of which are highly resistant to cisplatin, the modified clones expressing mJun (T98GdnJun) showed a significant loss of viability following treatment with cisplatin (Figure 4). Furthermore, the increase in cisplatin sensitivity correlated with the level of expression of mJun in several different clones (Figure 5). We observed a similar increase in sensitivity to cisplatin in MCF7 breast cancer cells, in PC-3 prostate cancer cells, and in U87 glioblastoma cells that were modified with the non-phosphorylatable mJun (not shown). We also observed enhanced sensitivity to cisplatin in cells modified with the TAM67 mutant of c-Jun (not shown). Tam67 has a truncated N-terminal domain and is known to be a dominant negative inhibitor of c-Jun phosphorylation (Grant *et al.*, 1996). However, we did not observe in mJun modified T98G cells nor in mJun modified PC-3 cells an increase in sensitivity to the anti-mitotic agent, taxotere™ (kindly provided by Dr. Pierre Potier, Centre Nationale de la Recherche Scientifique, Paris), whose primary target is the mitotic spindle rather than DNA (Figure 6). Taken together these results argue that the JNK/SAPK pathway plays a role in resistance to DNA damaging agents but not to agents that do not damage DNA, and that inhibition of this pathway could be a means to reverse resistance to DNA damaging therapies used in cancer treatment.

### 3.1.1 Inhibition of DNA repair by inhibition of the JNK/SAPK pathway.

T98G clones modified to express mutant Jun are compromised in repair of cisplatin-DNA adducts (Potapova *et al.*, 1997), an observation that further supports the rationale for enhancing sensitivity to DNA damage through inhibition of the JNK/SAPK pathway. DNA repair is known to play a role in acquired resistance to DNA damaging chemotherapies (Barret and Hill, 1998; Crul *et al.*, 1997; Reed, 1998; Fink, Aebi and Howell, 1998; Saves and Masson, 1998; Scanlon, 1989). Furthermore, as summarized in Table I, a number of the genes involved in DNA synthesis and repair are potentially regulated by the AP-1 transcription factor and related transcription factors targeted by the JNK/SAPK pathway (i.e., c-Jun and ATF2, components of AP-1 and c-Jun-ATF2 heterodimeric transcription activating complexes, respectively). Furthermore, down regulation of AP-1 by treatment of cells with a c-fos antisense ribozyme, has previously been shown to correlate with down regulation of expression of certain of these enzymes (thymidylate synthetase, DNA polymerase  $\beta$ ) and enhanced sensitivity to cisplatin (Scanlon *et al.*, 1991).

We analyzed DNA repair using a PCR-based assay developed by Jennerwein and Eastman (1991) based on their observations that DNA-cisplatin adducts block the progression of the Taq polymerase and lead to a decrease the yield of PCR product obtained from any given PCR amplicon in proportion to the extent of platination. The authors demonstrated that the relationship between the relative PCR signal strength (P) for a given amplicon from damaged versus undamaged templates, and overall platination level fits a Poisson distribution predicted from a random platination, so that  $P=e^{-n}$ , where n=adducts per amplicon-sized fragment.

We have used primers described by Oshita and Saijo (1994) to amplify a 2.7 Kb fragment of the human hypoxanthine phosphoribosyl transferase (HPRT) gene, a fragment large enough to sustain readily detectable levels of damage following cisplatin treatment of cells. As an internal control for the efficiency of the PCR reaction, we used a nested 5' primer which amplified a 150 base fragment of the same gene. At levels of cisplatin used to treat cells, damage to the smaller fragment was undetectable. PCR

reactions were performed under quantitative conditions such that the extent of reaction remained directly proportional to amount of template. Figure 7 shows an example of PCR amplification of the 2.7 Kb fragment and the 150 base fragment from DNA prepared from T98G glioblastoma cells treated with 0, 100, and 200  $\mu\text{M}$  cisplatin for 1 hour. Quantitation of band intensities was accomplished using Kodak digital camera and analysis software, and relative band intensity measurements were then used to calculate adducts per Kb based on the Poisson relationship described above.

Table 2 summarizes the cisplatin adducts per Kb observed on DNA from T98G glioblastoma cells treated for 1 hour with 200  $\mu\text{M}$  cisplatin and then harvested either immediately or after a 6 hour recovery period. As shown in the table, cisplatin adducts occur at greater frequency in DNA from T98G mutant Jun expressing cells than in DNA from parental T98G cells. Furthermore, parental T98G cells repair more than half of the adducts during the 6 hour recovery period, whereas little repair occurs in T98G mJun cells during that period of time. Thus the increase in cisplatin sensitivity observed in T98G mJun cells can be accounted for at least in part by a defect in their ability to repair damaged DNA.

### 3.2 Mechanism of Action of JNK/SAPK in DNA Repair.

How might the activation of JNK by genotoxic stress affect DNA repair? The answer to this question is not known in any detail, but a number of observations point to several testable hypotheses. It was noted that the promoters of certain genes known to be involved in carrying out cisplatin-DNA adduct repair contain AP-1-like or ATF2/CREB regulatory elements (section 3.1.1). The repair of DNA-cisplatin adducts is believed to require the nucleotide-excision repair process (Reed, 1998). In addition, a number of enzymes utilized for DNA synthesis are reported to be involved (reviewed in Zamble and Lippard, 1995). These included DNA polymerase  $\beta$ , topoisomerase I, topoisomerase II, uracyl glycosylase, PCNA, metallothionine and others (Table 1, and references therein). In each case the promoter regions contains one or more AP-1 or ATF2/CREB regulatory sequences. In several cases such as DNA polymerase beta, genotoxic stress in the form of UV-irradiation is known to induce the gene and that the ATF2/CREB sites are required for this event (Table 1 and references therein). Moreover, the N-terminal phosphorylation of c-Jun and ATF2 by the action of Jun Kinase leads to increased DNA binding and transactivation potential of heterodimeric complex formed by phosphorylated c-Jun and ATF2. Indeed, the c-Jun promoter itself is one of the better studied example of a gene that is up-regulated upon binding of the c-Jun-ATF2 heterodimer (van Dam *et al.*, 1995; Wilhelm *et al.*, 1995). N-terminal phosphorylation of both c-Jun and ATF2 is required for the activation of the c-jun gene (van Dam *et al.*, 1995; Wilhelm *et al.*, 1995). Other examples of gene that are up-regulated upon formation of c-Jun-ATF2 heterodimers include the ELAN promoter (De Luca, *et al.*, 1994) and the TNF-alpha promoter (Newell *et al.*, 1994). Thus, there is circumstantial evidence supporting the hypothesis that activation of the Jun Kinase pathway by genotoxic stress leading to the phosphorylation of both ATF2 and c-Jun and thereby causing preferential formation of ATF2-c-Jun heterodimers. These complexes preferentially bind promoters containing octameric ATF2/CREB regulatory elements. This hypothesis predicts that several of the genes known to be involved in cisplatin-DNA adduct repair may be coordinately upregulated upon activation of the JNK pathway

following damage to DNA by cisplatin. If verified, such an explanation suggests that the JNK pathway is a potentially useful target for intervention and that agents that inhibit JNK activity or formation may be useful in achieving enhanced sensitivity of tumor cells to cisplatin.

### 3.3 JNK/SAPK pathway with antisense approaches.

The above observations argue that targeting the JNK/SAPK pathway could have potential as a sensitizer to a variety of DNA damaging chemotherapies, a possibility that we have investigated directly using antisense oligonucleotides to either JNK 1 or 2 family of JNK isoforms.

Antisense mechanisms result most likely from oligonucleotide-target mRNA hybrid formation in the nucleus which stimulates the cleavage of the mRNA at one or more sites near the terminus of the hybrid complex by ribonuclease H (Crooke, 1992, 1998; Dean *et al.*, 1996), as well as from cytoplasmic complexes which may lead to translation arrest (Crooke, 1992, 1998; Dean *et al.*, 1996). Because steady state mRNA levels do not always predict steady state gene product levels, we monitor the effects antisense by the fractional reduction of the gene product. An enzymatic assay that discriminates among the various isoforms of Jun Kinase can be used (Hibi *et al.*, 1993), as well as Western analysis or PAGE analysis following immunoprecipitation.

The appropriate oligonucleotide controls for antisense efficacy have been described in detail (Stein and Kreig, 1994). and include a sense sequence, scrambled sequence or random control oligonucleotides, and antisense sequences bearing one or a small number of mismatched bases, i.e. mismatched with respect to the complementary target sequence.

For our studies we have used antisense oligonucleotides complementary to the JNK1 or JNK 2 families of JNK isoforms by selecting target sequences common to the major isoforms of human JNK1 and JNK2. Phosphorothioate backbone chemistry has been used as this formulation is nuclease resistant, readily available and a common element of second generation compounds (Crooke, 1992, 1998; Dean *et al.*, 1996; McKay *et al.*, 1999).

In collaboration with ISIS Pharmaceuticals, Inc. (Carlsbad, CA) we have identified effective antisense oligonucleotides capable of entering and inhibiting specifically JNK1 or JNK2 mRNA expression in A549 lung cancer cells (Bost *et al.*, 1997, 1999). As an example of a screening for JNK1 and JNK2, Figure 8 is included. As shown, most candidate oligonucleotides had only a small effect on the steady state level of JNK1 or JNK2 mRNA (Figure 8). However, their degree of activity greatly varied depending on the targeted region (Figure 8). Among the most potent oligonucleotides of the array complementary to JNK1 is ISIS 12539 (JNK1ASISIS12539) (5'-CTCTCTGTAGGCCCGCTTGG-3') located in the 3' end of the coding region. Treatment with this oligonucleotide leads to a reduction of steady state mRNA level by 95% (Figure 8A) as observed 24 hours after a 4 hour exposure of the cells to 0.4  $\mu$ M antisense oligonucleotides. ISIS 12560 (JNK2ASISIS12560) (5'-

GTCCGGGCCAGGCCAAAGTC-3'), located in the 5' end of the coding region of JNK2 genes, was the most efficient oligonucleotide in reducing JNK2 steady state mRNA levels. Lipofection with this oligonucleotide lead to a decrease in the steady-state JNK2 message level by 92% compared to the control JNK2 steady state mRNA level. The oligonucleotides targeted to the regions flanking either side of the sequences for JNK1ASISIS12539 and JNK2ASISIS12560 also inhibited JNK1 and JNK2 steady state mRNA but in a manner that decreased with increasing distance from the optimum sequence (Figure 8A and B) suggesting that discrete regions of the target mRNA are accessible and sensitive to the antisense-mediated elimination of steady-state mRNA as previously described (Crooke, 1992, 1998).

Cross inhibition tests demonstrated isoform class specificity. As shown in Figure 9, JNK1ASISIS12539 eliminates JNK1 mRNA and protein but does not affect JNK2 mRNA and protein and, conversely, JNK2ASISIS12560 has no effect on JNK1 mRNA and protein but abolishes JNK2 mRNA and protein. In the northern analysis we describe an example where two other antisense oligonucleotides from the initial gene screening are less efficient in reducing mRNA steady-state levels of their respective target gene (Figure 9). Similarly, western analysis shows that lipofections with the antisense oligonucleotides leads to complete elimination of their respective target steady state protein levels, whereas the scrambled sequence versions of the candidate oligonucleotides, JNK1Scr or JNK2Scr have no effect (Figure 10). Thus effective and specific reagents can be obtained.

These reagents have been used to examine the growth promoting roles of the Jun Kinase pathway in human T98G glioblastoma cells (Potapova *et al.*, 1998), human A549 NSCLC cells (Bost *et al.*, 1997, 1999), and human PC3 prostate carcinoma cells (Yang *et al.*, 1998) and shown to specifically inhibit growth and, in the case of A549 cells, anchorage independent growth. Moreover, these reagents have been used in systemic treatment of established PC3 xenografts and shown to block growth and promote regression of the established tumors in high frequency (Bost *et al.*, 1998). In this case, growth inhibition by antisense treatment of 78% was superior to that of cisplatin treatment alone (47%), however the effects of combined antisense JNK-cisplatin of 89% inhibition, was greater than either alone suggesting that, indeed, it may be possible to sensitize solid tumors to cisplatin by elimination of Jun Kinase. It will be of interest, therefore, to determine whether JNK is involved in a general mechanism utilized in other tumor cell lines and/or mediates DNA damage repair of other DNA-damaging agents.

#### 4. Conclusions

These results have clinical implications with regard to the application of therapies designed to alleviate drug resistance. As tumors progress, particularly if they have been exposed to DNA damaging therapies, they may upregulate their DNA repair response (see Reed, 1998 for review), which may in part involve AP-1 regulated DNA synthesis and repair genes. Elevated c-fos expression, one component of the AP-1 transcription factor, correlates with cisplatin resistance (Scanlon *et al.*, 1991; Funato *et al.*, 1992) and may directly affect the synthesis of AP-1 regulated DNA synthesis and repair genes, such as polymerase  $\beta$ , topoisomerase I and thymidylate synthetase (Scanlon and Kashini-Sabet, 1998). Loss of DNA damage-induced apoptosis through loss of wild-type p53

expression also correlates with drug resistance (O'Connor *et al.*, 1997) and represents an independent mechanism through which tumors acquire resistance to therapy. Because the success or failure of DNA repair could be critical in determining how a cancer cell responds to expression of p53, it may be necessary, in optimizing the benefits of p53-based approaches, to concurrently down-regulate the cellular stress and DNA damage response pathways such as the Jun Kinase pathway. Combination approaches targeting independently these two cellular responses to DNA damage can be foreseen today, and may provide an optimal strategy for reversing or alleviating drug resistance in advanced cancers.

## References

- Badie, B., Kramar, M. H., Lau, R., Boothman, D. A., Economou, J. S., Black, K. L., 1998, Adenovirus-mediated p53 gene delivery potentiates the radiation-induced growth inhibition of experimental brain tumors, *J. Neurooncol.* **37**:217-22.
- Bakalkin, G., Selivanova, G., Yakovleva, T., Kiseleva, E., Kashuba, E., Magnusson, K. P., Szekely, L., Klein, G., Terenus, L., and Wiman, K. G., 1995, p53 binds single stranded DNA ends through the C-terminal domain and internal DNA segments via the middle domain, *Nucl. Acids Res.* **23**:362-269.
- Barret, J. M., Hill, B. T., 1998, DNA repair mechanisms associated with cellular resistance to antitumor drugs: potential novel targets, *Anticancer Drugs* **9**:105-23.
- Binetruy, B., Smeal, T., and Karin, M., 1991, Ha-ras augments c-Jun activity and stimulates phosphorylation of its activation domain, *Nature* **351**:122-127.
- Cavigelli, M., Dolfi, F., Claret, F. X., Karin, M., 1995, Induction of c-fos expression through JNK-mediated TCF/Elk-1 phosphorylation, *EMBO J.* **14**:5957-64.
- Chelliah, J., Jarvis, W. D., 1996, Effect of 1-beta-D-arabinofuranosylcytosine on apoptosis and differentiation in human monocytic leukemia cells (U937) expressing a c-Jun dominant-negative mutant protein (TAM67), *Cell Growth Differ.* **7**:603-13.
- Clarke, A. R., Purdie, C. A., Harrison, D. J., *et al.*, 1993, Thymocyte apoptosis induced by p53-dependent and independent pathways, *Nature* **362**:849-852.
- Crooke, S. T., 1992, Therapeutic applications of oligonucleotides, *Annu. Rev. Pharmacol. Toxicol.* **32**:329-76.
- Crooke, S. T., 1998, Molecular mechanisms of antisense drugs: RNase H, *Antisense Nucleic Acid Drug Dev.* **8**:133-4.
- Crul, M., Schellens, J. H., Beijnen, J. H., Maliepaard, M., 1997, Cisplatin resistance and DNA repair, *Cancer Treat Rev.* **23**:341-66.
- Dean, N. M., McKay, R., Miraglia, L., Geiger, T., Muller, M., Fabbro, D., Bennett, C. F., 1996, Antisense oligonucleotides as inhibitors of signal transduction: development from research tools to therapeutic agents, *Biochem. Soc. Trans.* **24**:623-9.
- De Luca, L. G., Johnson, D. R., Whitley, M. Z., Collins, T., Pober, J. S., 1994, cAMP and tumor necrosis factor competitively regulated transcriptional activation through a nuclear factor binding to the cAMP-responsive element/activating transcription factor element of the endothelial leukocyte adhesion molecule-1 (E-selectin) promoter, *J. Biol. Chem.* **269**:19193-6.

- Derijard, B., Hibi, M., Wu, I. H., Barrett, T., Su, B., Deng, T., Karin, M., Davis, R. J., 1994, JNK1: a protein kinase stimulated by UV light and Ha-Ras that binds and phosphorylates the c-Jun activation domain, *Cell* **76**:1025-37.
- Dorigo, O., Turla, S. T., Lebedeva, S., and Gjerset, R. A., 1998, Sensitization of rat glioblastoma multiforme to cisplatin *in vivo* following restoration of wild-type p53 function, *J. Neurosurg.* **88**:535-540.
- Fink, D., Aebi, S., Howell, S. B., 1998, The role of DNA mismatch repair in drug resistance, *Clin. Cancer Res.* **4**:1-6.
- Fujiwara, T., Grimm, E. A., Mukhopadhyay, T., Zhang, W. W., Owen-Schaub, L. B., Roth, J. A., 1994, Induction of chemosensitivity in human lung cancer cells *in vivo* by adenovirus-mediated transfer of the wild-type p53 gene, *Cancer Res.* **54**:2287-91.
- Funato, T., Yoshida, E., Jiao, L., Tone, T., Kashani-Sabet, M., Scanlon, K. J., 1992, The utility of an anti-fos ribozyme in reversing cisplatin resistance in human carcinomas, *Adv. Enzyme Regul.* **32**:195-209.
- Gjerset, R. A., Turla, S. T., Sobol, R. E., Scalise, J. J., Mercola, D., Collins, H., Hopkins, P. J., 1995, Use of wild-type p53 to achieve complete treatment sensitization of tumor cells expressing endogenous mutant p53. *Molec. Carcinog.* **14**:275-285.
- Gjerset, R. A., Dorigo, O., Maung, V., *et al.*, 1997, Tumor regression *in vivo* following p53 combination therapy, *Cancer Gene Therapy* **4**:O-2.
- Grant, S., Fremerman, A. J., Birrer, M. J., Martin, H. A., Turner, A. J., Szabo, E., Reed, E., 1998, Platinum-DNA adduct, nucleotide excision repair and platinum based anti-cancer chemotherapy, *Cancer Treat Rev.* **24**:331-44.
- Gupta, S., Campbell, D., Derijard, B., Davis, R. J., 1995, Transcription factor ATF2 regulation by the JNK signal transduction pathway, *Science* **267**:389-93.
- Hibi, M., Lin, A., Smeal, T., Minden, A., Karin, M., 1993, Identification of an oncoprotein- and UV-responsive protein kinase that binds and potentiates the c-Jun activation domain, *Genes Dev.* **7**:2135-48.
- Jennerwein, M.M. and Eastman, A., 1991, A polymerase chain reaction-based method to detect cisplatin adducts in specific genes, *Nucleic Acids Res.* **19**:6209-6214.
- Lee, S., Elenbas, B., Levine, A., and Griffith, J., 1995, p53 and its 14kDa C-terminal domain recognize primary DNA damage in the form of insertion/deletion mismatches, *Cell* **81**:1013-1021.
- Levine, A. J., 1993, The tumor suppressor genes, *Annu. Rev. Biochem.* **62**:623-651.

- Levine, A. J., 1997, p53, the cellular gatekeeper for growth and division, *Cell* **88**:323-331.
- Livingstone, C., Patel, G., Jones, N., 1995, ATF-2 contains a phosphorylation-dependent transcriptional activation domain, *EMBO J.* **14**:1785-97.
- Lotem, J. and Sachs, L., 1993, Hematopoietic cells from mice deficient in wild-type p53 are more resistant to induction of apoptosis by some agents, *Blood* **82**:1092-1096.
- Lowe, S. W., Ruley, H. E., Jacks, T., Housman, D. E., 1993, p53-mediated apoptosis modulates the cytotoxicity of anti-cancer agents, *Cell* **74**:957-967.
- Lowe, S. W., Bodis, S., McClatchy A., Remington, L., Ruley, H. E., Fisher, D. E., Housman, D. E., Jacks, T., 1994, p53 status and the efficacy of cancer therapy *in vivo*, *Science* **266**:807-10.
- McKay, R. A., Miraglia, L. J., Cummins, L. L., Owens, S. R., Sasmor, H., Dean, N. M., Characterization of a potent and specific class of antisense oligonucleotide inhibitor of human protein kinase C-alpha expression, *J. Biol. Chem.* **274**:1715-22.
- Miyake, H., Hara, I., Gohji, K., Yamanaka, K., Arakawa, S., Kamidono, S., 1998, Enhancement of chemosensitivity in human bladder cancer cells by adenoviral-mediated p53 gene transfer, *Anticancer Res.* **18**:3087-92.
- Newell, C. L., Deisseroth, A. B., Lopez-Berestein, G., 1994, Interaction of nuclear proteins with an AP-1/CRE-like promoter sequence in the human TNF-alpha gene, *J. Leukocyte Biol.* **56**:27-35.
- Nguyen, D. M., Spitz, F. R., Yen, N., Cristiano, R. J., Roth, J. A., 1996, Gene therapy for lung cancer: enhancement of tumor suppression by a combination of sequential systemic cisplatin and adenovirus-mediated p53 gene transfer, *J. Thorac. Cardiovasc. Surg.* **112**:1372-6, discussion 1376-7.
- Nielsen, L. L., Lipari, P., Dell, J., Gurnani, M., Hajian, G., 1998, Adenovirus-mediated p53 gene therapy and paclitaxel have synergistic efficacy in models of human head and neck, ovarian, prostate, and breast cancer, *Clin. Cancer Res.* **4**:835-46.
- O'Connor, P. M., Jackman, J., Bae, I., Myers, T. G., Fan, S., Mutoh, M., Scuderio, D. A., Monks, A., Sausville, E. A., Weinstein, J. N., Friend, S., Fornace, A. J., Jr., Kohn, K. W., 1997, Characterization of the p53 tumor suppressor pathway in cell lines of the National Cancer Institute anticancer drug screen and correlations with the growth-inhibitory potency of 123 anticancer agents, *Cancer Res.*, **57**:4285-300.
- Oshita, F., and Saijo, N., 1994, Rapid polymerase chain reaction assay to detect variation in the extent of gene-specific damage between cisplatin- or VP-16-resistant and sensitive lung cancer cell lines, *Jpn J. Cancer Res.* **85**:669-73.

Potapova, O., Haghighi, A., Bost, F., Liu, C., Birrer, M. J., Gjerset, R., and Mercola, D., 1997, The JNK/stress-activated protein kinase pathway functions to regulate DNA repair and inhibition of the pathway sensitizes tumor cells to cisplatin, *J. Biol. Chem.* **272**:14041-14044.

Potapova, O., Bost, F., Dean, N., Mercola, D., 1998, Inhibition of the JNK pathway blocks cell cycle progression in human tumor cells, *Proc. AACR*, 89th Annual Meeting, abstract #1720, p. 251.

Reed, E., 1998, Platinum-DNA adduct, nucleotide excision repair and platinum based anti-cancer chemotherapy, *Cancer Treatment Reviews* **24**: 331-344.

Roth, J. A., Swisher, S. G., Merritt, J. A., Lawrence, D. D., Kemp, B. L., Carrasco, C. H., El-Naggar, A. K., Fossella, F. V., Glisson, B. S., Hong, W. K., Khurl, F. R., Kurie, J. M., Nesbitt, J.C., Pisters, K., Putnam, J. B., Schrupp, D. S., Shin, D. M., Walsh, G. L., 1998, Gene therapy for non-small cell lung cancer: a preliminary report of a phase I trial of adenoviral p53 gene replacement, *Semin. Oncol.* **25**:33-7.

Saves, I., Masson, J.M., 1998, Mechanisms of resistance to xenobiotics in human therapy, *Cell Mol Life Sci.* **54**:405-26.

Scanlon, K. J., Kashani-Sabet, M., 1988, Elevated expression of thymidylate synthase cycle genes in cisplatin-resistant human ovarian carcinoma A2780 cells, *Proc. Natl. Acad. Sci. USA.* **85**:650-3.

Scanlon, K. J., Kashani-Sabet, M., Miyachi, H., Sowers, L. C., Rossi, J., 1989, Molecular basis of cisplatin resistance in human carcinomas: model systems and patients, *Anticancer Res.* **9**:1301-12.

Scanlon, K. J., Jiao, L., Funato, T., Wang, W., Tone, T., Rossi, J. J., Kashani-Sabet, M., 1991, Ribozyme-mediated cleavage of c-fos mRNA reduces gene expression of DNA synthesis enzymes and metallothionein, *Proc. Natl. Acad. Sci. USA.* **88**:10591-5.

Smeal, T., Binetruy, B., Mercola, D., Birrer, M., and Karin, M., 1991, Oncogenic and transcriptional cooperation with Ha-ras requires phosphorylation of c-Jun on serines 63 and 73, *Nature* **354**:494-496.

Smeal, T., Binetruy, B., Mercola, D., Grover-Bardwick, A., Heidecker, G., Rapp, U. R., Karin, M., 1992, Oncoprotein-mediated signalling cascade stimulates c-Jun activity by phosphorylation of serines 63 and 73, *Mol. Cell. Biol.* **12**:3507-13.

Stark, G.R., 1993, Regulation and mechanisms of mammalian gene amplification, *Adv. Cancer Res.* **61**:87-113.

Stein, C. A. and Kreig, A. M., 1994, Problems in interpretation of data derived from *in vitro* and *in vivo* use of antisense oligodeoxynucleotides, *Antisense Res. Dev.* **4**:67-9.

Van Dam, H., Wilhelm, D., Herr, I., Steffen, A., Herrlich, P., Angel, P., 1995, ATF-2 is preferentially activated by stress-activated protein kinases to mediate c-jun induction in response to genotoxic agents, *EMBO J.* **14**:1798-811.

Wilhelm, D., van Dam, H., Herr, I., Baumann, B., Herrlich, P., Angel, P., 1995, Both ATF-2 and c-Jun are phosphorylated by stress-activated protein kinases in response to UV irradiation, *Immunobiology* **193**:143-8.

## Figure Legends

Figure 1. Viability assay showing that Ad-p53 suppresses growth and enhances sensitivity to DNA damaging chemotherapeutic drugs in p53-mutant-expressing cells (DLD-1 colon cancer, T47D breast cancer, PC-3 prostate cancer, and T98G glioblastoma). Infection efficiencies were 60-70% and drug treatments 1 day post-infection were as follows: 5-fluorouracil (5FU) 10  $\mu$ M 1 hour; doxorubicin (dox) 3.7  $\mu$ M 1 hour; cisplatin (CDDP) 30  $\mu$ M 1 hour for PC-3 and 20  $\mu$ M 1 hour for T98G. Viability was assayed 6 days post drug treatment in all cases except PC-3 which was 4 days post drug treatment, and expressed as a percent of control cells treated with Ad- $\beta$ gal.

Figure 2. Viability assay showing that Ad-p53 neither suppresses growth nor enhances sensitivity to DNA damaging chemotherapeutic drugs in wild-type p53-expressing cells (LS174T colon cancer cells and MCF7 breast cancer cells). Infection efficiencies were 60-70%, and drug treatments 1 day post-infection were 30  $\mu$ M cisplatin (CDDP) 1 hour for LS174T and 20  $\mu$ M 1 hour for MCF7. Viability was assayed 6 days post drug treatment.

Figure 3. Suppression of PC-3 prostate tumor growth in nude mice by Ad-p53 plus cisplatin. Vector ( $10^8$  pfu per tumor) was administered on days 1,3,5,8,10, and cisplatin was administered on days 1,8.

Figure 4. Viability assay showing that mutant Jun sensitizes T98G cells to cisplatin. Viability was assayed 5 days following a 1 hour treatment with cisplatin. Empty vector control cells (●); wild-type c-Jun-expressing cells (■); and mutant Jun-expressing cells (◆).

Figure 5. Dose response curve of the  $IC_{50}$  (cisplatin) versus total immunoreactive Jun (c-Jun + mutant Jun). Total immunoreactive Jun was determined by sequential immunoprecipitation of  $^{35}$ S-labeled cells using specific Jun B, JunD, followed by pan-Jun antiserum.

Figure 6. Viability assay showing that mutant Jun does not sensitize T98G cells to Taxotere<sup>TM</sup>. Viability was assayed 7 days following a 1 hour treatment with Taxotere<sup>TM</sup>.

Figure 7. PCR amplification of DNA from T98G cells that had been incubated 1 hour with 0, 100  $\mu$ M, and 200  $\mu$ M cisplatin. Products were analyzed on an agarose gel and stained with ethidium bromide, followed by quantitation of band intensities using the Electrophoresis Documentation and analysis System 120 (Kodak Digital Science<sup>TM</sup>).

Figure 8. "Messenger walk" survey for the elimination of JNK1 and JNK2 mRNA levels following treatment with phosphorothioate antisense oligonucleotides targeted to JNK1 or JNK2 mRNA. A, JNK1 mRNA steady state levels in A549 cells following treatment with 26 different phosphorothioate antisense oligonucleotides targeted to JNK1 mRNA. JNK1AS<sup>ISIS12539</sup> gave the most consistent results for the elimination of JNK1 mRNA steady state levels. B, Similar experiment to the previous one (Fig. 1A) was performed with 13 phosphorothioate antisense oligonucleotides complementary to the indicated regions of the JNK2 mRNA. JNK2AS<sup>ISIS12560</sup> yielded the most consistent results for the

elimination of JNK2 mRNA steady state levels. All oligonucleotides are arrayed relative to their complementary sequence along the JNK transcript. The asterisks indicate the oligonucleotides having a very similar nucleotide composition (2-4 bases) to the leading compound. These screenings have been repeated two times with similar results.

Figure 9. A549 cells were treated with 3 different antisense oligonucleotides complementary to JNK1 mRNA (including the active antisense oligonucleotide JNK1AS<sup>ISIS12539</sup> and 3 different antisense oligonucleotides complementary to JNK2 mRNA (including the active antisense oligonucleotide JNK2AS<sup>ISIS12560</sup>). 24 hours after a 4 hours transfection with 0.4  $\mu$ M antisense oligonucleotide, mRNA was prepared and examined by northern analysis, the same membrane was hybridized successively with JNK1 probe, JNK2 probe and the G3PDH probe.

Figure 10. A549 cells were treated with the indicated concentration of phosphorothioate 2'-O-methoxyethyl-modified antisense oligonucleotides JNK1AS<sup>ISIS15346</sup> or JNK2AS<sup>ISIS15353</sup> and 0.4  $\mu$ M of their respective control oligonucleotides JNK1Scr<sup>ISIS18076</sup> and JNK2Scr<sup>ISIS18078</sup>. Cell extracts were prepared 36 hours after the transfection and examined by western analysis using anti-JNK1 antibodies (SC-571). Protein level (below) was determined by comparison to respective protein level in untreated cells using the Electrophoresis Documentation and analysis System 120 (Kodak Digital Science <sup>TM</sup>).

TABLE 1: DNA REPAIR ASSOCIATED GENES WHICH CONTAIN POTENTIAL JNK-REGULATED SEQUENCES.<sup>1</sup>

REPAIR-ASSOCIATED GENE	ELEMENT	SEQUENCE (consensus sequence) <sup>2</sup>	POSITION <sup>3</sup>	LLG SCORE	REFERENCE FOR FUNCTION
DNA Polymerase $\beta$	AP-1/TRE	CTGACTCA (-t g a c t c a)	337	2.0	Known to be functional and TPA-activated classic TRE (1).  Known to be genotoxic-activated (1, 9).
	ATF/CREB	TTACGTAA (t t a c g t c a)	282	2.0	
DNA Polymerase $\alpha$ (26)	ATF/CREB	CACGTCA (t g a c g t c a) GGGGTCA (t g a g t c a)	-82 -149		Function of ATF/CREB (26) unknown.  AP-1 sites thought to be significant in DNA repair: DP $\alpha$ is over-expressed in cisplatin resistant cells and anti-Fos ribozyme sensitizes (27).
Topoisomerase I	AP-1	GGGGGCGG (t g a g t c a)	753	2.0	(2-3)  (2-3)  known to be functional & stress-activated (2-3).
	AP-1	TGACCCA (t g a c t c a)	217	2.0	
	ATF/CREB	TGACGTCA (t g a c g t c a)	792	2.0	
Topoisomerase II $\alpha$	ATF/CREB	TGACGCCG (t g a c g t c a)	286	2.0	(10-11); Topo II is UV-inducible and functions early in UV-induced DNA damage repair. (10) (12) (12)
Topoisomerase II $\beta$	AP-1	TGATTGG (t g a g t c a)	337	2.0	
	AP-1	TGACTCA (t g a c t c a)	3	2.0	
	AP-1	AGAGTCA (t g a g t c a)	65	1.6	
ATF-3	AP-1	TGAGTAA (t g a c g t c a)	-1600		(13) ATF-3 is stress-induced, anisomycin (JNK activator) induced, and induced by ATF-2/c-Jun coexpression suggesting a functional role for the ATF/CREB site. ATF-3/c-Jun heterodimers bind ATF/CREB sites and activate transcription (14-15) and ATF-3/c-Jun and ATF-3/JunD heterodimers have been shown to bind TTAGTTAC, a ATF/CREB sequence, which mediates EGF/ras/raf-stimulated transcription (28), however, a role in induction of DNA repair genes is not known.
	AP-1	ATAGTCA (t g a c g t c a)	-1353		
	AP-1	AGACTAA (t g a c g t c a)	-605		
	AP-1	GAGTCA (t g a c g t c a)	-380		
	ATF/CRE	TTACGTCA (t t a c g t c a)	-92		
<i>c-Jun</i>	ATF/CREB	TTACCTCA (t t a c g t c a)		2.0	(4-5); the "functional" association with DNA repair is strong induction of <i>c-Jun</i> by genotoxins known to activate JNK/SAPK
Uracil Glycosylase	AP-1	TGGGTCA (t g a g t c a)	141	2.0	not known
PCNA Proliferating Cell Nuclear Antigen	AP-1	TGACTCA (t g a c t c a)	489	2.0	DNA polymerase- $\alpha$ accessory protein function;  (7-8); Il-2, a potent JNK/SAPK activator, induces PCNA expression via ATF/CREB promoter sites which is blocked by rapamycin.
	ATF/CREB	TGAGGTCAGGG (t g a c g t c a - - -)	209	1.64	
	ATF/CREB	GTGACGTAC (-t t a c g t c a - -)	1253	1.60	

**Table I**  
Continued -

GADD153 (19) Growth Arrest and DNA-damage <sup>1</sup> Inducible Gene	ATF/CREB	ACTCCTGACCTT (t g t a c g t c a - - - -)	207	1.63	Induction requires phosphorylation-dependent event that is <i>not</i> PKA, PKC (16), or p38 (25) mediated consistent with a role for JNK/SAPK (16). Moreover GADD153 is induced by MMS (16) & cisplatin (17-18). The role of the ATF/CREB site is unknown. GADD153 is phosphorylated and activated by p38 in response to stress (25).
	AP-1	TGACTCA (t g a c t c a)	710	2.0	
XRCC1 (20) X-ray Damage Repair Cross Complementing Gene Product.	ATF/CREB	ACGTCA (a c g t c a)	1815	2.0	The site at 466 is consistent with c-Jun/ATF-3 vs. ATF-2 (TESS).  Functional roles of these ATF/CREB and AP-1 sites are not known zxxz.
	ATF/CREB	GGACGTCAA (t g a c g t c a)	1814	2.0	
	ATF/CREB	CCTGACCTCA (- - t g a c g t c a)	2029	1.64	
	ATF/CREB	GCTGACGTGACG (- - t g a c g t c a -) CCAATCA (t g t a c g t c a)	466 93	1.60 2.0	
MGMT (22) O6-Methylguanine-DNA-Methyltransferase	ATF/CREB	TGCGTCA (t g a c g t c a)	1661	2.0	MGMT is induced by genotoxic agents (21). The site at 1674 is consistent with c-Jun/ATF-3 (TESS). The functional significance of these sites is unknown.
	ATF/CREB	GTGACATCAT (- t g a c t c a -)	1195		
	AP-1	TGAGTCA (t g a g t c a)	734	2.0	
	AP-1	TACTCA (t t a c t c a)	285	1.73	
MSH2 (23)	ATF/CREB	TGGCGTCA (t g a c t c a)	108	1.62	TESS does not recognize c-Jun participation at 108 site. Role in cisplatin induced repair unknown. MSH2 has been reported to selectively bind to cisplatin-DNA adducts (
	AP-1	TGAATCA (t g a c / g t c a)	569	2.0	
	AP-1	TGATGAAA (t g a c / g t c a)	884	1.62	
Metallothionein IIA	AP-1	GAGCCGCAAGT (g a g t c a - - - - t GACTTCTAGCG g a c t c a a g t c CGGGCCGTG a - - - - - t g)	188	2.0	(6); TPA and UV-light activated

<sup>1</sup> Repair associated protein for which only partial promoter sequences are known (i.e. in Genbank) without recognizable AP-1 regulated sites include ADP ribose polymerase, *tif2/ref1*, *SSRP*, *Erc1* and thymidylate synthetase.

<sup>2</sup> AP-1 consensus: TG/TAC/GTCA; CREB/ATF-2 consensus: TG/TACGTCA.

<sup>3</sup> Positions are based on TESS numbering of promoter sequences unless preceded by (-).

**References:** 1. Srivastava *et al.* *J. Biol. Chem.*, 1995;270:16408. 2. Baumgärtner *et al.*, *Biochem. Biophys. Acta*, 1994;1218:123. 3. Heiland *et al.* *Eur. J. Biochem.* 1993;217:813. 4. Kharbanda *et al.* *Canc. Res.*, 1991;51:6636. 5. Kharbanda *et al.*, *J. Clin. Invest.*, 1990;86:1517. 6. Lee *et al.* *Nature*, 1987;325:368. 7. Feuerstein N., *et al.* *J. Biol. Chem.*, 1995;270:9454. 8. Huang D. *et al.* *Molec. Cell. Biol.*, 1994;14:4233; 9. Kedar *et al.* *PNAS USA*, 88:3729. 10. Hochhauser D. *et al.* *J. Biol. Chem.*, 1992;267:18796-5. 11. Popanda O; Thielmann HW. *Carcinogenesis*, 1992;13:2321. 12. Unpublished: Genbank Acc. #T29334. *Inst. Genomics Res.*, 1995. 13. Liang *et al.* *J. Biol. Chem.*, 1996;271:1695. 14. Hsu, J.-C. *et al.*, *Mol. Cell. Biol.*, 1992;12:4654. 15. Chu, H.-M. *et al.* *Mol. Endocrinol.* 1994;8:59. 16. Luethy, J. and Holbrook, N. *Cancer Res.* 1994;54:1902S. 17. Gately, D. *et al.* *Br. J. Cancer*, 1994;70:1102. 18. Delmastro, D. *et al.* *Canc. Chemoth. Pharmacol.*, 1997;39:245. 19. Park, J. *et al.*, *Gene*, 1992;116:259 (Acc. #S40707). 20. Lamerdin, J., *et al.*, *Genomics*, 1995;25:547 (Acc. #L34079). 21. Lefebvre, P. *et al.*, *Dna Cell Biol.*, 1993;12:233. 22. Iwakuma, T. *et al.*, *DNA Cell Biol.*, 1996;15:863. 23. Seib, T. *et al.* *Gene Bank direct submission Acc. #U232824*. 24. Leach, F. *et al.* *Cell*, 1993;75:1215. 24. Kolodner, R. *et al.* *Genomics*, 1994;24:515. 24. Mello, J. *et al.* *Chem. Biol.* 1996;3:579. 25. XiaoZhong, W. and Ron, D. *Science*, 1997;272:1347-49. 26. Pearson, B. *et al.* *Molec. Cell. Biol.*, 1991;11:2081. 27. Scanlon, K. *et al.* *PNAS USA*, 1994;91:11123. 28. Nilsson *et al.* *Cell Growth & Diff.* 1997;8:913.

**Abbreviations:** LLG, Log likelihood score which is 2 for a perfect match of the candidate response element with with the consensus sequence (TESS criteria) and all ambiguous matches yield a score of 0; AP-1, activator protein-1 complex, a Jun and a Fos family member; CREB/ATF, cAMP response element binding proteins, N-terminal phosphorylated c-Jun and N-terminal phosphorylated ATF-2 for a cAMP-independent complex which bind the CRE-like sequence TTACGTCA. XRCC., MMS, methyl methanesulfonate.

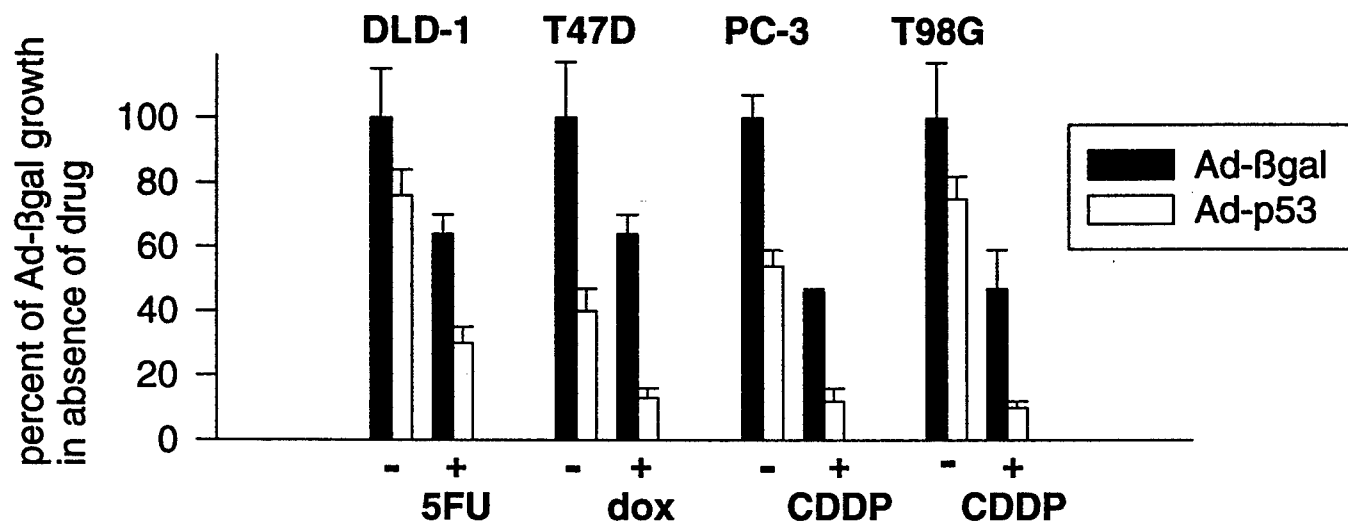
ctwps11qyqtdharpair.dh1

TABLE 2. CISPLATIN-DNA ADDUCTS PER 2.7 KBASE

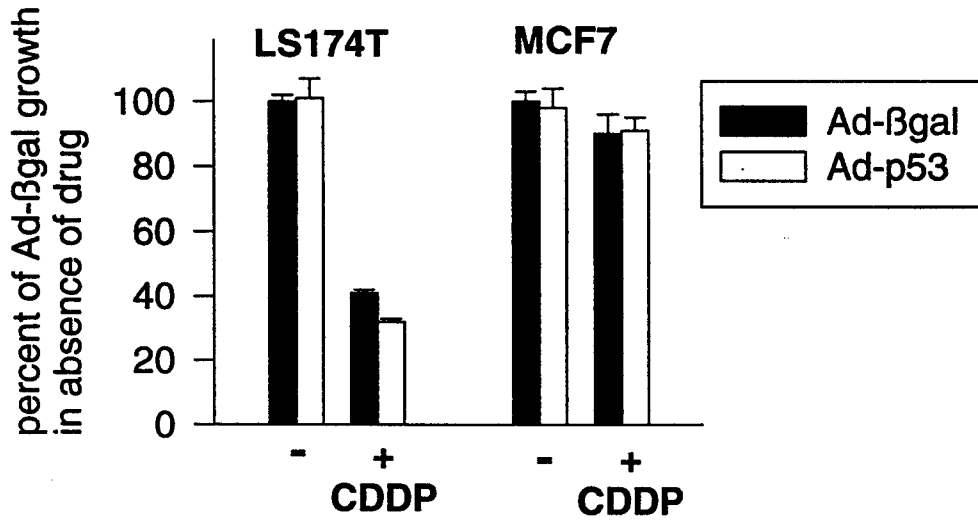
TREATMENT	T98G PARENTAL CELLS	T98G MUTANT JUN CELLS
200 $\mu$ M cisplatin 1 hour	0.48 $\pm$ 0.08	0.63 $\pm$ 0.2
200 $\mu$ M cisplatin 1 hour, 6 hour recovery	0.20 $\pm$ 0.05	0.55 $\pm$ 0.2

**ACKNOWLEDGEMENTS.** The authors would like to acknowledge financial support from the following: grants CA69546 (RAG), CA56834 (DM), CA76173 (DM) from the National Cancer Institute, grant DAMD17-96-1-6038 from the U.S. Army Breast Cancer Research Program (RAG), grant 1PF0140 from the California Cancer Research Program (RAG), grant 83401 from the California Breast Cancer Research Program (DM), and Introgen Therapeutics, Inc. (RAG). The authors would also like to thank Drs. Fred Bost and Olga Potapova for making available to us manuscripts prior to publication. We thank Deborah Wilson, Ph.D. of Introgen Therapeutics, Inc. for providing us with replication recombinant adenoviruses (Ad-p53, Ad-βgal, Ad-Luc). We also thank R. McKay, Ph.D. and N. Dean, Ph.D. of ISIS Pharmaceuticals for their support and materials for the studies reviewed here.

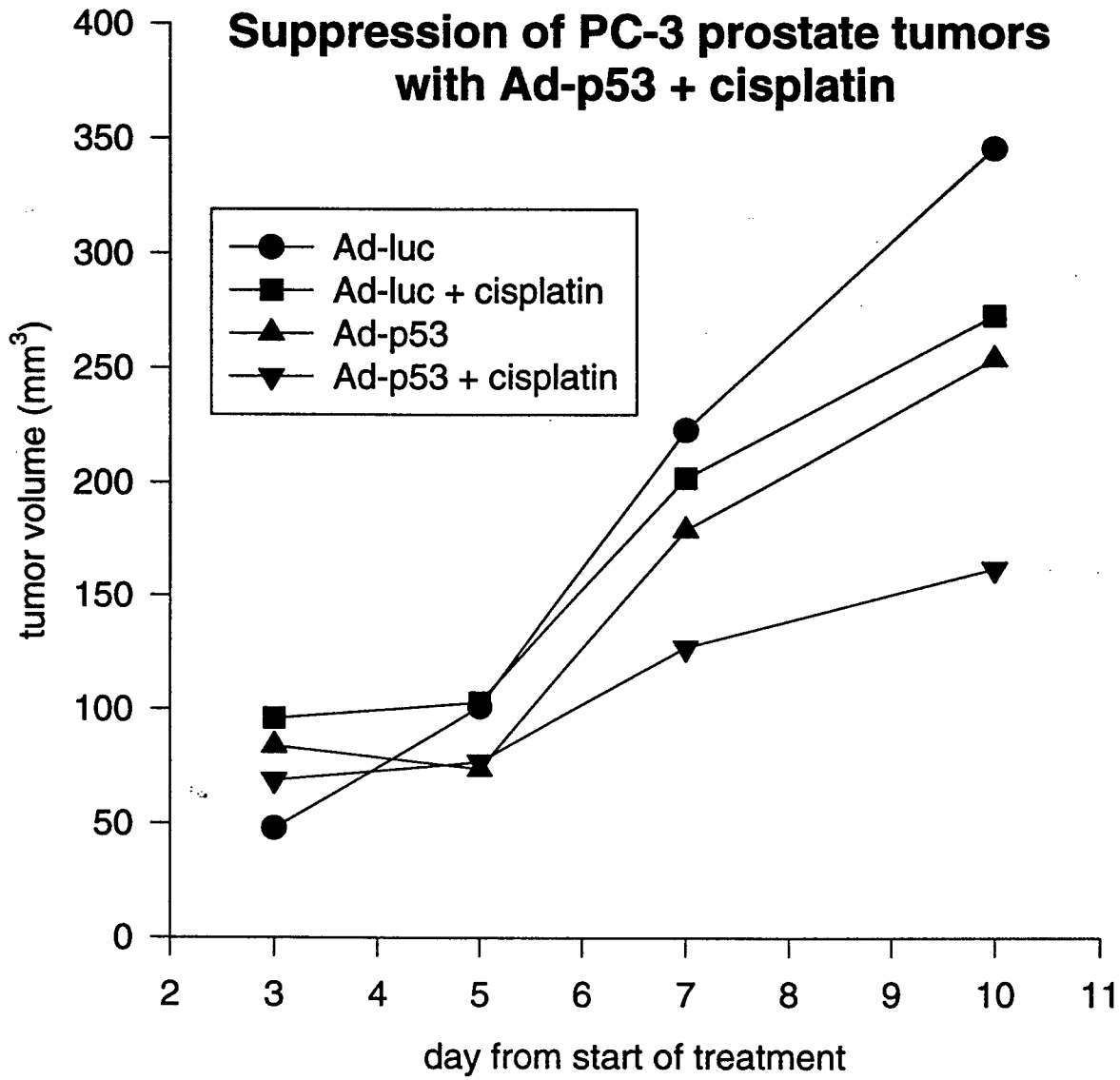
## Sensitivities of mutant p53-expressing cell lines to Ad-p53 and chemotherapeutic drugs

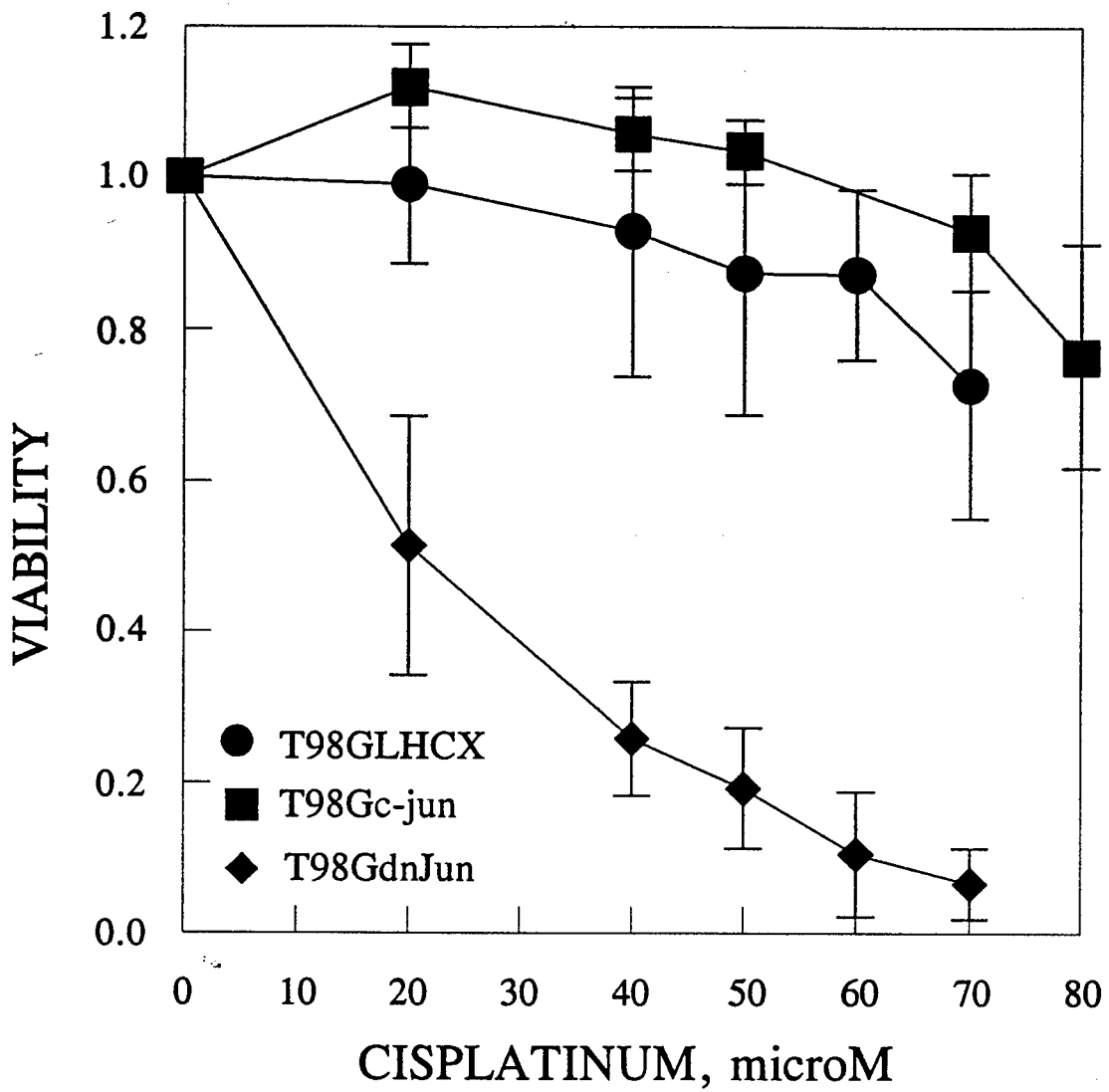


## Sensitivities of wild-type p53-expressing cell lines to Ad-p53 and chemotherapeutic drugs

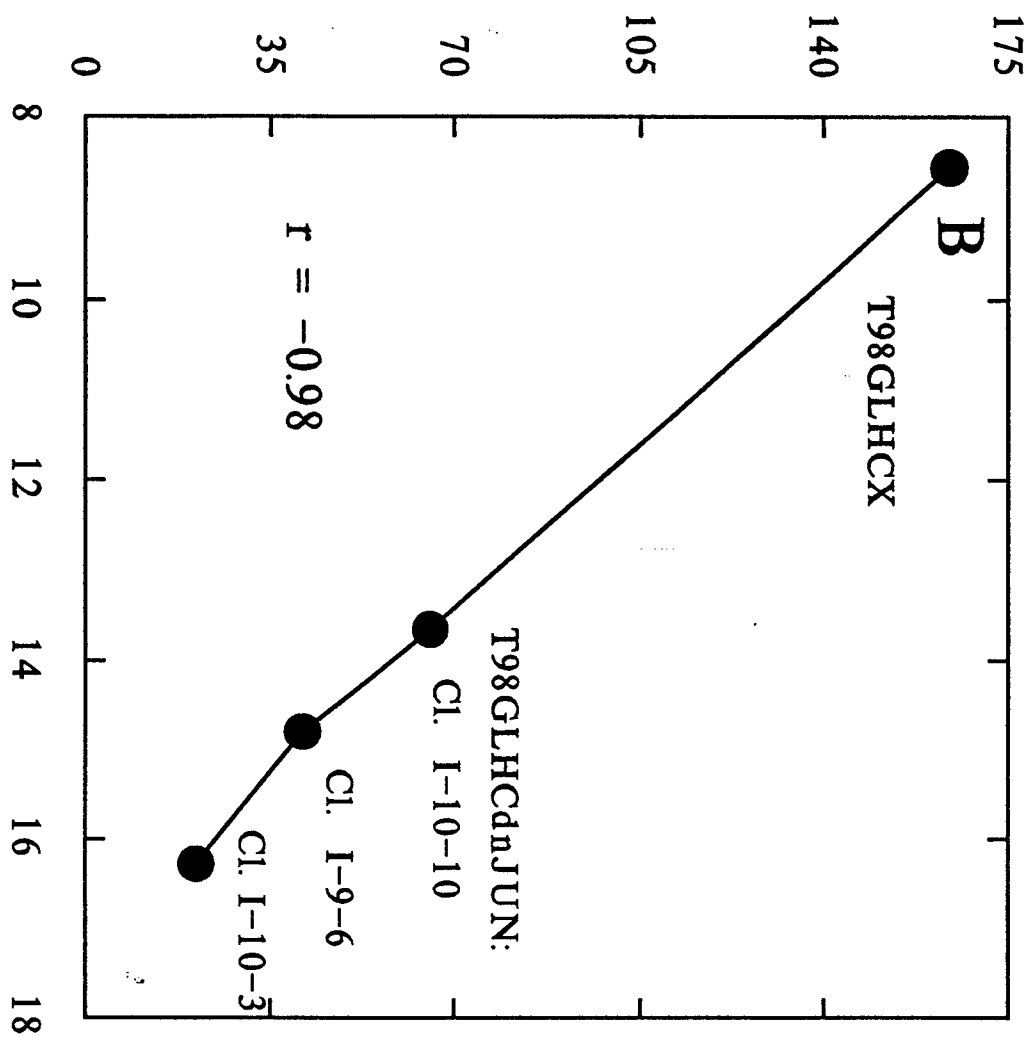


### Suppression of PC-3 prostate tumors with Ad-p53 + cisplatin





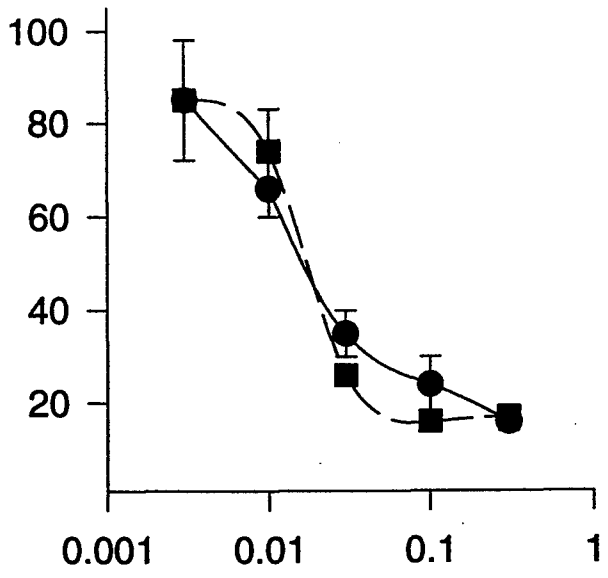
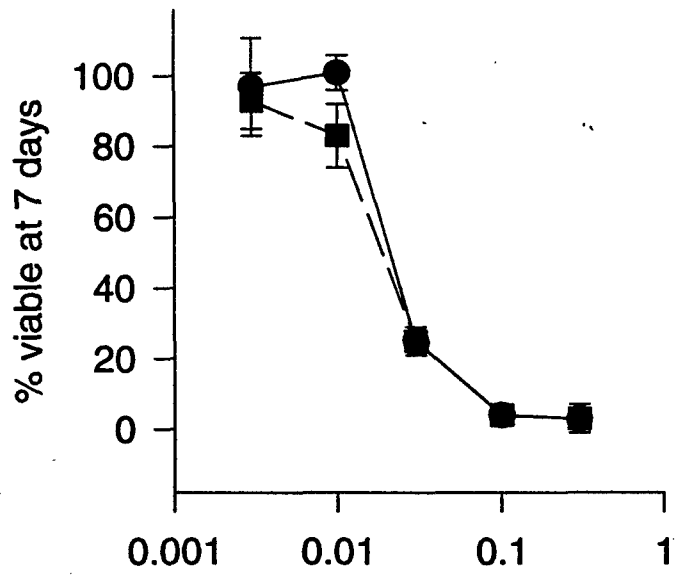
IC50 CISPLATIN (micromolar)



Expression of Total c-Jun Protein (cpm per 10<sup>6</sup> cells)

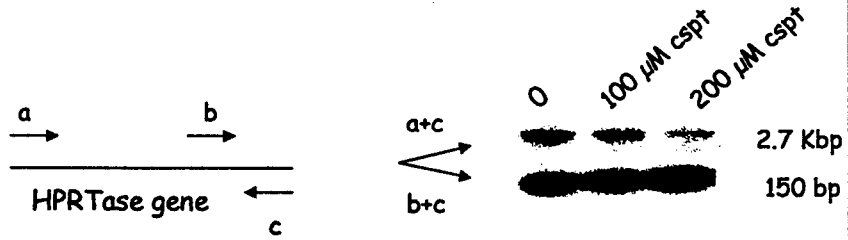
● control vector-modified T98G  
 ■ mutant Jun-modified T98G

● control vector-modified PC-3 cells  
 ■ mutant Jun-modified PC-3 cells



μM Taxotere™ (docetaxel)

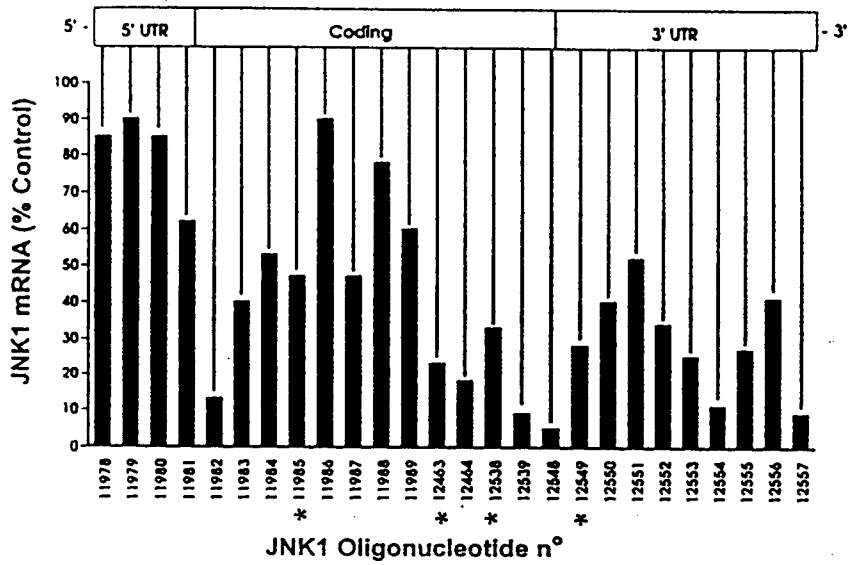
# PCR stop assay for DNA damage and repair



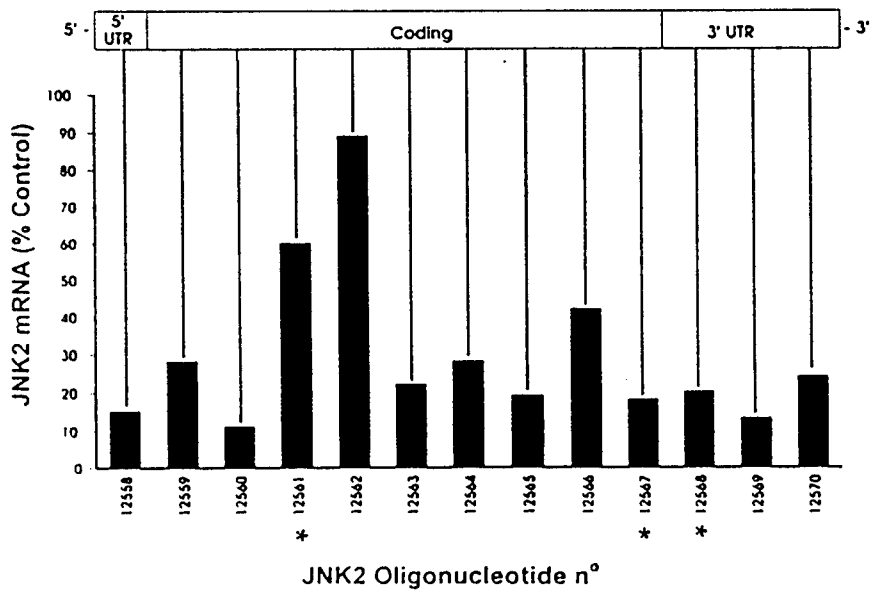
*PCR amplification of fragments of the HPRTase gene using end-labelled primers*

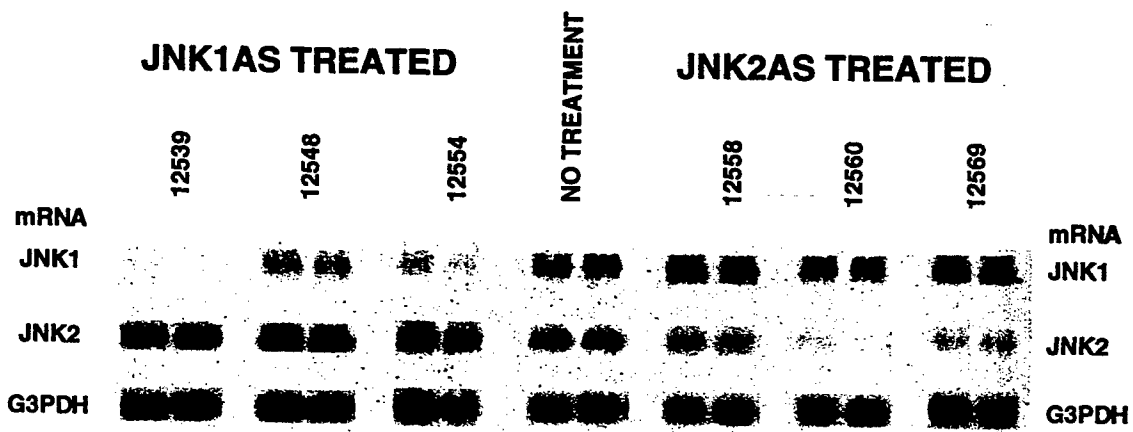
*1% agarase gel followed by quantification*

**A**



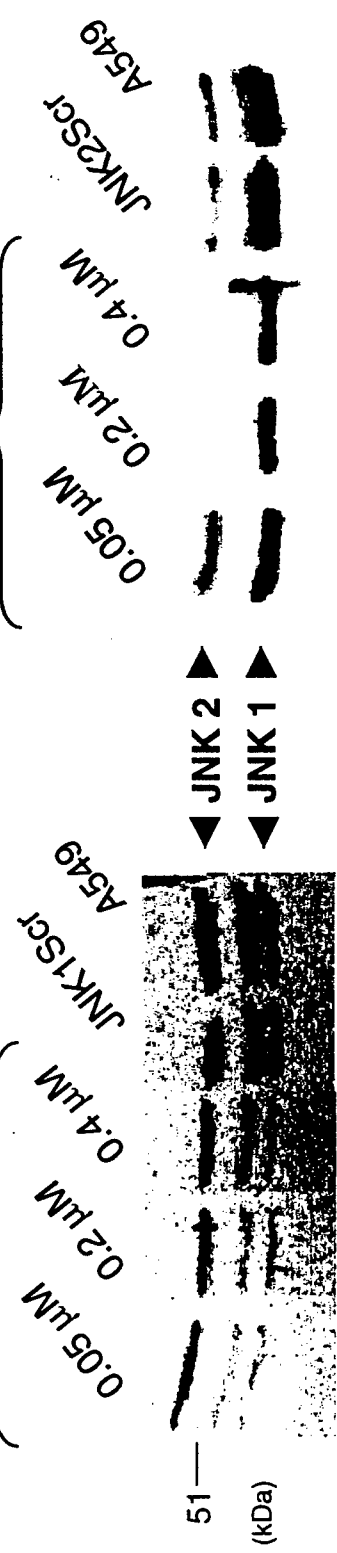
**B**





**JNK1AS**

**JNK2AS**



49

51

(kDa)

**JNK 1**

(% control) : 10

11

6.5

80

100

**JNK 2**

(% control) : 120

6

7

90

100

PREFERENTIAL PLATINATION OF AN ACTIVATED CELLULAR PROMOTER BY  
CIS-DIAMMINEDICHLOROPLATINUM †

Ali Haghighi, Svetlana Lebedeva, and Ruth A. Gjerset\*

Sidney Kimmel Cancer Center

10835 Altman Row, San Diego CA 92121

Running Title: Promoter platination by cisplatin

\*Corresponding author: Phone (619)-450-5990; FAX: (619)450-3251:

email:rgjerset@skcc.org

† This work was supported in part by grants (to R.A.G.) from the National Cancer Institute CA69546, from the U.S.Army Breast Cancer Research Program DAMD17-96-1-6038, and from Introgen Therapeutics, Inc.

## FOOTNOTES

<sup>1</sup>Abbreviations used: RAR $\beta$ : Retinoic Acid Receptor  $\beta$ ; RARE: retinoic acid response element; PCR: polymerase chain reaction; DHFR: dihydrofolate reductase; ATCC: American Type Culture Collection; PBS: phosphate buffered saline; Kb: Kilobase; bp:base pair; CDS: coding sequence.

## ABSTRACT

This study examines how accessibility to cisplatin on various genomic regions in T47D breast cancer cells, including the retinoic acid receptor  $\beta$  gene promoter and coding region and the dihydrofolate reductase gene promoter and coding region, is affected by treatment of the cells with 9-cis retinoic acid, a treatment that activates the retinoic acid receptor  $\beta$  gene promoter in these cells. A PCR-based assay was used to measure cisplatin adduct density based on the inhibition of PCR amplification of templates from cisplatin treated versus untreated cells.

Treatment of cells with 9-cis retinoic acid enhanced accessibility to cisplatin on the retinoic acid receptor  $\beta$  gene promoter region, but not on the coding regions of that gene nor on the dihydrofolate reductase gene promoter or coding regions, where accessibilities to cisplatin remained 2-4 times lower than on the activated retinoic acid receptor  $\beta$  gene promoter.

Examination of smaller regions within this promoter region, showed a repression of platination in the 500 bp region surrounding the TATA box in cells prior to 9-cis retinoic acid treatment, which was abolished following promoter activation. Differences in sequence composition between the various regions could not fully account for differences in platination, suggesting that structural features such as bends in retinoic acid receptor  $\beta$  gene promoter DNA following gene activation, create energetically favorable sites for platination and contribute to the cytotoxicity of the drug.

Cis-diamminedichloroplatinum (cisplatin) is a highly effective chemotherapeutic agent used in the treatment of a variety of human tumors (1). Its cytotoxicity derives from its ability to damage DNA, forming primarily bifunctional 1,2 intrastrand cross-links between adjacent guanines or adenine-guanine dinucleotides, as well as other minor adducts including interstrand cross-links (2). Adduct formation impedes DNA polymerase progression, inhibits DNA synthesis, and triggers apoptosis (3-5). While inhibition of DNA synthesis is believed to be a critical step in cisplatin's cytotoxicity, it does not by itself account for the marked anti-tumor efficacy of cisplatin. For example, adducts formed by the geometric isomer of cisplatin, trans-diamminedichloroplatinum (transplatin), also impede DNA polymerase progression and inhibit DNA synthesis (6). Yet transplatin does not induce apoptosis and has little anti-tumor activity. Furthermore, while cisplatin causes slowing of DNA synthesis, cells treated with cisplatin do not arrest in S phase, but progress and block in G2 (7). In addition, the extent to which DNA synthesis is slowed by cisplatin in sensitive versus resistant cells does not correlate with its relative toxicity to those cells (8). Several studies have pointed to transcription as a key target for cisplatin and have suggested that cisplatin's ability to target certain genetic regulatory elements and inhibit specific gene expression may contribute greatly to its toxicity (9-12).

A structural distortion in DNA occurs upon cisplatin binding that has been proposed to underlie the biological toxicity of cisplatin. Crystallographic studies reveal that the 1,2-cisplatin cross-link induces a bend of about 45° toward the major groove of the DNA helix accompanied by thermal destabilization (13). Such a bend appears to generate a structural motif with biological specificity, as certain chromosomal proteins bind with high affinity to these sites. These proteins include histone H1 (14), HMG1 (15), HMG2 (16), the human structure-specific recognition

protein SSRP1(17-18), and the human transcription factor hUBF (18), all of which are proteins known to bend DNA, and whose binding to DNA might be facilitated by the bends generated by cisplatin. In contrast, the structural effects of transplatin appear to be of greater variability (19), and transplatin adducts do not constitute high affinity binding sites for the above mentioned chromosomal proteins (see 20 for review). Cisplatin's toxicity may therefore be related to the structural consequences of adduct formation, which could involve a disruption of normal binding of chromosomal proteins, or an impediment to conformational changes that are necessary for biological regulation.

In the studies reported here we have addressed the possibility that cisplatin may actually target chromosomal regions such as transcriptional promoters, where DNA bends or partial unwinding of DNA may occur following transcription factor recruitment to an activated promoter. If so, such a structural motif may provide a preferential target for cisplatin and contribute to the cytotoxicity of this drug. We have examined cisplatin adduct formation on promoter and downstream regions of the retinoic acid receptor  $\beta$  (RAR $\beta$ )<sup>1</sup> gene in T47D breast cancer cells, where this gene undergoes retinoic acid-dependent activation. Adduct formation as determined by a quantitative PCR-based assay was observed to be significantly higher on the activated RAR $\beta$  promoter than on a downstream region of the same gene, as well as on the coding and promoter regions of the constitutively expressed housekeeping gene, dihydrofolate reductase (DHFR). Adduct formation on the DHFR promoter, which does not undergo retinoic acid-dependent activation, did not increase following retinoic acid treatment of cells. Cisplatin's cytotoxicity may therefore derive in part from its ability to target and disrupt the function of certain genetic regulatory loci such as the RAR $\beta$  promoter.

## EXPERIMENTAL PROCEDURES

**Cell culture.** T47D breast cancer cells were purchased from ATCC and maintained in RPMI medium supplemented with 10% heat-inactivated fetal bovine serum, 1 mM sodium pyruvate, 2 mM L-glutamine, 0.1 mM non-essential amino acids, 50 µg/ml gentamycin. Cell culture reagents were purchased from Irvine Scientific, Santa Ana, CA. All experiments were performed using charcoal-treated serum (600 mg activated charcoal per 50 mls serum for 10 minutes at 4° C, followed by filtration).

**Analysis of RAR $\beta$  and DHFR gene expression.** About  $5 \times 10^5$  T47D cells (at about 70% confluency) were treated as indicated and total cellular RNA was prepared using the Rneasy™ kit from Qiagen and following the manufacturer's procedure. 1 µg of RNA was reverse transcribed into cDNA in a 20 µl reaction containing 0.5 mM dNTPs (Pharmacia), 100 µg/ml oligo dT (Promega), 2 units RNasin (Promega), 10 units Moloney Murine leukemia virus reverse transcriptase (Promega), reverse transcriptase buffer (Promega). This cDNA was then used as a template for quantitative PCR. Primers were chosen so as to amplify a 178 base region of the RAR $\beta$  coding sequence encompassing parts of exons 4 and 5, as well as a 246 base region of the coding sequence of the dihydrofolate reductase from exons 1 to 4. As shown below:

RAR $\beta$  message (forward) 5' - GTGTACAAACCCTGCTTCGTCTGC - 3'

(reverse) 5' - CTGGAGTCGACAGTATTGGCATCG - 3'

DHFR message (forward) 5' - GGTTTCGCTAAACTGCATCGTCGC - 3'

(reverse) 5' – GTGGAGGTTTCCTTGAGTTCTCTG - 3'

Amplification conditions were as described below for the PCR-stop assay. Quantitative conditions were verified by preparing cDNA with 100 ng and 10 ng RNA (in addition to 1 µg RNA) and amplifying serial two fold dilutions of the cDNA from 2 µl to 0.25 µl template to show that product formation was proportional to input template under our conditions. Following amplification, products were analyzed by agarose gel electrophoresis followed by band quantitation using a Kodak digital camera.

**Cell viability.** Following treatments, cell viability was monitored by adding 10% Trypan blue and determining the fraction of cells that excluded the dye.

**Cisplatin treatments.** Cells were plated at 50% confluency in 6 well plates in medium supplemented with 10% charcoal-treated FBS in addition to the other standard additives described above. Following attachment, cultures were pre-treated 24 hours in the presence or absence of 1 µM 9-cis retinoic acid (Sigma, ST Louis, MO), followed by a 2 hour incubation in the presence or absence of 1 mM cisplatin (Platinol™, aqueous solution at 1 mg/ml, purchased from local pharmacies). The pre-incubation medium was then replaced, and genomic DNA was prepared 24 hours later as described below. Although DNA repair has been observed to occur over 24 hours in cells treated with lower doses of cisplatin (21-22), at the high levels used in our studies we observed an overall increase in adduct formation over 24 hours, so that adduct densities approached 1-4 adducts per 10Kb and were therefore readily detectable in our assay.

The increase in adduct formation over time suggests that residual cisplatin continued to cause DNA damage and that repair did not keep pace with adduct formation under our conditions.

**Preparation of genomic DNA.** DNA was prepared from treated cultures using the QIAmp blood kit essentially following the manufacturer's protocol, except that cells were lysed directly on the plate in the presence of PBS, Qiagen protease and lysis buffer supplied in the kit. Following purification, DNA was adjusted to 0.25 mg per ml in sterile water and stored at  $-20^{\circ}$  C until use.

**Analyses of DNA damage by PCR stop assay.** Quantitative PCR was used to compare cisplatin adduct formation on specific regions of DNA. The assay, known as the PCR stop assay has been described (23). Because Taq polymerase is blocked at cisplatin adducts, the relative efficiency of PCR amplification of genomic DNA from cisplatin-treated versus control cells decreases in proportion to platination levels. The relative PCR efficiency is equivalent to the frequency ( $P$ ) of undamaged strands within a population.  $P$  is related to the average number ( $n$ ) of cisplatin adducts per fragment, by the Poisson formula:  $P = e^{-n}$ , or  $-(\ln P) = n$ . Adducts per Kb would then be equal to  $-(\ln P) \div (\text{size of fragment in Kb})$ . We found that fragment sizes of around 1 Kb provided a sufficiently large target size to enable measurement of adduct densities in the range of 0.1-0.4 adducts per Kb observed here. A drop in the PCR signal of damaged DNA to 0.67 of the control signal would therefore reflect an average cisplatin adduct density of  $-(\ln 0.67) = 0.4$  adducts per fragment. Standard deviations among triplicate PCRs were in the range of  $\pm 5\%$ , meaning that adduct densities of less than about 0.05 adducts per fragment were undetectable. For each primer pair, we verified that product formation was directly proportional

to input template DNA by performing a pilot experiment with serial two fold dilutions of template, followed by electrophoresis on a 1% agarose gel containing 0.5  $\mu\text{g/ml}$  ethidium bromide. Bands were quantitated using Kodak digital camera and analysis software. Depending on the primer set, the amount of template used in the PCR reaction ranged from 0.03 to 0.25  $\mu\text{g}$  per 25  $\mu\text{l}$  reaction. Reactions were performed in 25  $\mu\text{l}$  containing template DNA, 25 pmole each of forward and reverse primer, 250  $\mu\text{M}$  dNTPs (Pharmacia) 1.25 units Taq polymerase (Qiagen), 1x buffer (Qiagen) and solution Q (Qiagen). The amplification program was as follows: 1 cycle ( $94^{\circ}\text{C}$ , 1 minute 30"); 25 cycles ( $94^{\circ}\text{C}$ , 1 minute,  $57^{\circ}\text{C}$ , 1 minute,  $70^{\circ}\text{C}$ , 2 minutes 30 seconds); 1 cycle ( $94^{\circ}\text{C}$ , 1 minute,  $57^{\circ}\text{C}$ , 1 minute,  $70^{\circ}\text{C}$ , 7 minutes). Two independent templates were prepared for each treatment condition, and each one was analyzed in triplicate. As an internal PCR control for each template, a 270 bp fragment of the dihydrofolate reductase gene was amplified. This fragment is too small to register significant levels of damage under the conditions we used, and its amplification product was seen to vary by less than 5% amongst the various templates. The primers (1) through (17) used for PCR amplification of various regions of genomic DNA are summarized in Table 1. Figure 1 shows a schematic representation of regions amplified from the RAR $\beta$  gene.

## RESULTS

**Transcriptional response of the RAR $\beta$  gene to 9-cis retinoic acid and cisplatin.** Figure 2 shows the results of an RT-PCR assay demonstrating retinoic acid-dependent activation of the RAR $\beta$  gene (lane 2 compared to lane 1) and cisplatin-mediated inhibition of this activation (lane 3). Under the same conditions, we observed little change in DHFR expression (lanes 4-6), indicating that expression of this gene is not retinoic acid dependent and that cisplatin has little immediate effect on its expression. This is consistent with another study in which treatment with cisplatin did alter levels of DHFR message (24), although long term *in vitro* selection for cisplatin resistant ovarian carcinoma cell lines by repeated exposure to cisplatin has been reported to generate variants that over-express DHFR (25). Genomic DNA from cells before and after treatment with 9-cis retinoic acid was then used to analyze platination of the RAR $\beta$  gene in its active and inactive state.

**Preferential cisplatin adduct formation on the activated RAR $\beta$  gene promoter.** We performed a PCR stop assay to examine cisplatin adduct density on genomic DNA templates from 9-cis retinoic acid treated (RA+) or untreated (RA-) cells. Regions spanning about 1 Kb in length of the RAR $\beta$  promoter (1043 bp), the RAR $\beta$  coding sequence (1036 bp), the DHFR promoter (1000 bp), and the DHFR coding sequence (1062 bp) were examined as defined by primers listed in Table 1. PCR products were analyzed on agarose gels (Figure 3A) and bands were quantitated in order to determine the relative PCR efficiencies from platinated versus unplatinated templates. Using templates from (RA-) cells (Figure 3A, lanes 1,2), the relative PCR efficiencies from platinated versus unplatinated templates (lane 2 versus lane 1) were as

follows: RAR $\beta$  promoter (0.88), RAR $\beta$  coding sequence (0.85), DHFR promoter (0.85), DHFR coding sequence (0.87). Using templates from (RA+) cells (lanes 3,4), the relative PCR efficiencies from platinated versus unplatinated templates (lane 4 versus lane 3) were as follows: RAR $\beta$  promoter (0.65), RAR $\beta$  coding sequence (0.88), DHFR promoter (0.9), DHFR coding sequence (0.88). Based on the PCR results, the cisplatin adduct densities were calculated by the Poisson equation described above. The results plotted in Figure 3B represent the averages and standard deviations of two separate experiments with independently prepared templates, with each experiment being performed in triplicate and corrected for variations in the 270 bp PCR product of the DHFR gene.

As shown in Figure 3B, in the case of the RAR $\beta$  CDS (1036 bp), the DHFR CDS (1062 bp), and the DHFR promoter (1000 bp), treatment of cells with 9-cis retinoic acid has little effect on cisplatin adduct density. Thus adduct densities (in adducts per Kb) on these regions in untreated cells (RA-) are observed to be  $0.16 \pm 0.03$ ,  $0.13 \pm 0.08$ , and  $0.17 \pm 0.04$ , respectively. Adduct densities on these same regions in 9-cis retinoic acid-treated cells (RA+) are observed to be  $0.13 \pm 0.06$ ,  $0.2 \pm 0.04$ , and  $0.11 \pm 0.07$ , respectively.

In contrast, cisplatin adduct density on the RAR $\beta$  promoter (1043 bp) is enhanced in cells following treatment of cells with 9-cis retinoic acid (Figure 3B). For this region, adduct densities increase from  $0.12 \pm 0.04$  adducts per Kb in untreated cells (RA-) to  $0.4 \pm 0.16$  adducts per Kb in treated cells (RA+). Cisplatin adduct density measured on the active RAR $\beta$  promoter region in RA+ cells is therefore about 2 times as high as on the DHFR CDS (1062 bp) or DHFR promoter regions in RA+ cells, and nearly 3.5 times as high as on the inactive RAR $\beta$  promoter in

RA- cells. Cisplatin adduct density on the constitutively expressed DHFR promoter does not increase following 9-cis retinoic acid treatment (Figure 3B).

To determine the extent to which differences in sequence composition might account for differences in adduct density, we examined the number of GG and AG dinucleotide pairs (the major sites of adduct formation in DNA) in the various DNA regions studied, as summarized in Table 2 (column 2). Clusters of 3 or 4 G's were scored as one site. The number of potential sites for adduct formation was in turn used to estimate the relative frequencies of cisplatin targets per Kb compared to the DHFR CDS (1062 bp) region (Table 2, column 5), given that AG is targeted by cisplatin only about 40% as frequently as GG dinucleotides (2). We find that cisplatin adducts form on the RAR $\beta$  promoter (1043 bp) about 2 times as frequently as we would anticipate on the basis of sequence composition alone. That is, the estimated frequency of targets is about the same for the RAR $\beta$  promoter (1043 bp) region and the DHFR CDS (1062 bp) region, yet the observed adduct frequency on the promoter region is about 2 times what it is on the DHFR CDS (1062 bp) region ( $0.4 \pm 0.16$  versus  $0.2 \pm 0.04$  adducts per Kb). Similarly, the estimated frequency of targets on the RAR $\beta$  promoter (1043 bp) is about 2 times the estimated frequency on RAR $\beta$  CDS (1036 bp), yet the observed adduct frequency is 3 times greater on the promoter compared to the CDS ( $0.4 \pm 0.16$  versus  $0.13 \pm 0.06$  adducts per Kb). This suggests that other factors contribute to the preferential targeting of cisplatin to the induced RAR $\beta$  promoter.

**Location of cisplatin adducts within the promoter region.** To further localize adduct formation within the promoter, we subdivided the RAR $\beta$  promoter (1043 bp) region into three

overlapping regions A (624 bp), B (483 bp), and C (592 bp) shown schematically in Figure 1, and defined by primers listed in Table 1. As shown in Figure 4, in the absence of promoter activation with 9-cis retinoic acid, adduct formation is virtually undetectable in the central region (B) encompassing the TATA box and RARE (retinoic acid response element), and approximately equivalent in regions A and C in adducts per Kb to what we observe on the larger 1043 base region of the promoter (0.17 adducts per Kb on each of regions A, C versus 0.12 adducts per Kb on the larger fragment overall). This suggests that some portion of the central region of the promoter included in fragment B is protected from platination in the uninduced state.

Following promoter activation, all three regions A, B, and C sustain elevated levels of damage, ( $0.34 \pm 0.07$ ,  $0.43 \pm 0.07$ ,  $0.27 \pm 0.11$  adducts per Kb, respectively), which is on the average what we observe on the larger 1043 base region of the activated promoter ( $0.4 \pm 0.16$  adducts per Kb). This confirms the measurement of adduct density on the larger 1043 base region (Figure 3, Table 3) and supports the conclusion drawn from the comparison of sequence composition in Table 3 that the activated RAR $\beta$  promoter sustains levels of cisplatin damage greater than would be expected on the basis of base composition alone. Because regions A, B, and C do not differ significantly between themselves in GG and AG sequence compositions, the result here suggests that cisplatin adducts are distributed evenly over the activated promoter and that protection from platination in region B is abolished by promoter activation.

## DISCUSSION

In these studies we have used a PCR-based assay to detect platination on genomic regions encompassing about 1 Kb of the RAR $\beta$  promoter, the RAR $\beta$  coding sequence (CDS), the DHFR promoter, and the DHFR CDS in T47D breast cancer cells. We see that treatment of these cells with 9-cis retinoic acid, a treatment that activates the RAR $\beta$  promoter but not the DHFR promoter, results in a three fold increase in accessibility of the RAR $\beta$  promoter region to cisplatin ( $0.4 \pm 0.16$  versus  $0.12 \pm 0.04$  adducts per Kb). In contrast, the accessibilities to cisplatin of the DHFR promoter, DHFR CDS, and RAR $\beta$  CDS are not significantly altered by treatment of cells with 9-cis retinoic acid, and observed adduct densities remain about 2-4 fold lower than on the activated RAR $\beta$  promoter ( $0.11 \pm 0.07$ ,  $0.2 \pm 0.04$  and  $0.13 \pm 0.06$  adducts per Kb, respectively). The activated RAR $\beta$  promoter appears therefore to be hypersensitive to cisplatin adduct formation. Preferential platination of the RAR $\beta$  promoter relative to the other regions examined could only be attributed in part to differences in sequence composition, suggesting that structural factors also play a role in directing adduct formation to certain sites.

The possibility that promoter-specific structural changes influence reactivity with cisplatin is further supported by the analysis of subregions of the larger RAR $\beta$  promoter fragment, where we see that accessibility to cisplatin increases over the entire promoter region following activation of the promoter. Furthermore, the accessibility to cisplatin of the central region of the promoter, including the TATA box and RARE appears to be suppressed in the inactive state, and this suppression is relieved upon promoter activation. In this case, inhibition of accessibility to cisplatin might be due to steric hindrance due to the possible positioning of a nucleosome at or

near the start site of transcription. A recent analysis of a large set of unrelated RNA polymerase II promoters, both TATA-containing and TATA-less, has revealed a common bendability profile of DNA just downstream of the start site of transcription, suggesting that the DNA could wrap around protein in a nucleosome (26). In addition, the complementary triplet pair, CAG/CTG, shown to correlate with nucleosome positioning (27-28) is over-represented in the region just downstream of the transcription start site (26). Complexation with nucleosomes near the transcription start site of the inactive promoter might therefore impede adduct formation by cisplatin, and displacement or destabilization of nucleosomes by the transcription initiation complex might remove this impediment.

Following transcriptional activation, the RAR $\beta$  promoter not only becomes more accessible to cisplatin than it was prior to transcriptional activation, but appears to bind more cisplatin than would be expected based on sequence composition alone. This suggests that some structural feature of the DNA of the activated promoter might make it an energetically favorable site for cisplatin adduct formation. One such feature might be an induced bend in the promoter DNA generated as a result of protein-protein interactions between transcription factors bound to distant sites (see 29, review). Such a bend might provide the stored energy required for strand separation and initiation of transcription, and this process could be blocked by the formation of a cisplatin adduct.

The retinoids all trans retinoic acid (ATRA) and 9-cis retinoic acid (9-cis RA), as well as several synthetic analogues of these natural retinoids, have attracted considerable attention as potential chemotherapeutic agents for the treatment of promyelocytic leukemia (30) and other cancers (31-

33). As ligands for nuclear retinoic acid receptors (RAR $\alpha$ , $\beta$ , or  $\gamma$ ) and retinoid X receptors (RXR $\alpha$ , $\beta$ , or  $\gamma$ ), retinoids regulate the expression of sets of overlapping genes involved in the regulation of cell proliferation, differentiation, and apoptosis (34-36). All trans retinoic acid, binding to RAR  $\alpha$ , $\beta$ , or  $\gamma$ , and 9-cis retinoic acid, binding to either RAR  $\alpha$ , $\beta$ , or  $\gamma$ , or RXR  $\alpha$ , $\beta$ , or  $\gamma$ , promote the heterodimerization of these receptors and facilitate the binding of the heterodimeric complex to specific response elements (RAREs) in the promoter regions of retinoic acid-responsive genes. This binding is believed to facilitate the recruitment of the components of the basal transcription complex to the promoter, and promote chromatin remodeling required for the onset of transcription. While these events may by themselves lead to partial suppression of some solid tumors, in most examples studied, retinoids showed more potential when used in combination with DNA damaging chemotherapies such as cisplatin, etoposide, and 5-fluorouracil (37-39). A synergistic activity between retinoids and cisplatin has been observed only when retinoid treatment preceded cisplatin treatment, and this correlated with a 1.5-fold increase in cisplatin adduct content of DNA without a change in cisplatin uptake (39). These data suggest that retinoid treatment induces an event or events that directly enhance cisplatin cytotoxicity and are consistent with the possibility suggested by our data, that retinoids may generate cisplatin-hypersensitive structures that contribute to an enhanced response to cisplatin.

These data implicate chromatin organization as a component influencing the toxicity of cisplatin, and add further support to a growing body of evidence pointing to the transcription process as a target for cisplatin mediated cytotoxicity. Cisplatin adduct formation may disrupt transcription through several mechanisms, including the following: (a) Cisplatin adducts may generate

inappropriate binding sites for transcription factors and chromosomal proteins with HMG domains, titrating them away from their natural sites (18). A variety of HMG-box chromosomal proteins involved in the transcription complex bind to cisplatin adducts (14-18). (b) Cisplatin may inhibit transcription factor binding to certain promoters, as has been shown for a stably integrated mouse mammary tumor virus promoter-driven reporter gene (40). In this case, cisplatin treatment prior to hormonal induction prevented activation of the reporter gene and blocked recruitment of the transcription complex to the promoter. (c) By targeting GG dinucleotides, cisplatin may inhibit certain regulatory elements rich in strings of guanines, leading to selective inhibition of such promoters (9,10), and (d) As suggested by our results, cisplatin may target a DNA structure generated in the active promoters of certain genes, such as the RAR $\beta$  gene. Assembled on activated promoters may be some of the factors needed to trigger apoptosis, including the transcription factor p53. Of interest is the recent identification of HMG-1, which is known to bind to cisplatin adducts, as a specific activator of p53 (41).

The differential toxicities of various platinum drugs may therefore be related to their respective abilities to mimic or disrupt chromatin structures critical to transcription. Further studies will be required to determine to what extent the observations made in this study extend to other promoters and to other DNA damaging agents.

## REFERENCES

1. Loehrer, P. J., and Einhorn, L. H. (1984) *Ann. Intern. Med.* 100, 704-713.
2. Eastman, A. (1986) *Biochemistry* 25, 3912-3915.
3. Pinto, A. L., and Lippard, S. J. (1985) *Proc. Natl. Acad. Sci. U. S. A.* 82, 4616-4619.
4. Howle, J. A., and Gale, G. R. (1970) *Biochem. Pharmacol.* 19, 2757-2762.
5. Chu, G. (1994) *J. Biol. Chem.* 269, 787-790.
6. Heiger-Bernays, W. J., Essigmann, J. M., and Lippard, S.J. (1990). *Biochemistry* 29, 8461-8466.
7. Sorenson, C. M., and Eastman, A. (1988) *Cancer Res.* 48: 4484-4488
8. Sorenson, C. M. and Eastman, A. (1988) *Cancer Res.* 48, 6703-6707.
9. Gralla, J.D., Sasse-Dwight, S., Poljak, L.G. (1987) *Cancer Res.* 47, 5092-5096.
10. Buchanan, R.L., and Gralla, J.D. (1990) *Biochemistry* 29, 3436-3442.
11. Evans, G.L., and Gralla, J.D. (1992) *Biochem. Biophys. Res. Commun.* 184: 1-8.
12. Evans, G.L., and Gralla, J.D. (1992) *Biochem. Pharmacol.* 44: 107-119.
13. Takahara, P. M., Rosenzweig, A. C., Frederick, C. A., and Lippard, S. J., (1995) *Nature* 377, 649-652.
14. Yaneva, J., Leuba, S. H., van Holde, K., and Zlatanova, J. (1997) *Proc. Natl. Acad. Sci. U.S.A.*, 94, 13448-13451.
15. Pil, P. M., and Lippard, S. J. (1992) *Science* 256, 234-237.
16. Billings, P. C., Davis, R. J., Engelsberg, B. N., Skov, K. A., Hughes, E.N. (1992) *Biochem. Biophys. Res. Commun.* 188, 1286-1294.

17. Bruhn, S. L., Pil, P. M., Essigmann, J. M., Housman, D. E., and Lippard, S. J. (1992) *Proc. Natl. Acad. Sci. U. S. A.* 89, 2307-2311.
18. Treiber, D. K., Zhai, X., Jantzen, H-M., and Essigman, J. M. (1994) *Proc. Natl. Acad. Sci. U.S.A.* 91, 5672-5676.
19. Bellon, S. F., Coleman, J. H., and Lippard, S. J. (1991) *Biochemistry* 30, 8026-8035
20. Zlatanova, J., Yaneva, J., and Leuba, S. H. (1998) *FASEB J.* 12, 791-799.
21. Bohr, V.A. (1991) *Carcinogenesis* 12: 1983-1992.
22. Rampino, N.J., and Bohr, V.A. (1994) *Proc. Natl. Acad. Sci. U.S.A.*, 91: 10977-10981.
23. Jennerwein, M. M., and Eastman, A. (1991) *Nucleic Acids Res.* 19, 6209-6214.
24. Sheibani, N., and Eastman, A. (1990) *Cancer Letters*, 52: 179-185.
25. Scanlon, K.J., and Kashani-Sabet, M. (1988) *Proc. Natl. Acad. Sci. U.S.A.*, 85: 650-653.
26. Pedersen, A. G., Baldi, P., and Chauvin, Y. (1998) *J. Mol. Biol.* 281, 663-673.
27. Baldi, P., Brunak, S., Cauvin, Y., and Krogh, A. (1996) *J. Mol. Biol.* 263, 503-510.
28. Liu, K., and Stein, A. (1997) *J. Mol. Biol.* 270, 559-573.
29. Van der Vliet, P.C. and Verrijzer, C.P. (1993) *Bioessays* 15, 25-32.
30. Huang, M. E., Ye, Y. C., and Chen, S. R. (1988) *Blood* 72, 567-572
31. Redfern, C. P., Lovat, P. E., Malcolm, A. J., and Person, A.D. (1995) *Eur. J. Cancer* 31A, 486-494.
32. Anzano, M.A., Byers, S.W., Smith, J.M., Peer, C.W., Mullen, L.T., Brown, C.C., Roberts, A.B., and Sporn, M.B. (1994) *Cancer Res.* 54, 4614-4617.
33. Gottardis, M.M., Lamph, W.W., Shalinsky, D.R., Wellstein, A., and Heyman, R.A. (1996) *Breast Cancer Res. Treat.* 38, 85-96.

34. Breitman, T., Selonic, S., and Collins, S. (1980) *Proc. Natl. Acad. Sci. U.S.A.* 77, 2936-2940.
35. Sporn, M., and Robert, A. (1984) *J. Natl. Cancer Inst.* 73, 1382-1387.
36. Martin, S., Bradley, J., and Cotter, T. (1990) *Clin. Exp. Immunol.* 79, 448-453.
37. Sacks, P. G., Harris, D., and Chou, T-C. (1995) *Int. J. Cancer* 61, 409-415.
38. Guchelaar, H.J., Timmer-Bosscha, H., Dam-Meiring, A., Uges, D.R., Oosterhuis, J.W., de Vries, E.G., and Mulder, N.H. (1993) *Int. J. Cancer* 55, 442-447.
39. Caliaro, M.J., Vitaux, P., Lafon, C., Lochon, I., Nehme, A., Valette, A., Canal, P., Bugat, R., and Jozan, S. (1997) *Br. J. Cancer* 75, 333-340.
40. Mymryk, J. S., Zaniewski, E., and Archer, T. K. (1995) *Proc. Natl. Acad. Sci. U.S.A.* 92, 2076-2080.
41. Jayaraman, L., Moorthy, N.C., Murthy, K.G., Manley, J.L., Bustin, M., and Prives, C. (1998) *Genes Dev.* 12, 462-472.

**TABLE 1**  
**Primers used for PCR-stop assay of genomic DNA**

Gene	Region amplified	Primer sequences (5'→3')	Product size (base pairs)
RAR B	RARB Promoter (Includes A,B,C below)	#1: CGAGTGCAGTCAATTCAGCCAGG (for) #2: GCTTATCCTCTAGGTGTGGAGGC (rev)	1043
	(A) Promoter, upstream and including TATA and RARE	#1: see above (for) #3: CTTCCTACTACTTCTGTCACACAG (rev)	624
	(B) Promoter region of TATA and RARE	#4: GGGAGAGAAGTTGGTGCTCAACG (for) #5: CCTTCCGAATGCGTTCGGGATC (rev)	483
	(C) Promoter, downstream and including TATA and RARE	#6: GCTTTTGCAGGGCTGCTGGGAG (for) #2: see above (rev)	592
	RARB CDS (1036 bp) (exon 10)	#7: GGTGCAGAGCGTGTAATTACCTTG(for) #8: CTGCCTTGGAGGCTATCATTACTG(rev)	1036
	RARB CDS (483 bp) (exon 10)	#7: see above (for) #9: GGTCTTTGCCATGCATCTTGAGTG (rev)	483
DHFR	DHFR Promoter	#10: CAGAATGGGAGTCAGGAGACCTG (for) #11: GCAGAAATCAGCAACTGGGCCTC (rev)	1000
	DHFR CDS (1062 bp) (exons 1,2,adjacent introns)	#12: CCGTAGACTGGAAGAATCGGCTC (for) #13: CAGTTGCCAATTCTGCCCCATGC (rev)	1062
	DHFR CDS (472 bp) (exon 1 and adjacent introns)	#14: CAATTCGCGCCAACTTGACCG (for) #15: GAGCTCTAAGGCACCTGACAAAC (rev)	472
	DHFR CDS (272 bp) (exon 1 and adjacent introns) (internal control)	#16: GGTTCGCTAAACTGCATCGTCGC (for) #17: CAGAAATCAGCAACTGGGCCTCC (rev)	272

TABLE 2

Comparison of expected versus observed adduct density in various gene fragments from cells treated with 9-cis retinoic and 1 mM cisplatin.

1	2	3		4	5	6	7
Gene fragment	Number of GG and AG sites	Cisplatin targets per fragment <sup>1</sup>		Targets/Kb	Targets/Kb relative to DHFR	Expected adducts per Kb based on observed DHFR <sup>2</sup> Column 5 x (0.2)	Observed adducts per Kb <sup>3</sup>
		(a)	(b) sum	<i>Column 3(b)</i> <i>Fragment length (Kb)</i>	<i>Column 4</i> <i>83</i>		
DHFR CDS 1062 bases	GG 77 AG 26	GG 77 AG 11	88	83	1.0	0.2	0.2 ± 0.04
RARβ CDS (1036 bp)	GG 25 AG 56	GG 25 AG 22	47	45	.54	0.11	0.13 ± 0.06
RARβ promoter (1043 bp)	GG 72 AG 50	GG 72 AG 20	92	88	1.1	0.21	0.40 ± 0.16
DHFR promoter (1000 bp))	GG 84 AG 55	GG 84 AG 22	106	106	1.3	0.26	0.11 ± 0.07

<sup>1</sup> AG adducts are about 40% as likely to form as GG adducts (16): therefore AG targets (column 3a) = AG sites (column 2) x 0.4.

<sup>2</sup> From column 7.

<sup>3</sup> Calculated from PCR data in Table 2 using Poisson equation relating adducts per fragment to PCR signal, and correcting for fragment size.

## FIGURE LEGENDS

Figure 1. Location and sizes of PCR amplification products from the RAR $\beta$  gene of T47D cells (see also Table 1). For the analysis in Figure 3, PCR primers were chosen so as to amplify a 1043 bp region of the RAR $\beta$  promoter, including the retinoic acid response element (RARE) and TATA box, and a 1036 bp region of the RAR $\beta$  coding sequence (CDS). For the analysis in Figure 4, PCR primers were chosen so as to amplify the subregions A, B, and C.

Figure 2. Quantitative RT-PCR analysis of RAR $\beta$  gene expression (lanes 1-3) and DHFR gene expression (lanes 4-6) in T47D cells under various conditions. Lanes 1,4: untreated T47D cells. Lanes 2,5: T47D cells treated 24 hours with 1  $\mu$ M 9-cis retinoic acid. Lanes 3,6: cells treated 24 hours with 9-cis retinoic acid, followed by 2 hours with 200  $\mu$ M cisplatin. Quantitative conditions for cDNA synthesis and PCR amplification were verified as described in Experimental Procedures. 10  $\mu$ l and 2  $\mu$ l, respectively, of the RAR $\beta$  and DHFR PCR reactions were analyzed.

Figure 3. Cisplatin adduct formation on various regions of T47D cell genomic DNA as assayed by PCR stop assay. Regions analyzed were the RAR $\beta$  CDS (1036 bp), the RAR $\beta$  promoter (1043 bp), the DHFR CDS (1062 bp), and the DHFR promoter (1000 bp). Genomic DNA was prepared from cells pre-treated in the presence (RA+) or absence (RA-) of 9-cis retinoic acid for 24 hours followed by 2 hours in the presence or absence of 1 mM cisplatin. (A) Agarose gel analysis of PCR products from one experiment. Lanes 1,2 (RA- cells). Lanes 3,4 (RA+ cells). Lanes 1,3 (no cisplatin). Lanes 2,4 (plus cisplatin). (B) Bar graph showing cisplatin adducts per

Kb as calculated from the PCR results as described in Experimental Procedures. The results represent the averages and standard deviations of two separate experiments with independently prepared templates, with each experiment being performed in triplicate. For each experiment, results were corrected for variations in the 270 bp PCR product of the DHFR gene.

Figure 4. Cisplatin adduct formation on three overlapping regions A (624 bp), B (483 bp), and C (592 bp) of the RAR $\beta$  promoter 1043 bp region shown schematically in Figure 1. Primers used are listed in Table 1. Cells were treated as in Figure 3. Results represent the average of triplicate assays.

Figure 1

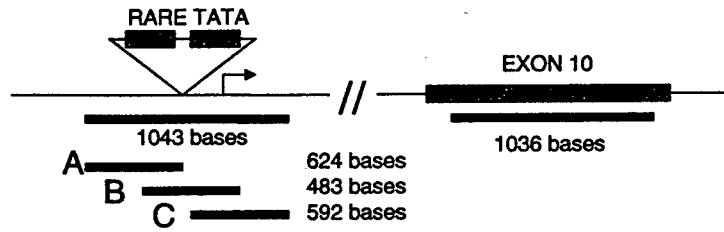


Figure 2

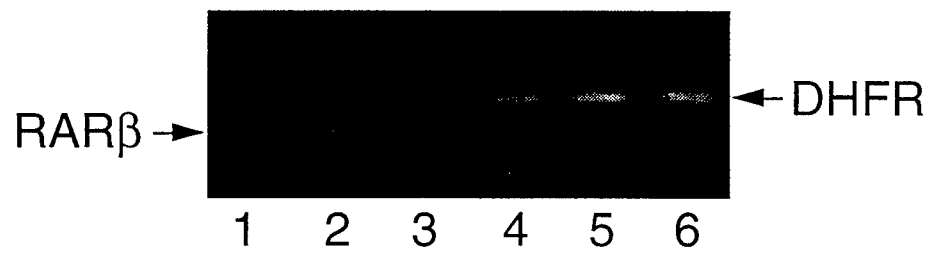


Figure 3A

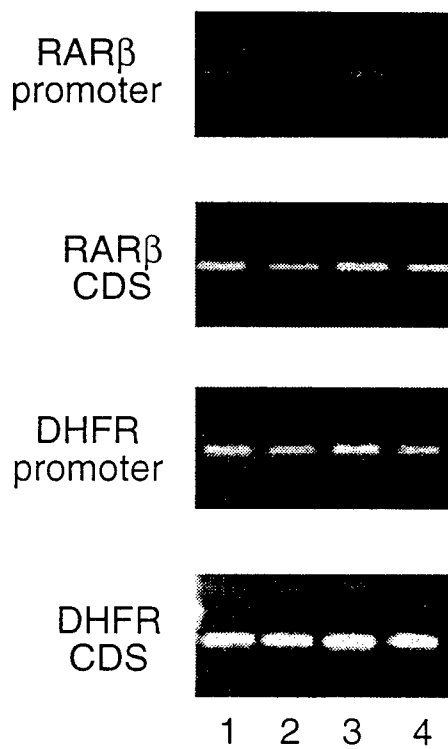


Figure 3B

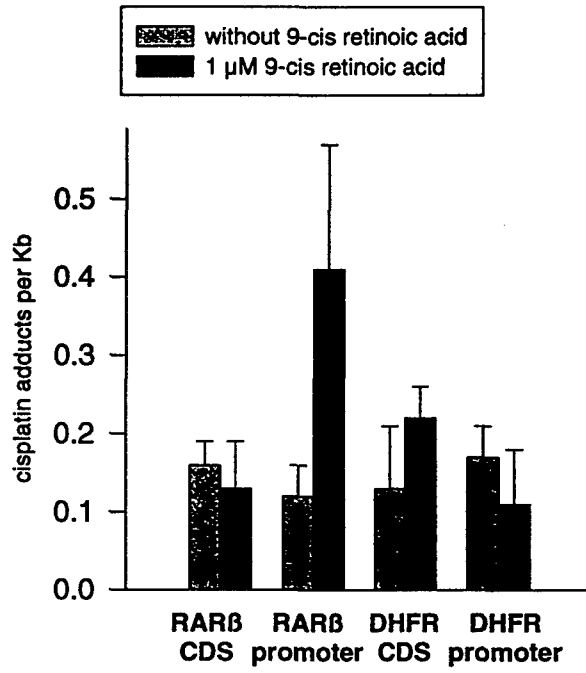
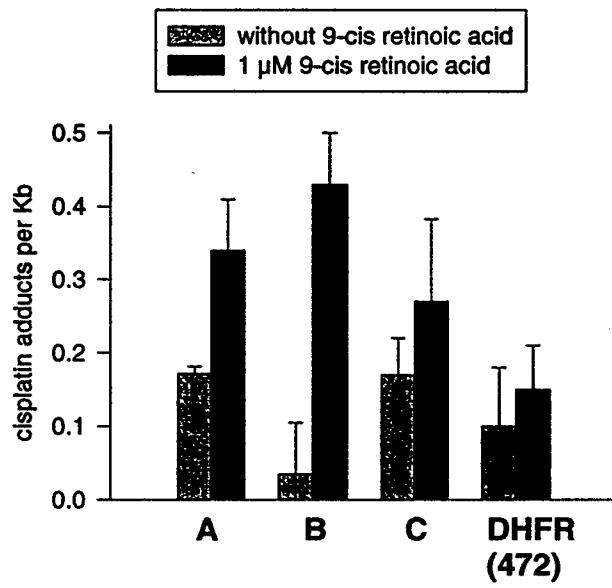


Figure 4



---

INHIBITION OF THE JUN KINASE PATHWAY BLOCKS DNA REPAIR,  
ENHANCES P53-MEDIATED APOPTOSIS AND PROMOTES GENE  
AMPLIFICATION<sup>1</sup>

RUTH A. GJERSET<sup>2</sup>, SVETLANA LEBEDEVA, ALI HAGHIGHI, SALLY T. TURLA, DAN  
MERCOLA,

*Sidney Kimmel Cancer Center, 10835 Altman Row, San Diego, CA 92121*

Running title: c-Jun phosphorylation and p53

Key words: p53, Jun kinase, gene amplification, DNA repair, glioblastoma

ABSTRACT

We have previously shown, by expression of a nonphosphorylatable dominant inhibitor mutant of c-Jun (cJun(S63A,S73A)), that activation of the N-terminal Jun kinase/stress-activated protein kinase (JNK/SAPK) by genotoxic damage is required for DNA repair. Here we examine the consequences of inhibition of DNA repair on p53-induced apoptosis in T98G cells, which are devoid of endogenous wild-type p53. Relative to parental or wild-type c-Jun expressing control cells, mutant Jun-expressing T98G clones show similar growth rates and plating efficiencies. However, these cells are unable to repair DNA (PCR-stop assays) and exhibit up to 80 fold increased methotrexate-induced colony formation due to amplification of the dihydrofolate reductase gene. Moreover, the mutant c-Jun clones exhibit increased apoptosis and elevated bax to bcl<sub>2</sub> ratios upon expression of wild-type p53. These results indicate that inhibition of DNA repair leads to accumulation of DNA damage in tumor cells with unstable genomes and this in turn enhances p53-mediated apoptosis.

## INTRODUCTION

Tumor progression involves the rapid accumulation of genetic alterations, some of which promote cell proliferation and enable cell survival in changing environments. Genomic instability, one of the unique features of cancer, may provide the driving force for progression by facilitating these rapid genetic alterations (see 1). Nevertheless, this instability generates strand breaks and other forms of DNA damage that could be deleterious to cell survival. There is therefore selective pressure on the cancer cell to modulate its DNA damage response so as to insure survival while accommodating this increased genetic instability.

One way in which a cancer cell may modulate its DNA damage response is loss of the tumor suppressor p53. p53 mediates apoptosis in response to DNA damage, possibly as a result of its ability to recognize and bind to damaged DNA, including DNA containing single stranded ends (2) and DNA in abnormal structures known as insertion-deletion loops (3). Stabilization of p53 protein occurs following DNA damage, in a process that involves DNA-PK/ATM as a key mechanism (4,5). Numerous studies correlate loss of p53 with increased genome instability (6-9), aneuploidy (10,11), and tumor progression (12), suggesting that loss of p53 renders cells permissive for further genome destabilizing events that accompany and promote tumor progression such as gene amplification and deletion. Restoration of p53 function in tumor cells that no longer express wild-type p53 restores the DNA damage recognition pathways and leads to G1 arrest or apoptosis (see 13, review).

DNA damage also leads to activation of the Jun kinase/Stress-activated protein kinase pathway (JNK/SAPK) (14). Jun kinase (JNK) phosphorylates the c-Jun component of the AP-1 complex and related transcription complexes on serines 63 and 73 in the N-terminal domain, thereby greatly activating transcriptional transactivation by AP-1 and related c-Jun-containing complexes such as the c-Jun/ATF2 heterodimer. JNK activity is strongly induced in response to a variety of DNA damaging treatments such as UV irradiation (15), cisplatin (15,16), camptothecin (17), and etoposide (18). We have previously shown that activation of the JNK pathway that follows DNA damage is required for DNA repair, suggesting an essential role of JNK in regulating the DNA repair process (16). Phosphorylation of c-Jun is also induced by certain oncogenes (19) and is required for c-Jun plus Ha-ras co-transformation of rat embryo fibroblasts (19,20). Complete loss of c-Jun in transgenic mouse embryo fibroblasts results in proliferation defects leading to prolonged passage through crisis and delay of spontaneous immortalization (21).

In order to more fully understand the role of the Jun kinase pathway and c-Jun phosphorylation in cellular transformation, tumorigenesis, and DNA repair, we have recently selected T98G glioblastoma cells modified to express a mutant Jun that acts as a dominant-negative inhibitor of wild-type c-Jun downstream targets. T98G cells express only mutant p53 (22), and unlike many other cell types, including normal lung epithelial cells (23), they express elevated, easily detectable levels of Jun kinase activity, which can be activated a further 5-10 fold by treatment with the DNA cross-linking agent cisplatin

(16). The Jun mutant construct used to modify T98G cells was originally derived by Karin and colleagues (19,20) and has alanine substitutions at serine positions 63 and 73. Mutant Jun therefore cannot be phosphorylated by Jun kinase. Expression of mutant Jun does not alter the basal or induced levels of Jun kinase activity in these cells, indicating that mutant Jun has no direct effect on the JNK enzyme<sup>3</sup>. However, it does strongly inhibit transactivation of AP-1 reporter plasmids in rodent fibroblasts (19,20), and T98G cells<sup>3</sup>, indicating that mutant Jun acts as a competitive inhibitor in the formation of an active AP-1 complex and therefore greatly impedes phosphorylation-dependent transactivation functions of c-Jun (19,20). Furthermore, in A549 human lung carcinoma cells, where the JNK pathway is known to be required for the EGF-stimulated cell growth (23), inhibition of the JNK pathway by the application of high affinity JNK oligonucleotides leads to inhibition of EGF-dependent growth in a manner indistinguishable from that caused by stable expression of mutant Jun (23). Thus, stable expression of mutant Jun appears to be a potent and specific inhibitor of phosphorylation-dependent effects of endogenous c-Jun that are usually promoted by the action of JNK.

T98G cells that express mutant Jun have a marked increase in sensitivity to the DNA damaging drug cisplatin, and to UV radiation, and this increased sensitivity to DNA damage correlates with an inability to repair DNA (16). This suggests that phosphorylation of the wild-type c-Jun subunit of transcription factors such as AP-1 and the c-Jun/ATF2 heterodimer may contribute to DNA repair and survival following DNA damage through induction of DNA synthesis and repair genes such as topoisomerase I and DNA polymerase  $\beta$ , both of which have functional AP-1 and ATF2/CREB sites

(which bind to c-Jun/ATF2) in their promoters (24-27). Phosphorylation of c-Jun may also contribute to cell survival during the crisis phase of tumorigenic transformation by promoting repair of DNA strand breaks generated by the mechanisms that destabilize the genome during tumor progression.

Restoration of p53 function in T98G glioblastoma cells by exposure to p53-adenovirus promotes low levels of apoptosis at gene transfer efficiencies of 50-80% (28). We have found that levels of apoptosis can be significantly increased in these cells when they are treated with p53 adenovirus in combination with DNA damaging agents such as cisplatin and radiation. This is consistent with a model in which the level of DNA damage sustained by the cell is a strong determinant of p53-mediated apoptosis as suggested by Chen *et al* (29). In this study we hypothesized that inhibition of DNA repair by expression of mutant Jun, would also enhance p53-mediated apoptosis. It is known that various forms of genetic instability characteristic of cancer cells, including gene amplification, gene deletion, and broken chromosomes, are related in origin through the involvement of strand breaks (see 30, review). By blocking DNA repair, mutant Jun is predicted to promote elevated levels of strand breaks which then serve as signals for p53-mediated apoptosis. The elevated level of strand breaks could also stimulate further gene amplification. In the studies reported here, we extend and confirm our earlier observations that mutant Jun expression leads to inhibition of DNA repair. Moreover, we show that mutant Jun expression predisposes cells to gene amplification as judged by the amplification of the dihydrofolate reductase (DHFR) gene. We further show that expression of mutant Jun greatly enhances p53-mediated apoptosis. These observations

provide support for the hypothesis that inhibition of DNA repair in cancer cells with unstable genomes enhances sensitivity to DNA damaging chemotherapy and p53-dependent apoptosis.

RESULTS

**T98G mutant Jun-expressing cells resemble parental T98G cells with respect to growth rate and plating efficiency.** We have previously shown that mutant Jun-expressing T98G clone I-10-10 has decreased viability following treatment with cisplatin and other DNA damaging agents likely due to a defect in DNA repair (16). Here we examine this and a second mutant Jun expressing clone, I-10-6, as well as a control c-Jun-expressing clone, T98GcJun, and parental T98G cells for the expression levels of total immunoreactive Jun, for proliferation rates, and for plating efficiencies. Figure 1 shows a Western blot of lysates from each of these four cell lines using an antibody that recognizes both mutant Jun and c-Jun. Equivalent loading was confirmed by stripping the blots and reprobing them with an anti- $\beta$ -actin antibody (not shown). As shown in the figure, mutant Jun modified clones I-10-10 and I-10-6, as well as control c-Jun modified clone T98GcJun, over express total Jun, consistent with expression of the exogenous constructs. The mutant Jun-expressing clones, as well as the control c-Jun-modified clone, show little difference from parental T98G cells with respect to proliferation rate or plating efficiency (Table 1). Only slight growth alterations were observed but these did not correlate with expression of mutant Jun, as clone I-10-10 proliferates about 20% faster than parental cells or c-Jun modified cells and clone I-10-6 proliferates about 20% slower. Therefore, expression of mutant Jun in T98G glioblastoma cells inhibits their ability to repair DNA damage (see below), but it is not growth suppressive in itself.

**T98G mutant Jun expressing cells are defective in repair of cisplatin adducts.**

Cisplatin adduct formation and repair was analyzed by a PCR-based assay (PCR-stop assay) as described in Materials and Methods. Because cisplatin adducts block PCR amplification by Taq polymerase, the intensity of the PCR signal derived from a given amplified region (in our case the hypoxanthine phosphoribosyl transferase (HPRT) gene) is inversely proportional to the platination level and can be used as a quantitative measure of the number of cisplatin-DNA adducts on that region (31). Platination levels determined by PCR amplification of a given housekeeping gene have been shown to correspond to determinations of platination levels on genomic DNA by atomic absorption, demonstrating that the PCR method reflects global DNA platination levels (31). We have also observed in a variety of tumor cell lines that cells shown to be DNA repair deficient by the PCR assay were also defective in repairing a cisplatin damaged reporter plasmid, as assayed by expression of the reporter gene two days following transfection (Gjerset and Haghighi, unpublished). The PCR assay was chosen for these studies as it measures repair of an endogenous genomic sequence. Figure 2 shows the results of a PCR stop assay performed on genomic DNA isolated from parental T98G cells, mutant Jun-expressing I-10-10 and I-10-6 cells, and control c-Jun-expressing T98GcJun cells following treatment with cisplatin, with and without a subsequent 16 hour recovery period. The bars represent the relative amounts of PCR product resulting from PCR amplification of a 2.7 Kb region of the HPRT gene of genomic DNA from cisplatin-treated versus untreated cells. In all cases, the results have been corrected for sample to sample fluctuations in PCR efficiency by normalizing the results to a 170 base PCR product of the same gene, i.e., a fragment too small to register significant levels of

Fig 2

platination and where fluctuation from sample to sample varied by less than 5%. The data show that treatment with 100  $\mu$ M cisplatin results in an immediate decrease in the PCR signal intensity to about 85% of control signals obtained from DNA from untreated cells. Based on a Poisson relationship, this corresponds to an adduct density of about 0.16 adducts per 2.7 KB. By 16 hours post-treatment, both T98G cells and c-Jun-expressing control cells (T98GcJun) have efficiently repaired the adducts and the PCR signal strengths are equal to controls (i.e., no detectable adducts at 16 hours). In contrast, mutant Jun-expressing clones I-10-10 and I-10-6 failed to repair the adducts and PCR signal strengths remain unchanged following the 16 hour recovery period (Figure 2). These observations confirm and extend our earlier results (16) and strongly indicate that inhibition of the JNK pathway effectively blocks DNA repair.

**T98G mutant Jun expressing cells give rise to methotrexate-resistant clones with higher frequency than do parental T98G cells or c-Jun-expressing cells.** Certain types of DNA repair defects contribute to tumorigenesis (32,33) and increased genome instability (34,35). We examined the T98G clones described above for DHFR gene amplification, one measure of genome instability known to correlate with increased tumorigenicity following *in vivo* implantation of cells (36-38). T98G cells were plated in the presence of concentrations of methotrexate 5 times the LD50 and 9 times the LD50 determined for these cells, i.e., concentrations at which gene amplification of DHFR is known to be the predominant mechanism of resistance to the cytotoxic effects of methotrexate (39,40). Thus the frequencies of appearance of methotrexate-resistant clones is a measure of genome instability. As shown in Table 2, T98G I-10-10 cells

produce methotrexate resistant colonies at about 20 times the frequency of the parental T98G cells, and T98G I-10-6 cells produce methotrexate resistant colonies at about 80 times the frequency of parental T98G cells ( $p=0.006$ ). In contrast, stable expression of wild-type *c-Jun* had no effect on the frequency of resistance indicating strongly that interference with a phosphorylation-dependent function of JNK predisposed cells to form resistant colonies.

In order to verify the occurrence of gene amplification in methotrexate resistant colonies, several colonies were picked from each selection condition and expanded. Genomic DNA was prepared and subjected to quantitative PCR analysis using  $^{32}\text{P}$ -labeled primers that define a 270 base fragment of the DHFR gene which includes part of exon 1 and intron A. PCR products were analyzed by agarose gel electrophoresis and quantitated by radioanalytic imaging as described in Material and Methods. The relative increase in PCR product from cellular DNA of methotrexate-resistant cells compared to unselected parental T98G cells was taken as a measure of the increased copy number of the DHFR gene and is indicated in Table 2. The methotrexate resistant clones derived from T98G mutant *Jun* expressing clones have from 2 to 4 times the gene dosage of the DHFR gene relative to parental T98G cells, indicating that the observed methotrexate resistance reflected an increased DHFR gene copy number. We conclude therefore, that inhibition of DNA repair by mutant *Jun* in T98G glioblastoma cells leads to accumulated DNA damage which can promote gene amplification.

**T98G mutant Jun cells are more susceptible than are parental cells to p53-mediated growth suppression.** T98G cells lack wild-type p53 function as a result of a methionine to isoleucine replacement in p53 at codon 237 (41). Restoration of wild-type p53 in T98G cells through gene transfer results in partial G1 arrest (41) or apoptosis (28). Furthermore, agents that promote DNA strand breaks and other forms of DNA damage enhance p53-mediated apoptosis (28). Based on the observations above indicating that mutant Jun-expressing cells are inhibited in DNA damage repair and predisposed to gene amplification, we predicted that strand breaks would accumulate in mutant Jun-expressing cells thereby leading to increased p53-dependent growth inhibition and apoptosis. Figure 3 compares the growth inhibition of Ad-p53-transduced cells relative to Ad-βgal-transduced cells 6 days post-infection. The results represent the average of two experiments performed on separate occasions, with each experiment being performed in triplicate. The infection efficiency, determined by X-gal staining of parallel cultures with Ad-βgal, was about 50% in all cases, low enough to cause incomplete growth suppression of parental T98G cells and control cells modified to stably express wild-type c-Jun as shown in Figure 3. Growth studies revealed that T98G I-10-10 and I-10-6 cells were considerably more growth suppressed upon expression of p53 under these conditions. Western blot analysis (Figure 4) of the p53-responsive gene product, p21<sup>waf1/cip1</sup> in cell lysates 48 hours post-infection shows induction of p21<sup>waf1/cip1</sup> in all cases. The data thus show that p21<sup>waf1/cip1</sup> is not a crucial player in this setting. Equivalent loading was confirmed by stripping the blots and reprobing them with an anti-β-actin antibody (not shown).

Fig 3

Fig 4

**T98G mutant Jun cells expressing cells are more susceptible to p53-mediated**

**apoptosis.** In order to determine whether the p53-mediated growth inhibition of T98G mutant Jun expressing cells observed in Figure 3 could be accounted for by the induction of apoptosis, we assayed the cytoplasmic fractions of Ad-p53 or Ad- $\beta$ gal-infected cells, 48 hours post-infection, for the presence of oligonucleosomal fragments (Figure 5).

These fragments are released from the nuclei of cells undergoing apoptosis, and can be detected by an ELISA assay using anti-histone antibodies and anti-DNA peroxidase antibodies. We assayed for apoptosis 48 hours following exposure to p53-adenovirus or  $\beta$ -gal adenovirus as this is the point at which we have observed maximal transgene expression in Ad- $\beta$ -gal-infected cells (unpublished observations). Figure 5A shows the results of the ELISA assay on the various T98G cell clones. Low levels of oligonucleosomal fragment release similar to levels observed in uninfected cells were observed in Ad- $\beta$ -gal-infected cells. Treatment of parental T98G cells and control wild-type c-Jun -expressing T98GcJun cells with Ad-p53 (100 pfu/cell, 3 hours) resulted in virtually no induction of apoptosis under our conditions, consistent with growth assays showing no suppression of overall growth following treatment of these cell lines with Ad-p53. However, readily detectable and significantly increased levels of apoptosis were observed in mutant Jun expressing clones I-10-10 and I-10-6. These results are consistent with the appearance of Ad-p53-treated cultures as shown in Figure 5B. Ad-p53-treated I-10-10 and I-10-6 cells lose contact with neighbors, become large and contain cytoplasmic vacuoles. Thus p53-mediated apoptosis is markedly enhanced in mutant Jun-expressing cells, possibly as a consequence of being triggered by endogenous strand breaks that fail to be repaired.

To confirm a p53-dependent mechanism of apoptosis, we carried out a Western blot analysis of the apoptosis regulatory proteins bax and bcl<sub>2</sub> in cells treated with Ad-p53 or Ad-βgal (Figure 6). The levels of the proapoptotic effector, bax, whose gene is induced by p53 (42), increase following treatment with Ad-p53, as expected, while levels of the antiapoptotic protein bcl<sub>2</sub> remain largely unchanged. A comparison of the bax to bcl<sub>2</sub> protein is indicated by the ratios under the lanes in Figure 6. The bax/bcl<sub>2</sub> ratio following treatment with Adp53 is significantly higher in mutant Jun-expressing cells I-10-10 and I-10-6 (ratios of 10 and 2.5, respectively) than in parental cells (ratio of 1.7) and c-Jun control cells (ratio of 0.8). Furthermore, a comparison of these ratios in uninduced *versus* induced cells (Adβgal-treated *versus* Adp53-treated) reveals a 3 to 4-fold increase for the Adp53-treated parental and cJun-expressing control cells compared to the same cells treated with Adβgal, whereas Adp53-treated mutant Jun-expressing cells I-10-10 and I-10-6 show an increase of some 8 to 25 fold, respectively, compared to the same cells treated with Adβgal. In accordance with other data suggesting that the bax to bcl<sub>2</sub> ratio is a critical determinant of apoptosis (see 43, review), these data support a role for bax in the increased apoptosis observed after Adp53 treatment of mutant Jun-expressing cells.

DISCUSSION

In this study we have examined how a dominant-negative inhibitor of phosphorylated wild-type c-Jun downstream targets affects cell proliferation, DNA repair, susceptibility to p53-mediated apoptosis, and DHFR gene amplification in T98G glioblastoma cells.

The JNK/SAPK pathway is a cellular DNA damage and stress response pathway that is activated by a variety of signals including mitogens such as EGF (23), oncogenes (19), and numerous DNA damaging agents such as UV radiation and cisplatin (15-17).

Phosphorylation of c-Jun by JNK, activates the transcriptional potential of AP-1 and related transcription factors such as c-Jun/ATF2, which employ c-Jun as a heterodimeric partner in the transcription complex. The non-phosphorylatable mutant Jun construct used in these and earlier studies resembles normal cellular c-Jun except for two alanine replacements at positions 63 and 73. This change has been shown to abrogate the co-transformation properties of c-Jun with H-ras in rat embryo fibroblasts (19,20), and to block EGF-induced proliferation of lung carcinoma cells (23). T98G glioblastoma cells expressing this mutant Jun have reduced viability following treatment with the DNA damaging drug cisplatin (16) and this result is due to an inability to repair cisplatin adducts, as we show here and in an earlier study (16). Thus, the JNK pathway may promote cell survival during transformation and in response to DNA damage.

In this study we extend the analysis of the T98G mutant Jun clones analyzed previously.

We observe that they grow with similar doubling times and have similar plating

efficiencies as parental T98G cells or c-Jun-modified control cells, indicating that stable expression of mutant Jun does not substantially alter DNA synthesis. However, methotrexate-resistant clones arising in the presence of  $\geq 5 \times \text{LD50}$  are generated at a 20 to 80 fold higher frequency in mutant Jun-expressing clones compared to parental T98G cells and the wild-type c-Jun expressing clone, T98GcJun. Under these conditions, resistance to methotrexate is known to be primarily due to amplification of the DHFR gene (39,40). We confirmed a low but detectable increase in DHFR gene copy number of about 2-4 fold compared to parental T98G cells by quantitative PCR analysis of genomic DNA isolated from several representative clones of methotrexate-selected T98G I-10-10 and I-10-6 cells. Though low, such an increase in copy number could explain the increase in methotrexate resistance observed in these cells, and is supported by previous studies which showed that a low level of DHFR gene amplification was sufficient to confer resistance to methotrexate (44). Furthermore, mutant Jun-expressing T98G cells, which do not express endogenous wild-type p53, exhibited increased growth suppression and apoptosis following exposure to p53 adenovirus and restoration of wild-type p53 function. Therefore, mutant Jun alone had little effect on the growth properties of T98G cells but manifested a negative effect on growth in the presence of wild-type p53.

Our results demonstrate that expression of a non-phosphorylatable mutant Jun but not c-Jun leads to a defect in DNA repair and contributes to increased gene amplification, one manifestation of genomic instability in mammalian cells. These observations are consistent with other examples where DNA repair defects are seen to underlie a genome instability phenotype (34,35). The results suggest that the DNA repair defect associated

with expression of mutant Jun may generate elevated levels of strand breaks in T98G cells compared to T98G parental cells and c-Jun-modified cells, both of which have an intact JNK pathway. The elevated level of breaks may in turn serve as initiation events for increased gene amplification (45) as well as triggers for DNA damage-induced stabilization of transduced wild-type p53 leading to apoptosis. Our results directly demonstrate both gene amplification and significantly increased p53-dependent apoptosis in mutant Jun-expressing cells in support of this hypothesis.

One possible explanation for our observations is that one or more downstream targets of wild-type c-Jun promotes repair of endogenous strand breaks. Candidate targets include DNA polymerase  $\beta$ , PCNA (proliferating cell nuclear antigen), topoisomerase I, topoisomerase II, and GADD153, all of which have potential AP-1 or c-Jun/ATF2 binding sequences in their promoter regions (see 24-27, 46, review). In the cases of DNA polymerase  $\beta$  and topoisomerase I, these c-Jun/ATF2 binding sites are known to be functional and stress activated (46). Moreover, all of these gene products have been implicated in the repair of cisplatin-DNA adducts (47). Thus while an intact JNK pathway in T98G parental cells and in c-Jun modified control cells would not directly prevent DNA damage-induced p53 stabilization, the pathway would act indirectly to attenuate p53-mediated apoptosis by efficiently promoting repair of endogenous strand breaks that would trigger p53 stabilization.

An additional mechanism also may play a role in cells expressing endogenous wild-type p53. Shreiber *et al* (21) have recently shown that c-Jun directly down-regulates p53

expression through binding to a variant AP-1 site in the endogenous cellular p53 promoter. In their study, negative regulation of p53 by c-Jun appeared to be crucial to cellular transformation in that transgenic mouse embryo fibroblasts (MEFs) lacking c-Jun displayed proliferation defects, elevated p53 expression, and prolonged transit through crisis prior to spontaneous immortalization. Thus c-Jun may attenuate p53-mediated apoptosis both by down-regulating expression of p53 and by promoting repair of endogenous DNA damage that could trigger p53 stabilization and apoptosis.

Two independently derived mutant Jun-expressing clones show a similar properties, whereas a third clone expressing wild-type c-Jun and maintained in culture for a similar period did not share any of these properties. These observations strengthen the argument that down regulation of DNA repair as a consequence of mutant Jun expression underlies the elevation in DHFR gene amplification, and enhanced predisposition to p53-mediated apoptosis. Our results suggest in addition that increased expression of the p53-regulated proapoptotic effector, bax, leads to an increased bax/bcl<sub>2</sub> ratio that contributes to enhanced apoptosis in mutant Jun-expressing cells following exposure to p53 adenovirus. This is consistent with a variety of observations in other systems showing the importance of the bax/bcl<sub>2</sub> ratio in determining apoptosis (see 43, review). Thus, an elevated level of endogenous DNA strand breaks in mutant Jun-expressing cells may result in increased stabilization and activation of p53 and increased induction of bax.

The recent identification of p53 as a physiological substrate for JNK (48) indicates that the JNK response extends to other targets besides c-Jun, and these could mediate the

various aspects of the stress response. Although inhibited in c-Jun phosphorylation, T98G cells modified with mutant Jun express constitutively active JNK at levels similar to the parental T98G cells. They would therefore be expected to carry out phosphorylation of other JNK substrates similarly to parental cells. The ability of T98G mutant Jun cells to carry out apoptosis following restoration of p53 activity suggests that any JNK-related apoptotic functions are not disrupted by the mutant Jun modification.

Consistent with our observations that the mutant Jun modification has no significant effect on cell growth or plating efficiency of T98G cells, is a study demonstrating that embryonal stem (ES) cells lacking c-Jun had similar viability and growth rate as parental ES cells, and were able to efficiently transactivate AP-1 reporter constructs (49). Thus most of the functions of c-Jun in ES cells appeared to be complemented by other Jun proteins. In our case, mutant Jun itself may be able to carry out the c-Jun functions required for basal growth. However, phosphorylation of c-Jun appears to be critical in the cellular response to DNA damage.

Our results can be understood in light of a growing body of evidence supporting a role for p53 in modulating apoptosis in response to DNA damage (see review, ref. 50), and in proportion to the extent of damage (29). p53 is a DNA damage recognition protein known to bind to a variety of types of DNA damage, including single stranded ends (2), and insertion-deletion loops (3). These types of damage, which could serve as triggers for p53-mediated apoptosis are likely to be generated in tumor cells by the mechanisms that promote spontaneous gene rearrangements, deletions, and amplifications. As such, a

failure of DNA repair in mutant Jun-expressing cells would promote the accumulation of strand breaks, which would, on the one hand, favor gene amplification and other manifestations of genome instability, and on the other hand, promote DNA damage-induced stabilization of p53 and apoptosis.

As depicted in the scheme in Figure 7, we hypothesize that activation of JNK and loss of p53 represent independent mechanisms by which tumor cells undergoing progression accommodate increased levels of genomic instability and insure survival while sustaining potentially lethal genome destabilizing events. By promoting DNA repair, the JNK pathway may limit damage to levels compatible with survival. Loss of p53 would further enhance survival owing to a down-regulated apoptotic response to unrepaired damage.

#### MATERIALS AND METHODS

**Cell Lines.** T98G glioblastoma cells were obtained from Dr. Hoi U (University of California, San Diego) and cultured at 37° C in 10% CO<sub>2</sub> in Dulbecco's Modified Eagles Medium (DMEM) supplemented with 10% newborn calf serum. The T98G clones that had been modified to express mutant Jun, termed T98G-dnJun-I-10-10 and I-10-6 (see 16), or simply T98G I-10-10 and T98G I-10-6, were cultured in the same way as were T98G cells except that 100 µg/ml hygromycin was added to the culture medium. The pLHC*mjun* vector encodes a dominant negative mutant of c-Jun and was prepared as previously described (51) by insertion of DNA encoding mutant Jun (obtained by site-directed mutagenesis by M. Karin and colleagues (20)) into the retroviral vector pLHCX.

Mutant Jun has ser → ala substitutions at positions 63 and 73, two sites of DNA damage-induced phosphorylation in wild-type c-Jun and cannot be phosphorylated at these sites. As a control T98G cells modified to overexpress wild-type c-Jun (T98GcJun) were obtained by cotransfection with a *c-jun* expression vector, pSV2*cjun* and with pSV2neo, and were cultured similarly, with the addition of 100 µg/ml G418.

**Western blot analysis.** Levels of total cellular Jun protein (c-Jun + mutant Jun), as well as levels of the gene products of the p53-regulated genes p21<sup>waf1</sup>, bax, and bcl<sub>2</sub> were determined by western blot analysis. Cell lysates (20-40µg) were electrophoresed on a 12% acrylamide gel and blotted onto nylon membranes. Membranes were then treated with rabbit polyclonal anti c-Jun (1:200), or with mouse monoclonal anti p21<sup>waf1</sup> (1:200), or with rabbit polyclonal anti bax (1:200), or with mouse monoclonal anti bcl<sub>2</sub> (1:100) followed by an appropriate anti-rabbit or anti-mouse secondary antibody conjugated with horseradish peroxidase. All antibodies were purchased from Santa Cruz Biotechnology, Inc.(Santa Cruz CA) and used according to the protocol recommended by the manufacturer. Antibody reactive bands were revealed using the ECL Western detection system (Amersham Life Sciences, U.K.). For quantitation of bands, we used Kodak digital camera and analysis software.

**Analysis of repair of cisplatin-DNA adducts.** Cisplatin (cis-diamminedichloroplatinum) adduct formation and repair was analyzed by a PCR-based DNA damage assay (PCR-stop assay)(31). The assay is based on observations that Taq polymerase is blocked at cisplatin adducts, was used to analyze cisplatin adduct formation and repair. Since DNA

fragments are platinated randomly, the distribution of damage fits a Poisson distribution, where a mean level of one adduct per fragment (i.e., the portion of the genome defined by the forward and reverse PCR primers) will leave 37% of the fragments undamaged and these will be amplified to produce a PCR signal 37% of that from control DNA. For cisplatin treatments, cells were plated at 50% confluency in three wells of a 6 well plates in standard medium described above. Following attachment, duplicate wells were treated with 100  $\mu$ M cisplatin (Platinol™, aqueous solution at 1 mg/ml, purchased from local pharmacies) for one hour 15 minutes, and one well was left untreated. Following treatment, the untreated cells, and one well of 100  $\mu$ M cisplatin-treated cells were harvested and genomic DNA was prepared. The remaining treated well was incubated an additional 16 hours in the absence of cisplatin before harvesting. DNA was prepared using the QIAmp blood kit essentially following the manufacturer's protocol, except that cells were lysed directly on the plate in the presence of PBS, Qiagen protease and lysis buffer supplied in the kit. Following purification, DNA was adjusted to 0.5 mg per ml in sterile water and stored at  $-20^{\circ}$  C. Quantitative PCR was used to compare cisplatin adduct formation on a 2.7 kilobase region of the HPRT gene. As an internal control for PCR efficiency, we PCR-amplified from the same templates, a 170 base non-overlapping region of the same gene. The smaller region represents a target too small to register significant levels of damage under our conditions. We found that both the 2.7 Kb and 170 base products increased linearly with input template over the range 0.1 to 0.5  $\mu$ g DNA per 25  $\mu$ l reaction, and we therefore routinely used 0.125 to 0.25  $\mu$ g template per reaction. Reactions were performed in 25  $\mu$ l using 0.125 – 0.25  $\mu$ g DNA, 25 pmole each of forward and reverse primer, 250  $\mu$ M dNTPs (Pharmacia) 1.25 units Taq polymerase

(Qiagen), 1x buffer (Qiagen) and solution Q (Qiagen). Bands were quantitated using a Kodak digital camera and analysis software. The amplification program was as follows: 1 cycle (94° C, 1 minute 30 seconds); 25 cycles (94° C, 1 minute, 57° C, 1 minute, 70° C, 2 minutes 30 seconds); 1 cycle (94° C, 1 minute, 57° C, 1 minute, 70° C, 7 minutes). All assays were performed in triplicate on two separate occasions.

***Virus.*** Replication-defective Adenoviruses (Ad-p53 and Ad-βgal) in which the human p53 coding sequence or the bacterial β-galactosidase gene, respectively, replaced the viral early region E1A and E1B genes were provided by Introgen Therapeutics, Inc. (Houston, TX).

***Virus treatments.*** Cells at 80% confluence were placed in DMEM supplemented with 2% heat-inactivated fetal bovine serum and infected for 3 hours at a multiplicity of 100 pfu per cell. The efficiency of infection was determined by X-gal (5-bromo-4-chloro-3-indolyl-β-D-galactopyranoside) staining a sample of the β-gal virus-infected cells (see 28), and was usually ≥ 50%.

***Viability and growth assays.*** Following infection, triplicate aliquots of cells were replated in 96-well plates at a density of 1000 cells per well. Plates were incubated for 5-7 days and surviving cells were determined by adding a solution containing MTS (3-(4,5'-dimethylthiazol-2-yl)-5-(3-carboxymethoxyphenyl)-2-(4-sulfophenyl)-2H-tetrazolium inner salt) and PMS (phenazine methosulfate) (both purchased from Promega, Madison, WI.) for 1 hour and determining A590 nm of the resulting formazan

product, following procedures provided by the manufacturer. For growth assays, cells were plated at 1000 cells per well in 96-well plates. On successive days from day 1 through day 8, triplicate samples were stained with MTS as described above.

***Generation of methotrexate-resistant clones.*** LD50 values for methotrexate were determined for the cell lines to be tested. Cells were seeded at a starting density of  $10^3$  cells per  $\text{cm}^2$  and allowed to attach for 16 hours. Methotrexate (Sigma, St. Louis, MO) was then added to a concentration of 5 x LD50 or 9 x LD50, concentrations known to select for DHFR gene amplification (39,40). Medium with fresh methotrexate was replaced weekly. When colonies developed and reached a size of about 100-200 cells (about 5 weeks), plates were washed in PBS and stained with 1% methylene blue in 70% methanol.

***Analysis of DHFR gene copy number.*** To verify DHFR gene amplification following selection in methotrexate as described above, several clones were picked and expanded. Genomic DNA from these clones, as well as from parental unselected cells was prepared from about  $10^6$  cells in each case using the QIAamp Blood Kit™ (Qiagen Inc., Chatsworth, CA) and resuspended at 0.5 mg/ml in sterile  $\text{H}_2\text{O}$ . Quantitative PCR was performed in 50  $\mu\text{l}$  aliquots containing 0.2  $\mu\text{g}$  DNA, 50 pmol each of forward and reverse primers defining a 270 base pair region of exon 1 and intron A of the dihydrofolate reductase gene (see below), 50 mM KCL, 10 mM Tris pH 8.3, 1.5 mM  $\text{MgCl}_2$ , 250 mM dNTPs, 0.5  $\mu\text{l}$  Tac polymerase (Qiagen Inc., Chatsworth, CA), 10  $\mu\text{l}$  Q buffer™ (Qiagen, Inc., Chatsworth, CA) and 1 pmol radioactively end-labeled reverse primer (labeled with

$\gamma$ -<sup>32</sup>P-dATP). PCR conditions were as follows: 1 cycle: 94° C (1'30"); 25 cycles: 94°(1 min)-57°(1 min)-70°(2'30"); 1 cycle: 94°(1 min)-57°(1 min)-70°(7'). Following PCR, 10  $\mu$ l aliquots were electrophoresed on a 1% agarose gel. The gel was vacuum-dried for two hours onto filter paper and the PCR-amplified 270 base pair band was quantitated using an Ambis4000 Radioanalytic Imaging system (Ambis, Inc., San Diego, CA). Quantitative conditions were established by demonstrating in control reactions with known amounts of DNA in two-fold dilutions that product formation was directly proportional to input template. Primer sequences for the dihydrofolate reductase gene were as follows: (forward primer) 5'-GGTTCGCTAAACTGCATCGTCGC-3' and (reverse primer) 5'-CAGAAATCAGCAACTGGGCCTCC-3'. An increase in DHFR gene copy number was then equal to the fold increase in the PCR product from cellular DNA of methotrexate-resistant clones compared to that of unselected parental cells.

***Apoptosis assay.*** Apoptosis was assayed using the Cell Death Detection ELISA (Boehringer Mannheim, Indianapolis, IN), a quantitative photometric peroxidase immunoassay that detects cytoplasmic histone-associated DNA fragments (mono- and oligonucleosomes) that are released from the nuclei of cells undergoing apoptosis.  $2 \times 10^5$  cells were plated in 24-well plates and infected the next day (when the cells were about 80% confluent) with Ad-p53 or Ad- $\beta$ gal as described above. 48 hours post-infection, cells were collected and cytoplasmic fractions were prepared and assayed for the presence of mono- and oligonucleosomes by following the manufacturer's protocol.

Acknowledgements: We thank M. Karin for providing the mutant Jun expression vectors, and Dr. Hoi U for providing the T98G cells.

Footnotes

<sup>1</sup>This work was supported in part by funds provided by grants from the National Cancer Institute CA69546 (RAG), CA63783-05 (DAM), CA76173-01 (DAM), the Department of Defense (RAG), Introgen Therapeutics, Inc., Houston, Texas (RAG), and the Breast Cancer Research Program of the University of California 83401 (DAM).

<sup>2</sup> To whom requests for reprints should be addressed. Phone: 619-450-5990, FAX: 450-3251, email:rgjerset@skcc.org.

<sup>3</sup>Potopova, O. and Mercola, D., unpublished observations

Table 1. *Culture characteristics of T98G clones*

clone	Relative doubling time <sup>a</sup>	plating efficiency <sup>b</sup>
T98G	1	47% ± 3%
T98GcJun (control)	1.0 ± 0.14	52% ± 17%
I-10-10	0.83 ± 0.10	42% ± 13%
I-10-6	1.2 ± 0.04	45% ± 2%

- a) Average of 2 experiments on different occasions, each in triplicate.  
b) Average of 3 experiments on different occasions, each in triplicate.

Table 2. *Frequency of methotrexate-resistant colonies arising from T98G, T98GcJun and T98G mutant Jun clones I-10-10 and I-10-6.*

Cells were plated at a density of  $10^5$  cells per 10-cm culture dish and incubated 4 weeks in the presence of methotrexate at the indicated concentrations. Plates were then stained with 70% methylene blue in methanol and colonies were counted. For analysis of DHFR gene amplification, several colonies were picked prior to staining, expanded and cellular DNA was prepared and subjected to quantitative PCR analysis.

Clone	methotrexate dose <sup>a</sup>	Frequency of colonies per $10^5$ cells (average of 3 experiments)	DHFR gene dosage relative to parental in representative colonies
T98G parental	5 x LD50	$2.3 \pm 2.5$	1
	9 x LD50	$0.3 \pm 0.6$	
T98GcJun (control)	5 x LD50	2 <sup>b</sup>	n/t
	9 x LD50	0	
I-10-10	5 x LD50	$38 \pm 19$	3-4
	9 x LD50	$6 \pm 5$	
I-10-6	5 x LD50	$174 \pm 21$	2
	9 x LD50	$16 \pm 12$	

a) LD50 = 0.1  $\mu$ M (T98G, T98GcJun) or 0.04  $\mu$ M (I-10-10, I-10-6)

b) One experiment.

Figure Legends

Figure 1. Western blot analysis of total c-Jun plus mutant Jun in lysates of control c-Jun-modified clone, T98GcJun (lane 1), T98G mutant Jun expressing clones, I-10-6 (lane 2) and I-10-6 (lane 3), and parental T98G cells (lane 4). Each lane represents the electrophoresis of 40  $\mu$ g of total protein.

Figure 2. PCR-stop assays of cisplatin adduct formation and repair. A 2.7 Kb region of the HPRT gene was PCR amplified from genomic DNA from untreated cells or from cells treated 1 hour 15 minutes with 100  $\mu$ M cisplatin and harvested either immediately or 16 hours after treatment. The bars represent the relative amounts of PCR product obtained from damaged versus undamaged templates. The results represent the averages of triplicate PCR reactions performed on two independent occasions.

Figure 3. 6 day viability assay of T98G subclones following treatment with Ad-p53, 100 pfu/cell for 3 hours. Viability of Ad-p53-treated cultures is represented as a percentage of the same culture treated under identical conditions with Ad- $\beta$ gal.

Figure 4. Western blot analysis of p21<sup>waf1</sup> protein in lysates from T98G parental cells, mutant Jun-expressing clones I-10-10 and I-10-6, and control c-Jun expressing clone T98GcJun, 48 hours after treatment with Ad- $\beta$ gal or Ad-p53, 100 pfu per cell for 3 hours. Each lane represents 40  $\mu$ g of protein and are as follows: Lane 1 (T98G parental-Ad $\beta$ gal), Lane 2 (T98G parental-Adp53), Lane 3 (mutant Jun clone I-10-10-Ad $\beta$ gal), Lane 4

(mutant Jun clone I-10-10-Adp53), Lane 5 (mutant Jun clone I-10-6-Ad $\beta$ gal), Lane 6 (mutant Jun clone I-10-6-Adp53), Lane 7 (control T98GcJun-Ad- $\beta$ gal), Lane 8 (control T98GcJun-Adp53).

Figure 5. (A) ELISA apoptosis assay of cytoplasmic nucleosomes in untreated cells, or in cells 48 hours after being treated with 100 pfu per cell of Ad- $\beta$ gal or Ad-p53 for 3 hours. (B) Light microscopy (40x) of untreated cells (top row), or cells 72 hours following treatment with Ad- $\beta$ gal (middle row) or Ad-p53 (bottom row). Columns are as follows: (Column A) T98G parental cells, (Column B) c-Jun-modified clone T98GcJun, (Column C) mutant Jun modified clone I-10-6, (Column D) mutant Jun modified clone I-10-10.

Figure 6. Western blot analysis of bax and bcl<sub>2</sub> protein in lysates from T98G parental cells, mutant Jun-expressing clones I-10-10 and I-10-6, and control c-Jun-expressing clone T98GcJun, 48 hours after treatment with Ad- $\beta$ gal or Adp53, 100 pfu per cell for 3 hours. Each lane represents 15  $\mu$ g protein for the bax analysis and 30  $\mu$ g protein for the bcl<sub>2</sub> analysis. Following immunostaining and band detection with ECL Western reagent, bands were quantitated using Kodak digital software. Ratios of bax to bcl<sub>2</sub> are indicated below the lanes. Experiment was carried out twice with similar results.

Figure 7. Model explaining how, through inhibition of potential c-Jun downstream targets leading to DNA repair (e.g., DNA polymerase  $\beta$ , topoisomerase I, II, PCNA), mutant Jun promotes the accumulation of endogenous DNA strand breaks in genomically

unstable tumor cells and thus collaborates with p53 to promote p53-mediated induction of bax and apoptosis.

References

1. Nowell, P.C. The clonal evolution of tumor cell populations. *Science (Washington DC)*, 194: 23-28, 1976.
2. Bakalkin, G., Selivanova, G., Yakovleva, T., Kiseleva, E., Kashuba, E., Magnusson, K.P., Szekely, L., Klein, G., Terenus, L., and Wiman, K.G. p53 binds single stranded DNA ends through the C-terminal domain and internal DNA segments via the middle domain. *Nucl. Acids Res.*, 23: 362-369, 1995.
3. Lee, S., Elenbas, B., Levine, A., and Griffith, J. p53 and its 14kDa C-terminal domain recognize primary DNA damage in the form of insertion/deletion mismatches. *Cell*, 81: 1013-1021, 1995.
4. Shieh, S-Y., Ikeda, M., Taya, Y., and Prives, C. DNA damage-induced phosphorylation of p53 alleviates inhibition by MDM2. *Cell*, 91:325-34, 1997.
5. Woo, R.A., McLure, K.G., Lees-Miller, S.P., Rancourt, D.E., and Lee, P.W. DNA-dependent protein kinase acts upstream of p53 in response to DNA damage. *Nature (London)*, 394:700-704.
6. Tainsky, M.A., Bischoff, F.Z., and Strong, L.C. Genomic instability due to germline p53 mutations drives preneoplastic progression toward cancer in human cells. *Cancer Metastasis Rev.*, 14: 43-48, 1995.
7. Agapova, L.S., Ilyinskaya, G.V., Turovets, N.A., Ivanov, A.V., Chumakov, P.M., and Kopnin, B.P. Chromosome changes caused by alterations of p53 expression. *Mutat. Res.*, 354: 129-138, 1996.

8. Bertrand, P., Rouillard, D., Boulet, A., Levalois, C., Soussi, T., and Lopez, B.S. Increase of spontaneous intrachromosomal homologous recombination in mammalian cells expressing a mutant p53 protein. *Oncogene*, *14*: 1117-1122, 1997.
9. Bouffler, S.D., Kemp, C.J., Balmain, A., and Cox, R. Spontaneous and ionizing radiation-induced chromosomal abnormalities in p53-deficient mice. *Cancer Res.*, *55*: 3883-3889, 1995.
10. Donehower, L.A., Godley, L.A., Aldaz, C.M., Pyle, R., Shi, Y.-P., Pinkel, D., Gray, J., Bradley, A., Medina, D., and Varmus, H.E. Deficiency of p53 accelerates mammary tumorigenesis in wnt-1 transgenic mice and promotes chromosomal instability. *Genes Dev.*, *9*: 882-895, 1995.
11. Lanza, G. Jr., Maestri, I., Dubini, A., Gafa, R., Santini, A., Ferretti, S., and Cavazzini, L. p53 expression in colorectal cancer: relation to tumor type, DNA ploidy pattern and short-term survival. *Am. J. Clin. Pathol.*, *105*:604-612, 1996.
12. Gryfe, R., Swallow, C., Bapat, B., Redston, M., Gallinger, S., and Couture, J. Molecular biology of colorectal cancer. *Curr. Probl. Cancer*, *21*:233-300, 1997.
13. Levine, A.J. p53, the cellular gatekeeper for growth and division. *Cell*, *88*: 323-331, 1997.
14. Derijard, B., Hibi, M., Wu, I.H., Barrett, T., Su, B., Deng, T., Karin, M., and Davis, R.J. JNK1: a protein kinase stimulated by UV light and Ha-ras that binds and phosphorylates the c-Jun activation domain. *Cell*, *76*: 1025-1037, 1994.
15. Adler, V., Fuchs, S.Y., Kim, J., Kraft, A., King, M.P., Pelling, J., and Ronai, Z. Jun-NH<sub>2</sub>-terminal kinase activation mediated by UV-induced DNA lesions in melanoma and fibroblast cells. *Cell Growth Differ.*, *6*: 1437-1446, 1995.

23. Bost, F., McKay, R., Dean, N., and Mercola, D. The Jun kinase/stress-activated protein kinase pathway is required for epidermal growth factor stimulation of growth of human A549 lung carcinoma cells. *J. Biol. Chem.*, 272:33422-33429, 1997.
24. Srivastava, D.K., Rawson, T.Y., Showalter, S.D., and Wilson, S.H.. Phorbol ester abrogates up-regulation of DNA polymerase beta by DNA-alkylating agents in Chinese hamster ovary cell. *J. Biol. Chem.*, 270:16402-16408. 1995.
25. Kedar, P.S., Widen, S.G., Englander, E.W., Fornace, A.J. Jr., and Wilson, S.H. The ATF/CREB transcription factor-binding site in the polymerase beta promoter mediates the positive effect of N-methyl-N-nitro-N-nitrosoguanidine on transcription. *Proc. Natl. Acad. Sci. USA*, 88:3729-3733, 1991.
26. Baumgartner, B., Heiland, S., Kunze, N., Richter, A., and Knippers, R. Conserved regulatory elements in the type I DNA topoisomerase gene promoters of mouse and man. *Biochim. Biophys. Acta*, 1218:123-127, 1994.
27. Heiland, S., Knippers, R., and Kunze, N. The promoter region of the human type-I-DNA-topoisomerase gene. Protein-binding sites and sequences involved in transcriptional regulation. *Eur. J. Biochem.*, 217:813-22 1993.
28. Gjerset, R.A., Turla, S.T., Sobol, R.E., Scalise, J.J., Mercola, D., Collins, H., and Hopkins, P.J. Use of wild-type *p53* to achieve complete treatment sensitization of tumor cells expressing endogenous mutant *p53*. *Mol. Carcinog.*, 14: 275-285, 1997.
29. Chen, X., Ko, L.J., Jayaraman, L., and Prives, C. *p53* levels, functional domains, and DNA damage determine the extent of the apoptotic response of tumor cells. *Genes Dev.*, 10: 2438-2451, 1996.

16. Potapova, O., Haghighi, A., Bost, F., Liu, C., Birrer, M.J., Gjerset, R., and Mercola, D. The JNK/stress-activated protein kinase pathway functions to regulate DNA repair and inhibition of the pathway sensitizes tumor cells to cisplatin. *J. Biol. Chem.*, *272*: 14041-14044, 1997.
17. Saleem, A., Datta, R., Yuan, Z.M., Kharbanda, S., and Kufe, D. Involvement of stress-activated protein kinase in the cellular response to 1-beta-D-arabinofuranosylcytosine and other DNA damaging agents. *Cell Growth Differ.*, *6*: 1651-1658, 1995.
18. Osborne, M.T. and Chambers, T.C. Role of stress-activated/c-Jun NH<sub>2</sub>-terminal protein kinase pathway in the cellular response to adriamycin and other chemotherapeutic drugs. *J. Biol. Chem.*, *271*: 30950-30955, 1996.
19. Binétruy, B., Smeal, T., and Karin, M. Ha-ras augments c-Jun activity and stimulates phosphorylation of its activation domain. *Nature (London)*, *351*: 122-127, 1991.
20. Smeal, T., Binétruy, B., Mercola, D.A., Birrer, M., and Karin, M. Oncogenic and transcriptional cooperation with Ha-ras requires phosphorylation of c-Jun on serines 63 and 73. *Nature (London)*, *354*: 494-496, 1991.
21. Schreiber, M., Kolbus, A., Piu, F., Szabowski, A., Mohle-Steinlein, U., Tian, J., Karin, M., Angel, P., and Wagner, E.F. Control of cell cycle progression by c-Jun is p53 dependent. *Genes Dev.*, *13*:607-619, 1999.
22. Takahashi, J.A., Fukumoto, M., Kozai, Y., Ito, N., Oda, Y., Kikuchi, H., and Hatanaka, M. Inhibition of cell growth and tumorigenesis of human glioblastoma cells by neutralizing antibody against human basic fibroblast growth factor. *FEBS Lett.*, *288*: 65-71, 1991.

30. Stark, G.R. Regulation and mechanisms of mammalian gene amplification. *Adv. Cancer Res.*, *61*: 87-113, 1993.
31. Jennerwein, M.M. and Eastman, A. A polymerase chain reaction-based method to detect cisplatin adducts in specific genes. *Nucleic Acids Res.*, *19*: 6209-6214, 1991.
32. Robbins, J.H. and Burk, P.G. Relationship of DNA repair to carcinogenesis in xeroderma pigmentosa. *Cancer Res.*, *33*: 929-935, 1973.
33. Nacht, M., Strasser, A., Chan, Y.R., Harris, A.W., Schlissel, M., Bronson, R.T., and Jacks, T. Mutations in the p53 and SCID genes cooperate in tumorigenesis. *Genes Dev.*, *10*: 2055-2066, 1996.
34. Melton, D., Ketchen, A.M., Nuñez, F., Bonatti-Abbondandolo, S., Abbondandolo, A., Squires, S., and Johnson, R. Cells from ERCC1-deficient mice show increased genome instability and a reduced frequency of homologous recombination. *J. Cell. Sci.*, *111*: 395-404, 1998.
35. Lengauer, C., Kinzler, K.W., and Vogelstein, B. Genetic instability in colorectal cancers. *Nature (London)*, *386*: 623-627, 1997.
36. Sager, R., Gadi, I.K., Stephens, L., and Grabowy, C.T. Gene amplification: an example of accelerated evolution in tumorigenic cells. *Proc. Natl. Acad. Sci. USA*, *82*: 7015-7019, 1985.
37. Otto, E., McCord, S., and Tlsty, T.D. Increased incidence of CAD gene amplification in tumorigenic rat lines as an indicator of genomic instability of neoplastic cells. *J. Biol. Chem.*, *264*: 3390-3396, 1989.
38. Tlsty, T.D. Normal diploid human and rodent cells lack a detectable frequency of gene amplification. *Proc. Natl. Acad. Sci. USA*, *87*: 3132-3136, 1990.

39. Brown, P.C., Tlsty, T.D., and Schimke, R.T. Enhancement of methotrexate resistance and dihydrofolate reductase gene amplification by treatment of mouse 3T6 cells with hydroxyurea. *Mol. Cell. Biol.*, 3: 1097-1107, 1983.
40. Tlsty, T.D., Brown, P.C., and Schimke, R.T. UV-radiation facilitates methotrexate resistance and amplification of the dihydrofolate reductase gene in cultured 3T6 mouse cells. *Mol. Cell. Biol.*, 4: 1050-1056, 1984.
41. Mercer, W.E., Shields, M.T., Amin, M., Sauve, G.J., Appela, E., Roman, J.W., and Ullrich, S.J. Negative growth regulation in a glioblastoma tumor line that conditionally expresses human wild-type p53. *Proc. Natl. Acad. Sci. USA*, 87: 6166-6170, 1990.
42. Miyashita, T. and Reed, J.C. Tumor Suppressor p53 is a direct transcriptional activator of the human bax gene. *Cell*, 80: 293-299, 1995.
43. Basu, A. and Haldar, S. The relationship between Bcl<sub>2</sub>, Bax and p53: consequences for cell cycle progression and cell death. *Mol. Hum. Reprod.*, 4:1099-1109, 1998.
44. Windle, B., Draper, B.W., Yin, Y.X., O'Gorman, S., and Wahl, G.M. A central role for chromosome breakage in gene amplification, deletion formation, and amplicon integration. *Genes Dev.*, 5: 160-174, 1991.
45. Smith, K.A., Agarwal, M.L., Chernov, M.V., Chernova, O.B., Deguchi, Y., Ishizaka, Y., Patterson, T.E., Poupon, M.F., and Stark, G.R.. Regulation and mechanisms of gene amplification. *Philos. Trans. R. Soc. Lond. B. Biol. Sci.*, 347: 49-56, 1995
46. Gjerset, R.A. and Mercola, D. Sensitization of tumors to chemotherapy through gene therapy. *In: N. Nagy (ed.) Cancer Gene Therapy: Past Achievements and Future Challenges*, New York, London, Moscow, Plenum Publishing Corporation, *in press*.
47. Zamble, D.B. and Lippard, S.J. Cisplatin and DNA repair in cancer chemotherapy.

Trends Biochem. Sci., 20: 435-439, 1995.

48. Milne, D.M., Campbell, L.E., Campbell, D.G., and Meek, D.W. P53 is phosphorylated in vitro and in vivo by an ultraviolet radiation-induced protein kinase characteristic of the c-Jun kinase, JNK1. *J. Biol. Chem.*, 270: 5511-5518, 1995.
49. Hilberg, F. and Wagner, E.F. Embryonic stem (ES) cells lacking functional c-Jun: consequences for growth and differentiation, AP-1 activity and tumorigenicity. *Oncogene* 7: 2371-2380, 1992.
50. Harris, C.C. Structure and function of the p53 tumor suppressor gene: clues for rational cancer therapeutic strategies. *J. Natl. Cancer Inst.*, 88: 1442-1445, 1996.
51. Potapova, O., Fakhrai, H., Baird, S., and Mercola, D. Platelet-derived growth factor-B/*v*-sis confers a tumorigenic and metastatic phenotype to human T98G glioblastoma cells. *Cancer Res.*, 56: 280-286, 1996.

Figure 1

## Increased expression of immunoreactive Jun in stable transfectants

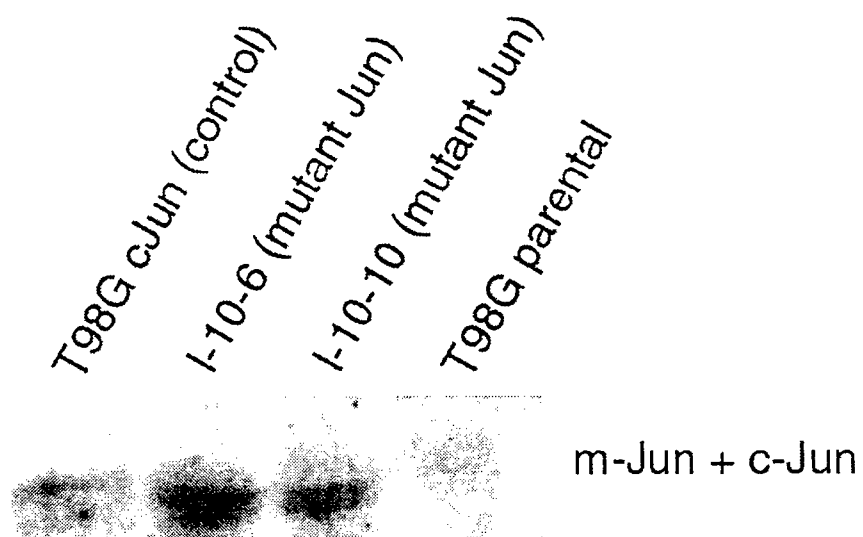


Figure 2

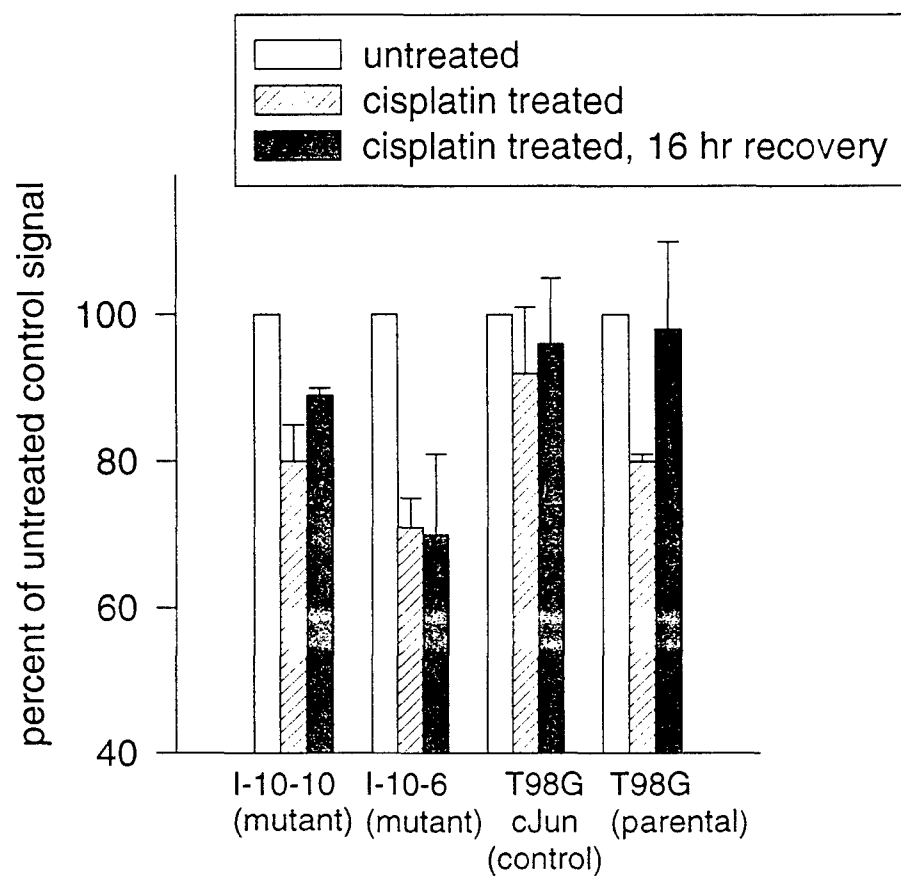


Figure 3

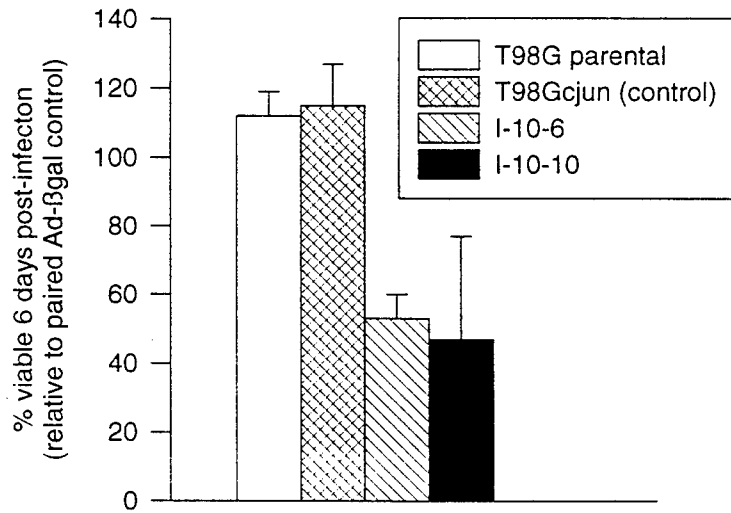


Figure 4

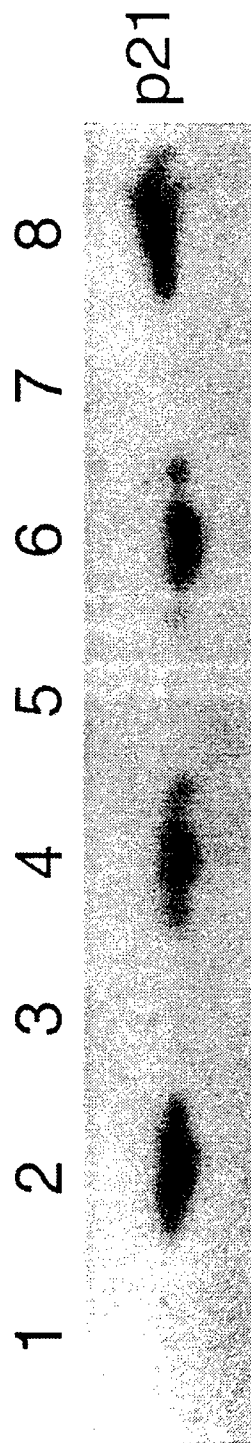


Figure 5 (A)

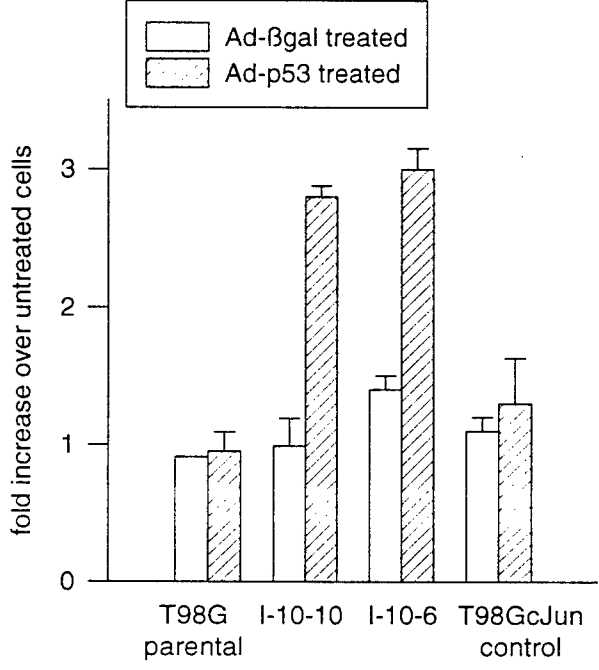


Figure 5 (B)

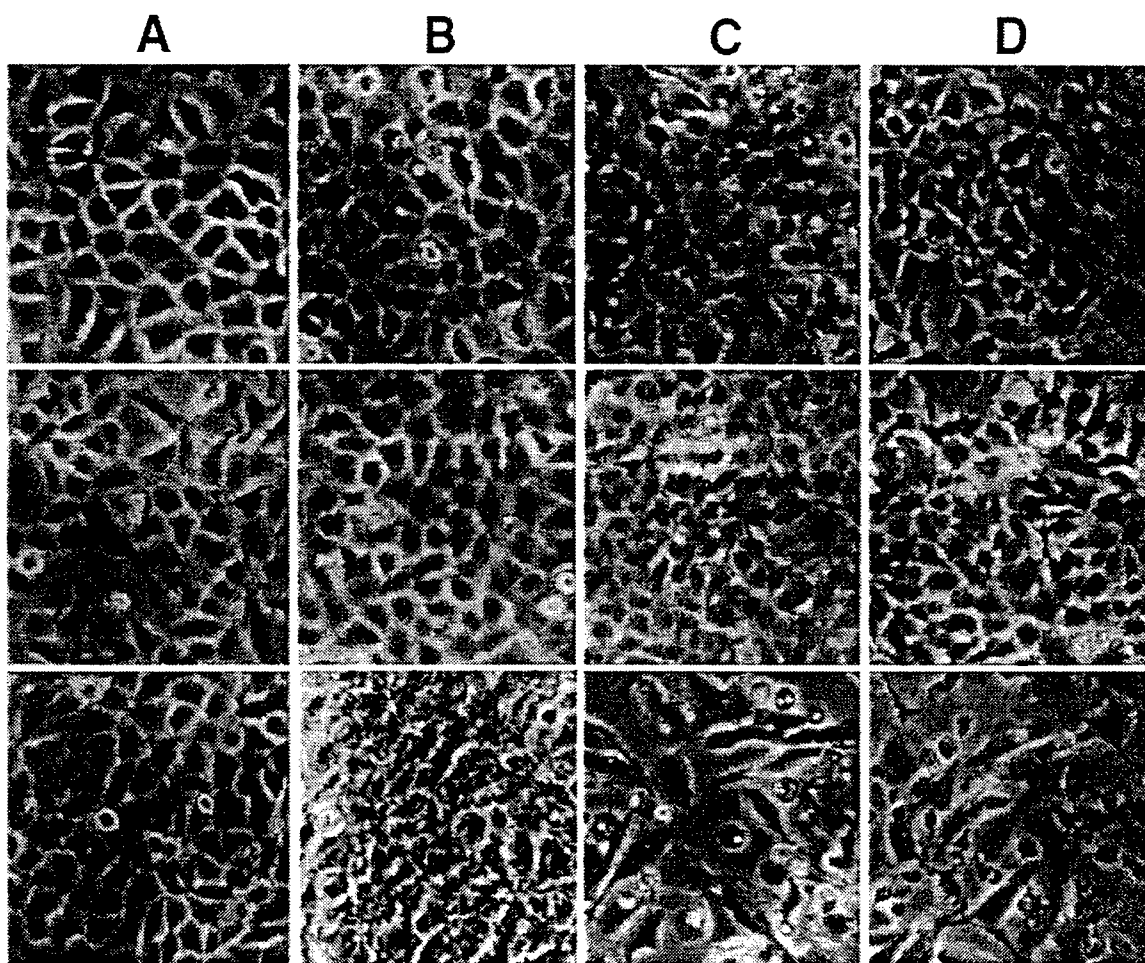


Figure 6

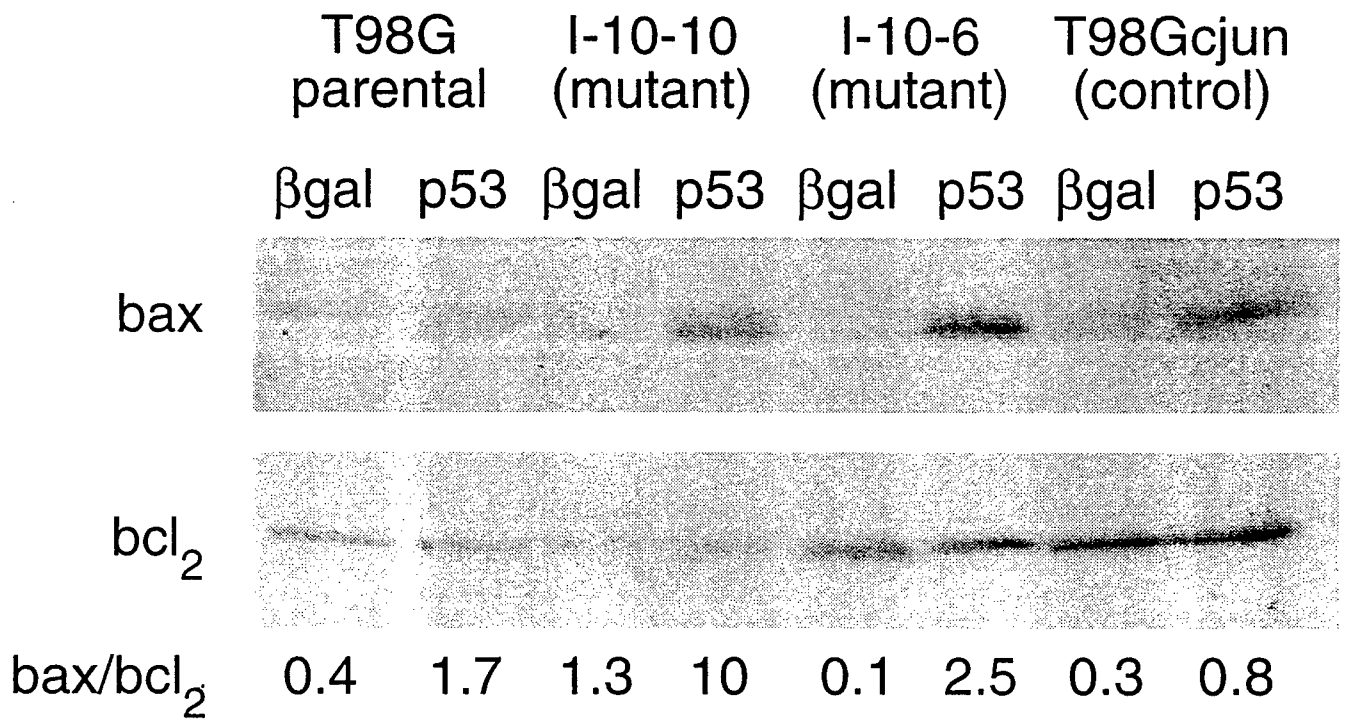
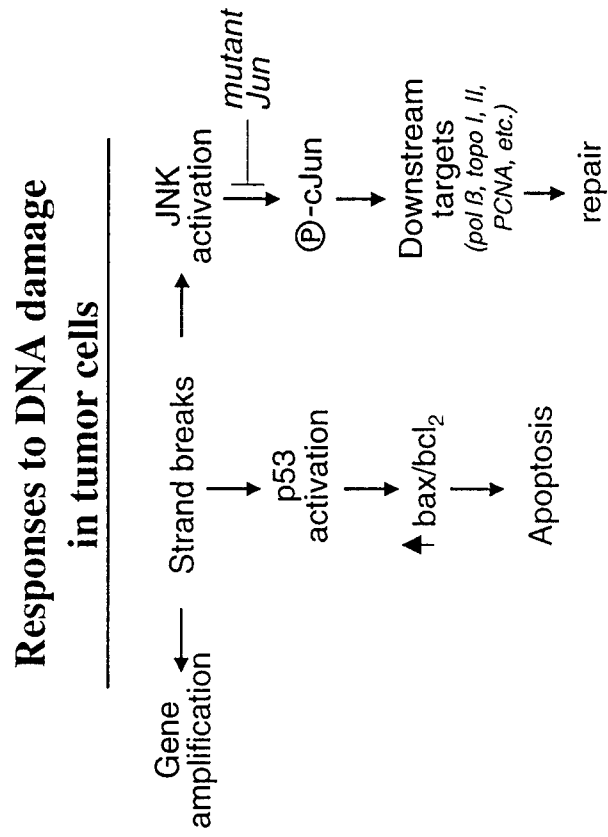


Figure 7





DEPARTMENT OF THE ARMY  
US ARMY MEDICAL RESEARCH AND MATERIEL COMMAND  
504 SCOTT STREET  
FORT DETRICK, MARYLAND 21702-5012

REPLY TO  
ATTENTION OF:

MCMR-RMI-S (70-1y)

26 Aug 02

MEMORANDUM FOR Administrator, Defense Technical Information  
Center (DTIC-OCA), 8725 John J. Kingman Road, Fort Belvoir,  
VA 22060-6218

SUBJECT: Request Change in Distribution Statement

1. The U.S. Army Medical Research and Materiel Command has reexamined the need for the limitation assigned to technical reports written for this Command. Request the limited distribution statement for the enclosed accession numbers be changed to "Approved for public release; distribution unlimited." These reports should be released to the National Technical Information Service.

2. Point of contact for this request is Ms. Kristin Morrow at DSN 343-7327 or by e-mail at Kristin.Morrow@det.amedd.army.mil.

FOR THE COMMANDER:

Encl

  
PHYLIS M. RINEHART  
Deputy Chief of Staff for  
Information Management

ADB274369  
ADB256383  
ADB264003  
ADB274462  
ADB266221  
ADB274470  
ADB266221  
ADB274464  
ADB259044  
ADB258808  
ADB266026  
ADB274658  
ADB258831  
ADB266077  
ADB274348  
ADB274273  
ADB258193  
ADB274516  
ADB259018  
ADB231912✓  
ADB244626  
ADB256677  
ADB229447  
ADB240218  
ADB258619  
ADB259398  
ADB275140  
ADB240473  
ADB254579  
ADB277040  
ADB249647  
ADB275184  
ADB259035  
ADB244774  
ADB258195  
ADB244675  
ADB257208  
ADB267108  
ADB244889  
ADB257384  
ADB270660  
ADB274493  
ADB261527  
ADB274286  
ADB274269  
ADB274592  
ADB274604

ADB274596  
ADB258952  
ADB265976  
ADB274350  
ADB274346  
ADB257408  
ADB274474  
ADB260285  
ADB274568  
ADB266076  
ADB274441  
ADB253499  
ADB274406  
ADB262090  
ADB261103  
ADB274372